Inaugural dissertation

for

obtaining the doctoral degree

of the

Combined Faculty of Mathematics, Engineering and Natural Sciences

of the

Ruprecht - Karls - University

Heidelberg

Presented by

Shivohum Bahuguna, M.Sc.

born in Mumbai, India

Oral Examination: 12th May 2025

Decoding the Genetic Regulation of Stem Cells Using *Drosophila melanogaster* Tumor Models

Referees:

Prof.Dr. Michael Boutros

Prof.Dr. Aurelio Teleman

Table of Contents

List of Abbreviations

AMPs	Antimicrobial peptides
AS-C	Acheate scute complex
bHLH	Basic Helix-Loop-Helix
ccRCC	Clear cell renal cell carcinoma
CNS	Central Nervous system
CRC	Colorectal cancer
CRD	Cysteine-rich domain
CRISPR	Clustered Regularly Interspersed Short Palindromic Repeats (CRISPR)
crRNA	CRISPR RNA
DSB	Double stranded breaks
dsRNA	Double-stranded RNA
E(spl)-C	Enhancer of Split Complex
EBs	Enteroblasts
Ecc15	*Erwinia carotovora carotovora 15*
ECs	Enterocytes
EEPs	Enteroendocrine progenitors
EEs	Enteroendocrine cells
F/O	Flipout
gRNA	Guide RNA
HDR	Homology-directed repair
Indel	Insertion or deletion
ISCs	Intestinal stem cells
mRNA	Messenger RNA
MT	Malpighian tubules
NEXT	Notch extracellular truncation
NHEJ	Non-homologous end joining
NICD	Notch intracellular domain
OD	Optical density
PAM	Protospacer adjacent motif

pH3	Phospho-Histone H3
RCC	Renal cell carcinoma
RISC	RNA-induced silencer complex
RNAi	RNA interference
RSCs	Renal stem cells
RT-qPCR	Quantitative reverse transcription polymerase chain reaction
scRNA seq	Single-cell RNA sequencing
siRNA	small interfering RNA
TLR	Toll-like receptors
ts	Temperature sensitive
UAS	Upstream activation sequence
uORF	Upstream open reading frame
VM	Visceral muscles

List of Tables

List of Figures

1 Abstract

Regenerative organs maintain a dynamic equilibrium throughout the life of the organism by resisting and repairing damage from both internal and external threats. This balance is achieved by replacing lost or damaged cells through a process primarily mediated by stem cells, which are capable of self-renewal to maintain their pool and differentiate to form specialized cell types. The decision to either divide or differentiate is tightly regulated by a genetic network, disruption of which can trigger uncontrolled stem cell proliferation and differentiation, leading to the formation of large tumors. While several studies have used *Drosophila melanogaster* to explore the roles of Notch, JNK, EGFR, and Wnt signaling pathways in regulating stem cell function, many genes that interact with these pathways remain unidentified. In this study, I generated tumor models of the *Drosophila* midgut and malpighian tubules to identify and characterize novel genes involved in stem cell regulation.

Using the CRISPR/Cas9 system, I developed a method to introduce mutations in the progenitor cells of the midgut. With this approach, I generated a Notch loss-of-function midgut tumor model, characterized by increased stem cell proliferation and secretory enteroendocrine cells. Through single-cell RNA sequencing (scRNA seq), I identified several differentially expressed genes, from which I found 28 genes whose knockdown reduced tumor growth and proliferation. I further showed that one of the candidate genes, *nerfin-1*, is required for the proliferation of stem cells during Apc^{RNAi};Ras^{V12}-mediated midgut tumorigenesis, infection-induced regeneration, and homeostasis.

From the scRNA seq dataset, I also observed that Notch loss-of-function tumors activated the Toll signaling pathway in the midgut. I demonstrated that active Toll signaling is required for promoting the proliferation of both the Notch loss-of-function and Apc^{RNAi};Ras^{V12} tumors in the midgut. Additionally, I showed that genetic activation of the Toll signaling pathway in progenitor cells was sufficient to trigger the rapid proliferation of stem cells via the JNK signaling pathway. I also demonstrated that the activation of the Toll signaling pathway in enterocytes serves as a niche signal, that drives stem cell proliferation in the midgut.

Lastly, I generated a renal cell carcinoma fly tumor model by introducing Apc^{RNAi};Ras^{V12} in renal stem cells of the malpighian tubules. I showed that tumor-bearing malpighian tubules activate the

Wnt, Pi3K/Akt/mTor, and Raf/MEK/ERK signaling pathways, all of which are essential for tumor proliferation. Additionally, I identified five genes whose knockdown reduced tumor proliferation in the malpighian tubules, the human homologs of which are upregulated in renal cell carcinoma patients.

In summary, my research demonstrates that *Drosophila melanogaster* is a valuable model, which can be used to decode the genetic networks that regulate stem cell function. By generating tumor models in the midgut and malpighian tubules, identifying transcriptomic changes, and characterizing gene function, my work lays the groundwork for further research in flies and higher model organisms, including humans.

Zusammenfassung

Regenerative Organe halten während des gesamten Lebens des Organismus ein dynamisches Gleichgewicht aufrecht, indem sie Schäden durch innere und äußere Bedrohungen abwehren und reparieren. Dieses Gleichgewicht wird erreicht, indem verlorene oder geschädigte Zellen durch einen Prozess ersetzt werden, der in erster Linie durch Stammzellen vermittelt wird, die zur Selbsterneuerung fähig sind, um ihren Pool zu erhalten und sich in spezialisierte Zelltypen zu differenzieren. Die Entscheidung, sich zu teilen oder zu differenzieren, wird durch ein genetisches Netzwerk streng reguliert, dessen Störung eine unkontrollierte Vermehrung und Differenzierung von Stammzellen auslösen kann, was zur Bildung großer Tumore führt. In mehreren Studien wurde die Rolle von Notch-, JNK-, EGFR- und Wnt-Signalwegen bei der Regulierung der Stammzellfunktion untersucht, doch viele Gene, die mit diesen Signalwegen interagieren, sind noch nicht identifiziert. In dieser Studie habe ich Tumormodelle des Mitteldarms und der malpighischen Tubuli von Drosophila erstellt, um neue Gene, die an der Stammzellregulation beteiligt sind, zu identifizieren und zu charakterisieren.

Ich habe eine Methode entwickelt, um mittels CRISPR-Cas9 in die Vorläuferzellen des Mitteldarms Mutationen herbeizuführen. Dadurch erzeugte ich ein Notch-Tumormodell mit Funktionsverlust im Mitteldarm, das sich durch erhöhte Stammzellproliferation und eine Anreicherung sekretorischer enteroendokriner Zellen kennzeichnet. Durch Einzelzell-RNA-Sequenzierung (scRNA-seq) identifizierte ich mehrere differentiell exprimierte Gene, von denen bei 28 Genen ein Knockdown das Tumorwachstum und die Proliferation reduzierte. Darüber hinaus habe ich gezeigt, dass eines der Kandidatengene, *nerfin-1*, für die Vermehrung von Stammzellen während der Apc^{RNAi};Ras^{V12}-vermittelten Mitteldarmtumorigenese, infektionsinduzierten Regeneration und Homöostase erforderlich ist.

Anhand des scRNA seq-Datensatzes konnte ich außerdem feststellen, dass Notch-Loss-of-Function-Tumoren den Toll-Signalweg im Mitteldarm aktivieren. Des Weiteren konnte ich zeigen, dass ein aktiver Toll-Signalweg für die Förderung der Proliferation sowohl von Notch-Loss-of-Function- als auch von Apc^{RNAi};Ras^{V12}-Tumoren im Mitteldarm erforderlich ist. Darüber hinaus habe ich gezeigt, dass die genetische Aktivierung des Toll-Signalwegs in Vorläuferzellen ausreicht, um eine schnelle Vermehrung von Stammzellen über den JNK-Signalweg auszulösen. Ich habe auch gezeigt, dass die Aktivierung des Toll-Signalwegs in

Enterozyten als Nischensignal dient, das die Stammzellproliferation im Mitteldarm antreibt.

Schließlich habe ich ein Nierenzellkarzinom-Tumormodell für Fliegen entwickelt, indem ich Apc^{RNAi};Ras^{V12} in Nierenstammzellen der malpighischen Tubuli eingeführt habe. Ich konnte zeigen, dass tumortragende malpighische Tubuli die Wnt-, Pi3K/Akt/mTor- und Raf/MEK/ERK-Signalwege aktivieren, die alle für die Tumorproliferation wichtig sind. Darüber hinaus habe ich fünf Gene identifiziert, deren Knockdown die Tumorproliferation in den malpighischen Tubuli reduzierte und deren menschliche Homologe bei Patienten mit Nierenzellkarzinom hochreguliert sind.

Zusammenfassend lässt sich sagen, dass meine Forschung zeigt, dass *Drosophila melanogaster* ein wertvolles Modell ist, das zur Entschlüsselung der genetischen Netzwerke verwendet werden kann, die die Stammzellfunktion regulieren. Durch die Erzeugung von Tumormodellen im Mitteldarm und in den malpighischen Tubuli, die Identifizierung von Transkriptomveränderungen und die Charakterisierung von Genfunktionen legt meine Arbeit den Grundstein für weitere Forschung in Fliegen und höheren Modellorganismen, einschließlich des Menschen.

2 Introduction

2.1 Regenerative organs require stem cells to maintain homeostasis

Organismal health is maintained through the coordinated functioning of cells, tissues, and organs, all of which are influenced by environmental conditions. However, both internal and external challenges can disrupt homeostasis and threaten overall health. To counteract these threats, organisms have evolved mechanisms to restore normal function, primarily through recognition and repair of cellular damage. One such mechanism is the replacement of damaged or dead cells with new ones, a process driven by stem cells in regenerative organs. Stem cells are a special group of cells that divide and differentiate to give rise to new, differentiated cells while maintaining their own pool. Signals derived from damaged or dying cells prompt stem cells to activate their division and differentiation processes when necessary. Maintaining strict control over these processes is critical, as any defects in this regulation can lead to tumor formation [1, 2].

2.1.1 The *Drosophila* midgut

The *Drosophila* midgut performs key functions similar to those of the human small intestine, including food digestion, nutrient absorption, immune defence, and interaction with the gut microbiome. Both the human intestine and the *Drosophila* midgut also share similarities in their cell types. The *Drosophila* midgut is a monolayer epithelium and is composed of five major cell types: Intestinal stem cells (ISCs), Enteroblasts (EBs), Enteroendocrine progenitors (EEPs), Enterocytes (ECs), and Enteroendocrine cells (EEs). ISCs, EBs, and EEs are diploid with a small nucleus, while ECs are polyploid with a larger nucleus. These cell types are distributed along the entire length of the midgut, with functional roles that are analogous to their human counterparts **(Figure 1A)** [1].

ISCs reside at the base of the midgut epithelium and divide asymmetrically to produce a daughter stem cell and a transient EB or EEP [3, 4, 5]. Collectively, ISCs, EBs, and EEPs are referred to as progenitor cells and they all express the transcriptional factor Escargot (Esg) [4, 5]. Apart from the expression of *esg*, ISCs express the ligand Delta, EBs express the transcription regulator Suppressor of Hairless (Su(H)), and EEPs express the transcription factor Prospero (pros) [4, 5, 6]. Post-mitotic progenitor EBs differentiate into ECs, while transient

progenitor EEPs differentiate into EEs [5]. ECs are the most abundant cell type in the midgut; they are absorptive cells responsible for nutrient absorption and interaction with luminal contents and serve as a barrier between the lumen and the internal organs of the fly. EEs are secretory cells that primarily produce hormones and cytokines, which are essential for the proper functioning of the midgut [1, 6] **(Figure 1B)**.

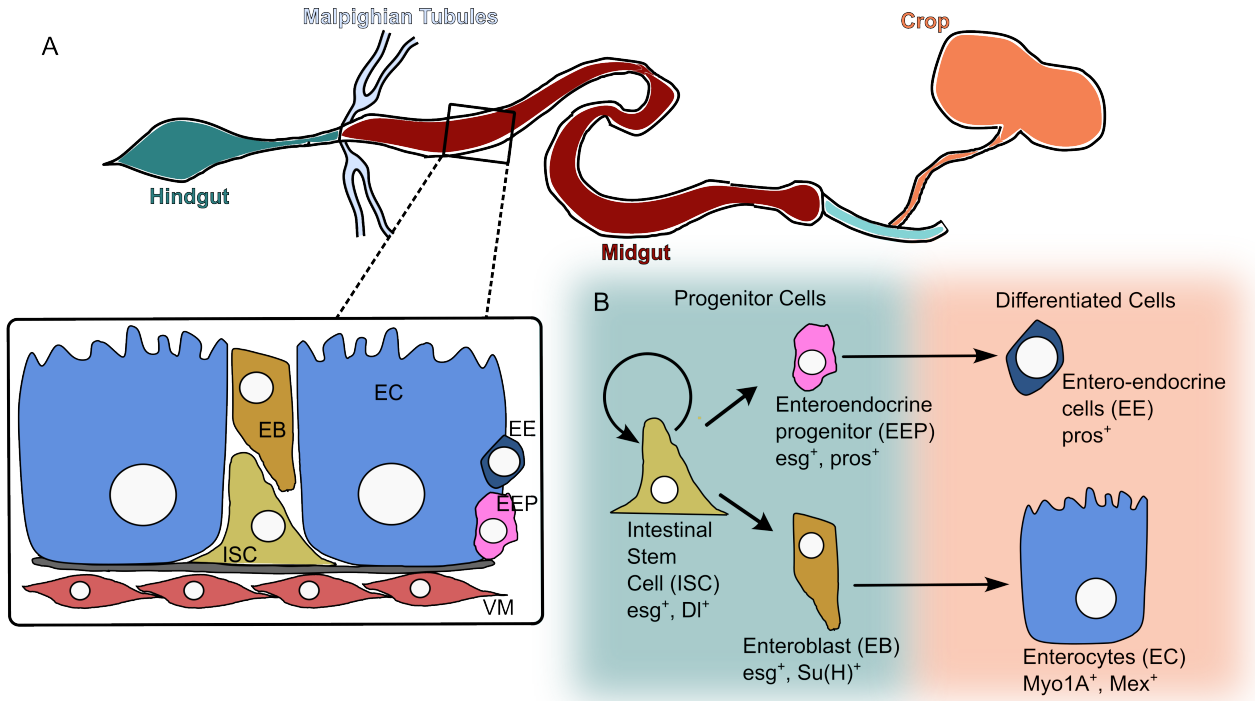

Figure 1: *Drosophila* midgut and its cell types. (A)The midgut comprises of dividing Intestinal Stem Cells (ISCs), transient Enteroblasts (EBs), Enteroendocrine progenitors, absorptive Enterocytes (ECs), secretory Enteroendocrine cells (EEs), and Visceral Muscles (VM). **(B)** ISCs, EBs, and EEPs together constitute the progenitor population, while ECs and EEs constitute the differentiated cell population. ISCs divide asymmetrically to give rise to one ISC and one EB or EEP. A transient EB differentiates into an EC, while EEP differentiates into an EE.

The mechanism of ISC division and subsequent differentiation into ECs or EEs are accelerated in response to stress signals, such as infection or toxin exposure. Damage to the midgut triggers the activation of various signaling pathways in different cell types, which act either autonomously or non-autonomously to promote division, differentiation, and repair, ultimately maintaining gut integrity [7]. Key signaling pathways involved in this process include: Notch, Wnt, EGFR, Jak-Stat, and JNK signaling [3, 4, 7, 8, 9, 10, 11]. The mechanism by which these pathways maintain midgut integrity and how disruption of these pathways cause tumor formation will be explained in sections 2.2 to 2.6.

2.1.2 The *Drosophila* Malpighian Tubule

The adult fly Malpighian Tubule (MT) is an important excretory organ responsible for maintaining electrolyte and water balance, a function analogous to the human kidney. The MTs are attached to the midgut at the midgut-hindgut boundary and consist of the ureter, initial segment, main segment, and lower segment. Together, the MTs work alongside the midgut and hindgut to facilitate the excretion of waste and toxins [12]. In addition to their excretory role, the MTs are regenerative organs that contain renal stem cells (RSCs) located in the ureter and lower tubule [13]. These stem cells are derived from the same pool of larval progenitor cells that produce ISCs in the midgut, and therefore also express *esg* [14]. However, unlike the midgut ISCs, the RSCs are generally quiescent. Nonetheless, they are capable of responding to injury and can divide and replace lost cells, employing similar signaling pathways as those used by ISCs [15].

2.2 The Notch signaling pathway

2.2.1 Signaling components of the Notch signaling pathway

The Notch signaling pathway plays a critical role in determining cell fate and regulating cell proliferation and differentiation in flies. The canonical Notch pathway relies on the communication between two adjacent cells to transmit a complete signal. In the signal-receiving cell, the Notch (N) receptor undergoes post-translational modifications and proteolytic cleavage (S1) in the endoplasmic reticulum (ER) and Golgi apparatus before being transported to the plasma membrane [16, 17, 18]. The extracellular domain of the N receptor binds to the ligands Delta or Serrate (Ser) from the adjacent signal-sending cell. Upon this interaction, the Delta ligand exerts a physical force on the N receptor, triggering its second proteolytic cleavage (S2) by Kuzbanian (Kuz) [19]. The Delta ligand is endocytosed in the signal-sending cell, where it is ubiquitinated by Neuralized (Neur) or Mind bomb 1 (Mib1) and eventually degraded [20, 21, 22].

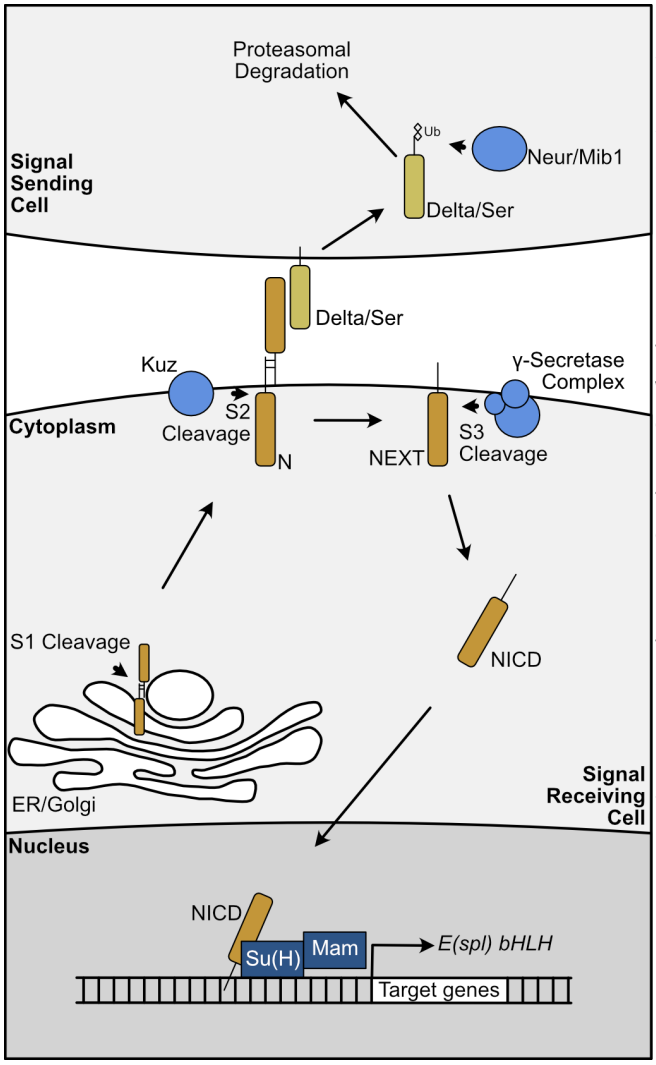

Figure 2: The *Drosophila* Notch Signaling Pathway: Signal-sending cell - Delta, Serrate (Ser), Neuralized (Neur), Mindbomb (Mib1).
Signal-receiving cell - Notch (N), Kuzbanian (Kuz), γ-Secretase Complex (Psn, Nct, Aph-1, Pen-2), Suppressor of Hairless (Su(H)), Hairless (H), Mastermind (Mam).
In the signal-receiving cell, N receptor first undergoes S1 cleavage at the ER/Golgi, from where it translocates to the cell membrane. Here it interacts with the Delta or Ser ligands from the signa- sending cell. This interaction triggers S2 cleavage mediated by Kuz, resulting in the formation of Notch extracellular truncation (NEXT). The γ-Secretase Complex further cleaves NEXT to form Notch intracellular domain (NICD), which translocates into the nucleus. In the nucleus, NICD forms a complex with Su(H) and Mam to transcribe Notch target genes including Enhancer of Split Complex (*E(spl)-C)* basic Helix-Loop-Helix (*bHLH)* genes. In the signal sending cell, Delta/Ser undergoes ubiquitination by Neur/Mib1 and is subsequently degraded.

S2 cleavage of the N receptor in the signal-receiving cell generates a truncated form by shedding the extracellular domain, known as Notch extracellular truncation (NEXT) [23]. This truncated form undergoes a third proteolytic cleavage (S3) by the γ-Secretase Complex, resulting in the release of the Notch intracellular domain (NICD) [19, 24, 25]. The NICD is then translocated into the nucleus, where it displaces Hairless (H) and forms a transcriptional activation complex with Suppressor of Hairless (Su(H)) and Mastermind (Mam) [26, 27, 28]. This active NICD-Su(H)-Mam complex recruits co-activators to initiate the transcription of Notch target genes, most common of which are the Enhancer of Split Complex (E(spl)-C) basic Helix-Loop-Helix (bHLH) proteins [29, 30, 31] **(Figure 2)**.

2.2.2 Notch signaling in stem cell homeostasis and tumorigenesis

The maintenance and differentiation of ISCs are primarily regulated by the Notch signaling pathway. ISCs express high levels of the ligand Delta, which interacts with the Notch receptor on adjacent EBs. Strong Delta-Notch activity in EBs promotes their differentiation into ECs, while weaker Delta-Notch signaling favours EE differentiation via the formation of transient EEPs [5, 6]. The transcription factor Klumpfuss (Klu) regulated by Notch signaling, restricts the differentiation of EBs to ECs [32], while activation of Scute (Sc) and Asense (Ase) promotes EE differentiation [33]. The bHLH transcription factor Daughterless (Da) is essential for maintaining ISC identity and is inhibited by the E(spl)-C complex to promote differentiation [34]. Disruption of the Notch signaling pathway in progenitor cells leads to defects in EC differentiation, resulting in tumorigenic clusters composed of ISCs and EEs [6].

Differentiation-defective Notch mutant progenitors give rise to tumors through a series of signaling events. At an early stage, mitogenic signals resulting from Notch knockdown initiate the formation of small stem cell clusters. The growth of these clusters is further promoted by autocrine Spi/EGFR signaling, which contributes to tumor formation. As the tumors grow larger, they disrupt the surrounding epithelial architecture, forcing the cells to detach and extrude. This breakdown of the epithelial structure triggers stress-induced signaling pathways, such as JNK and Hippo/Yorkie signaling, leading to the production of growth factors (e.g., Pvf, Wg, Vn, and Dilp3) and cytokines (Upd2/3). These growth factors and cytokines further fuel tumor growth and form a positive feedback loop to create a stem cell niche [35].

2.3 The Canonical Wnt signaling pathway

2.3.1 Signaling components of the Canonical Wnt signaling pathway

Canonical Wnt signaling is a key regulator of the development, patterning, and functioning of various organs such as wings, and midgut in flies.

In the **"Wnt OFF"** state, the absence of Wingless (Wg) leads to the inactivated state of Frizzled (Fz) and Arrow (Arr) receptors. As a consequence, the β-Catenin Destruction Complex composed of the scaffold proteins Axin (Axn), Adenomatous polyposis coli (Apc), and kinases Shaggy (Sgg), Casein kinase 1α (Ck1α), phosphorylates Armadillo (Arm) in the cytoplasm [36,

37, 38]. This phosphorylation creates a docking site for the E3 ubiquitin ligase β-Transducing repeat-containing protein (β-Trcp), which ubiquitinates Arm, targeting it for proteasomal degradation [39, 40]. The lack of nuclear Arm prevents the activation of Wnt target gene expression, as co-repressor Groucho (Gro) binds to the transcription factor Pangolin (Pan), inhibiting gene expression [41].

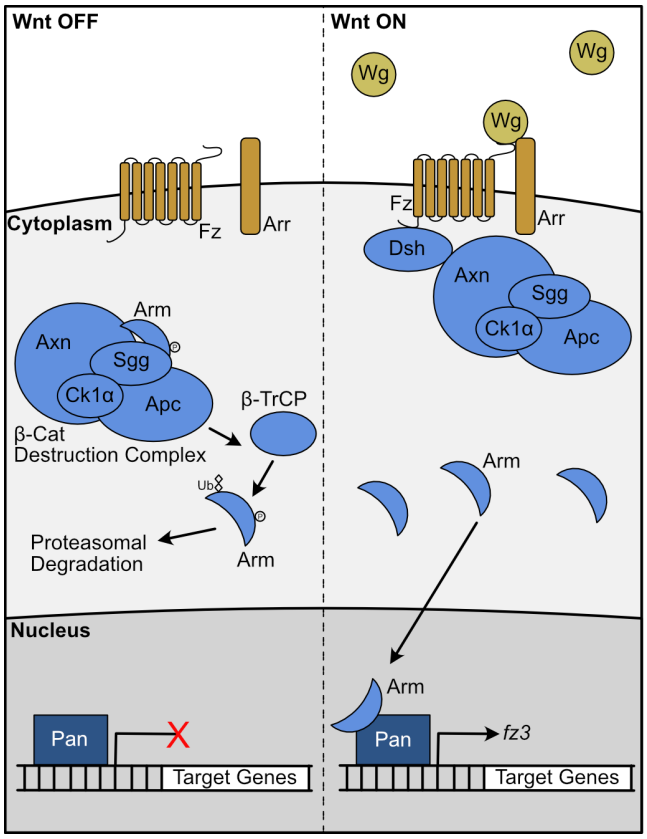

Figure 3: The *Drosophila* Wnt Signaling Pathway:
Extracellular ligand - Wingless (Wg).
Transmembrane receptors - Frizzled (Fz), Arrow (Arr).
Cytoplasmic proteins - Dishevelled (Dsh), Armadillo (Arm) and β-Catenin Destruction Complex (Axin (Axn), Adenomatous Polyposis Coli (Apc), Shaggy (Sgg), Casein kinase 1 alpha (Ck1α)), Beta-Transducing repeat-Containing Protein (β-TrCP).
Nuclear factors - Pangolin (Pan), Groucho (Gro).
Wnt OFF - In the absence of Wg, the receptors Fz and Arr remain in an inactive state. The cytoplasmic β-Cat destruction complex (Axn, Apc, Sgg, Ck1α) phosphorylates Arm. Phosphorylated Arm is ubiquitinated by β-TrCP and degraded. This prevents the activation and transcription of Wnt target genes by Pan in the nucleus.
Wnt ON - Wg binds to Fz-Arr complex at the plasma membrane and recruits Dsh to the Fz receptor. This brings the β-Cat Destruction Complex at the plasma membrane, which prevents phosphorylation and subsequent degradation of Arm. Stable Arm translocates into the nucleus, and together with Pan promotes transcription of Wnt target genes such as *fz3*.

In the **"Wnt ON"** state, Wg ligand binds to the extracellular cysteine-rich domain (CRD) of the Fz receptor [42]. This interaction triggers the recruitment and dimerization of Fz with Arr at the plasma membrane [43]. The Wg-Fz-Arr complex promotes the oligomerization of Dishevelled (Dsh) at the cytoplasmic domain of Fz [44]. Dsh brings Axin (Axn), which is complexed with the kinases Sgg and Ck1α, to the plasma membrane, where it serves as a platform for the phosphorylation of the cytoplasmic tail of Arr [45]. The dimerization of Fz-Arr together with Dsh, Axn, Apc, Sgg, and Ck1α at the plasma membrane, prevents the phosphorylation and subsequent degradation of Arm by the "β-Catenin Destruction Complex" in the cytoplasm. Stable Arm then translocates into the nucleus, where it displaces the repressor Gro and forms a complex with DNA-bound Pan, leading to the transcription of Wnt target genes such as *frizzled 3 (fz3)* [46, 47, 48] **(Figure 3)**.

2.3.2 Wnt signaling in stem cell homeostasis and tumorigenesis

Wnt signaling plays a crucial role in regulating stem cell homeostasis in both the mammalian intestine and the *Drosophila* midgut. In both, loss of the canonical Wnt signaling pathway components under homeostasis leads to impaired regeneration capacity of intestinal stem cells [49]. In flies, Wg is secreted from the surrounding visceral muscles (VM) and at major compartment boundaries of the gut epithelium [8, 50, 51]. Under normal conditions, Wnt signaling is predominantly active at the intestinal compartment boundaries, as indicated by the Wnt target gene reporter Fz3-RFP [51]. However, during a regenerative response, Wg is produced by Esg-positive progenitor cells, leading to stem cell overproliferation through activation of the canonical Wnt signaling pathway [52].

Inactivating mutation of the *Apc* gene is the first step in the formation of colorectal cancer in humans. These mutations lead to Wnt pathway hyperactivation, which drives early stages of tumorigenesis [53]. In flies, Apc is mainly expressed in progenitor cells, loss of which activates Wnt signaling and causes stem cell overproliferation and intestinal hyperplasia [9, 50, 54]. This phenotype is dependent on the canonical Wnt signaling pathway [9, 54]. Additionally, loss of Apc confers a competitive advantage to mutant stem cells over wild-type cells and promotes JNK-dependent cell death of surrounding healthy cells, further fueling tumor proliferation [55]. Beyond Wnt-driven stem cell proliferation, Apc mutant cells rely on other signaling pathways, such as JNK, JAK/STAT, and EGFR signaling to sustain growth and proliferation [52, 54, 56]. Therefore, Wnt signaling serves as an important regulator of stem cell proliferation, and its hyper-activation drives the early onset of tumor formation.

2.4 The EGFR signaling pathway

2.4.1 Signaling components of the EGFR signaling pathway

Epidermal growth factor receptor (EGFR) signaling is a well-known regulator of stem cell proliferation and an oncogenic signaling pathway.

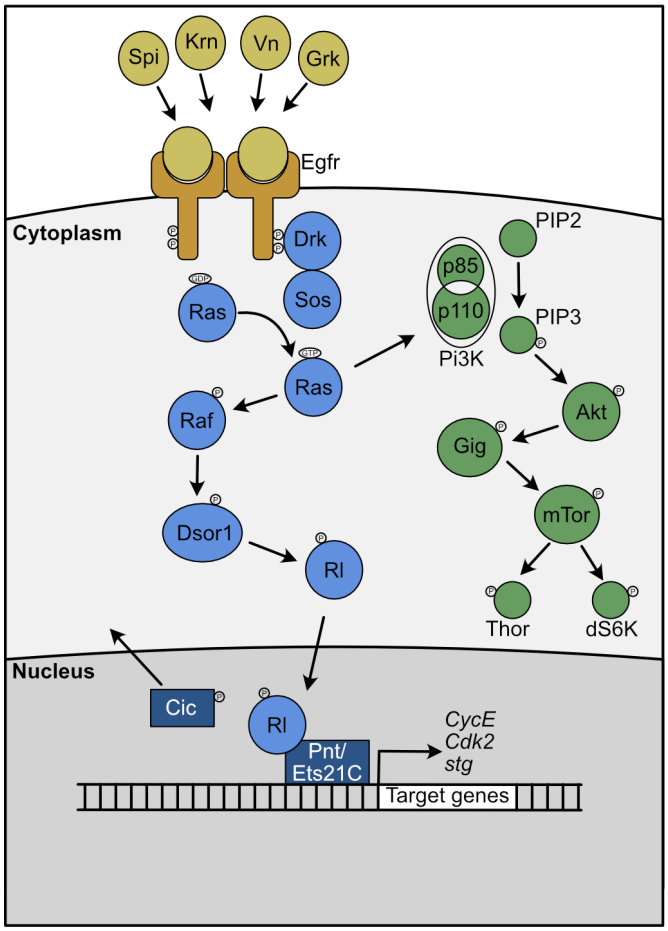

Figure 4: The *Drosophila* EGFR Signaling Pathway:
Extracellular ligands - Spitz (Spi), Keren (Krn), Vein (Vn), Gurken (Grk).
Transmembrane receptor - Epidermal growth factor receptor (Egfr).
Cytoplasmic proteins - Downstream of receptor kinase (Drk), Son of sevenless (Sos), Ras85D/Ras, Raf, Downstream of raf1 (Dsor1), Rolled (Rl), Phosphoinositide 3-kinase (Pi3K), Akt kinase (Akt), Gigas (Gig/dTsc2), mechanistic Target of rapamycin (mTor), Thor (d4EBP), Ribosomal protein S6 kinase (dS6K).
Nuclear factors - Pointed (Pnt), Capicua (Cic), Ets21C.
Ligands Spi, Krn, Vn, or Grk bind to the Egf receptor (Egfr) at the cell membrane. Binding induces dimerization, and auto-phosphorylation of the intracellular domain of Egfr. Drk and Sos are recruited to the receptor, where Sos activates Ras by exchanging GDP to GTP. This activation signal is relayed through a series of kinase-dependent phosphorylations involving Raf, Dsor1, and ultimately Rl. Phosphorylated Rl translocates into the nucleus, displaces Cic, and activates Pnt and Ets21C, leading to the transcription of target genes such as *CycE, Cdk2*, and *stg*. Ras also activates Pi3K, which generates PIP3, subsequently activating Akt kinase. Phosphorylated Akt kinase activates mTor by inactivating its negative regulator, Gig (dTSC2). mTor promotes cell growth and protein synthesis by phosphorylating downstream effectors Thor and dS6K.

The Epidermal growth factor receptor (Egfr) is a monomeric receptor belonging to the receptor tyrosine kinase (RTK) family, consisting of a ligand-binding extracellular domain, a transmembrane domain, and an intracellular tyrosine kinase domain [57]. EGF ligands, such as Spitz (Spi), Keren (Krn), Vein (Vn), and Gurken (Grk) bind to the extracellular domain of Egfr in flies [58, 59, 60, 61]. Upon binding, Egfr undergoes dimerization and subsequent auto-transphosphorylation of its intracellular domain [62]. These intracellular phosphorylated regions of the Egfr serve as docking sites for the adaptor protein Downstream of receptor kinase (Drk) at the plasma membrane [63]. The interaction recruits the guanine exchange factor Son of sevenless (Sos), leading to the activation of Ras85D/Ras by exchanging GDP for GTP [64, 65].

Activated Ras transduces the signal through a cascade of kinase-dependent phosphorylations in the mitogen-activated protein kinase (MAPK) pathway. This pathway involves the sequential

activation of Raf oncogene (Raf) [66, 67], Downstream of raf 1 (Dsor1) [68], and Rolled (Rl) [69]. Once phosphorylated, Rl translocates into the nucleus and triggers the removal of the repressor Capicua (Cic) from the nucleus to the cytoplasm [70]. The activation of Rl and the release of Cic-mediated repression results in the activation of ETS transcription factors Pnt and Ets21C. Both these transcription factors regulate target gene expression required for cell cycle, such as *CycE*, *Cdk2*, and *stg* [71] **(Figure 4)**.

Another major downstream effector of Ras is phosphoinositide 3-kinase (Pi3K), which activates the Pi3K/Akt/mTor signaling cascade [72, 73]. The activation of Pi3K by Ras catalyzes the phosphorylation of phosphatidylinositol (4,5)-bisphosphate (PIP2) to produce phosphatidylinositol (3,4,5)-trisphosphate (PIP3), which in turn activates Akt kinase [74]. Akt then activates mTor kinase by phosphorylating its inhibitor, Gigas (Gig/dTsc2). Activated mTor promotes cell growth and protein synthesis by phosphorylating its downstream effectors *Drosophila* Ribosomal protein S6 kinase (dS6K) and Thor (d4E-BP) [75] **(Figure 4)**.

2.4.2 EGFR signaling in stem cell homeostasis and tumorigenesis

In the *Drosophila* midgut, EGFR signaling plays a crucial role in regulating ISC proliferation under both homeostatic and stress conditions. During homeostasis, ISCs stain positive for diphosphorylated form of ERK (dpERK), which is indicative of active EGFR signaling. Additionally, ISCs carrying loss of EGFR signaling components Ras, and Egfr, fail to grow and proliferate [76]. Flies mutant for Pi3K and mTor function had significantly reduced ISC division as well as decreased DNA endoreplication in ECs during homeostasis [77]. The visceral muscles (VMs) serve as a niche for EGFR signaling in ISCs through the secretion of the ligand Vn [10, 78].

Epithelial stress in the *Drosophila* midgut triggers the production of EGFR ligands from various sources: 1) Vn from VMs, 2) Spi primarily from progenitor cells and also from some ECs, and 3) Krn from ECs. These ligands are necessary for activating EGFR signaling in ISCs thereby promoting their proliferation [10]. Infection-induced damage enhances EGFR signaling in progenitor cells, disruption of which suppresses infection-induced stem cell overproliferation in the midgut [79]. Additionally, Notch loss-of-function tumors also activate EGFR signaling, which autonomously drives stem cell proliferation and tumor growth [35].

Ectopic expression of active EGFR signaling components, such as *Egfr*$^{\lambda Top}$, *Ras*^{V12}, *Raf*^{GOF}, and *pnt*, drives stem cell overproliferation by promoting the transcription of genes involved in cell growth and cell cycle [10, 71]. Overexpression of *Ras*^{V12} induces oncogenic proliferation of stem cells, loss of cell polarity, epithelial disruption, and metastasis in the fly midgut, making it a good *in-vivo* cancer model for genetic and drug screening [80, 81]. In the fly malpighian tubules, *Ras*^{V12}-expressing renal stem cells activate MAPK signaling and cause renal stem cell overproliferation. Inhibition of signaling components Dsor1, Raf, and mTor suppressed *Ras*^{V12}-mediated renal stem cell overproliferation in the malpighian tubules [82]. Moreover, tumors driven by *Ras*^{V12} in the *Drosophila* accessory gland activate the MAPK and Pi3K/Akt/mTor pathways, both of which are required for tumorigenesis [83].

2.5 The JNK signaling pathway

2.5.1 Signaling components of the JNK signaling pathway

The c-Jun NH 2 -terminal kinase (JNK) signaling pathway is a stress response pathway that senses various stress signals and mediates cellular responses that regulate cell survival, repair, and homeostasis.

Tumor necrosis factor (TNF) ligand Eiger (Egr) activates JNK signaling by binding to TNF receptors Wengen (Wgn) and Grindelwald (Grnd) [84, 85, 86]. This interaction triggers a cascade of sequential phosphorylation events involving a series of kinases: Misshapen (Msn), TGF-β activated kinase 1 (Tak1), Hemipterous (Hep), and Basket (Bsk) [87, 88, 89, 90]. Phosphorylated Bsk then activates Kayak (Kay) and Jun-related antigen (Jra) by phosphorylating them, leading to the formation of the AP1 transcription factor complex [91]. The AP1 complex translocates to the nucleus and regulates the transcription of JNK target genes, such as *puckered (puc)*, *Matrix metalloproteinase (Mmp1)*, and *unpaired (upd)*. These genes are essential for cell proliferation and survival [92] **(Figure 5)**.

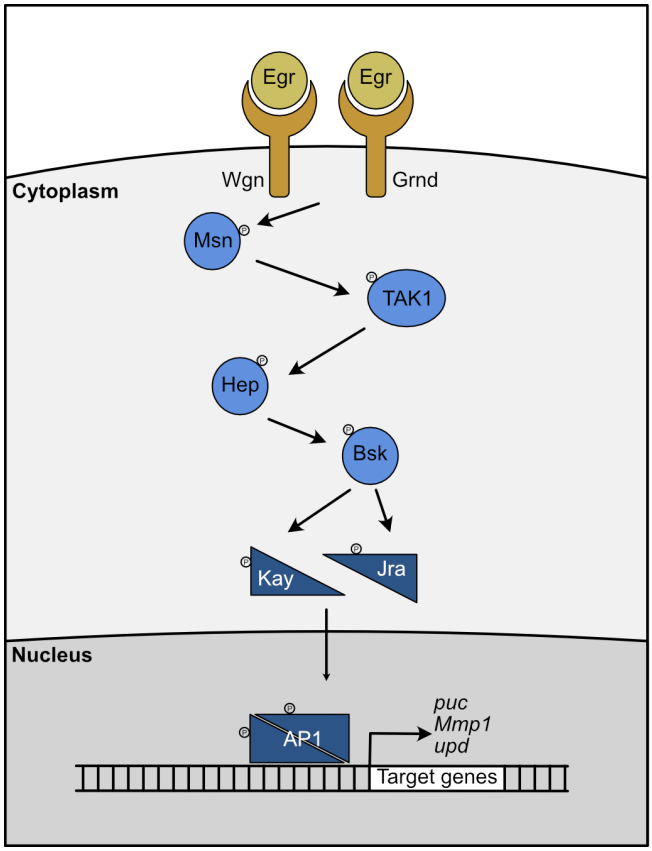

Figure 5: The *Drosophila* JNK Signaling Pathway:
Extracellular ligand - Eiger (Egr).
Transmembrane receptors - Grindelwald (Grnd), Wengen (Wgn).
Cytoplasmic proteins - Misshapen (Msn), Tak1, Hemipterous (Hep), Basket (Bsk).
Nuclear factors - AP1 complex- Kayak (Kay), Jun-related antigen (Jra).
Ligand Egr binds to the receptors Wgn or Grnd resulting in the phosphorylation of Msn. This further phosphorylates TAK1, which relays the signal to Bsk via Hep. Active Bsk phosphorylates Kay and Jra. which together forms the AP-1 complex and transcribe target genes such as *puc, Mmp1*, and *upd* in the nucleus.

2.5.2 JNK signaling in stem cell homeostasis and tumorigenesis

Epithelial renewal of the fly gut in response to stress signals occurs in two major steps: 1) Loss of damaged ECs, and 2) Increased ISC proliferation. During stress, JNK signaling is activated in ECs and ISCs, which facilitates both of these major steps in epithelial renewal [11].

In ISCs, active JNK signaling is required for proliferation in response to oxidative stress, such as *Ecc15* infection, paraquat damage, and aging [11, 93]. In the absence of infection, forced activation of JNK signaling by overexpressing *hep* in stem cells causes a significant overproliferation of ISCs [93]. Furthermore, JNK signaling contributes to the autonomous growth of midgut tumors [92, 94]. JNK signaling promotes its pro-proliferative effects through several transcription factors, including AP1, Sox21a [95], and Ets21c [96], as well as by maintaining spindle orientation through the recruitment of Wdr62 and repression of Kif1a [97].

JNK signaling also acts non-autonomously to trigger stem cell proliferation. Stress-induced activation of JNK signaling in ECs enhances the expression of Unpaired (Upd) cytokines, which, in turn, triggers ISC proliferation via the JAK/STAT signaling pathway [7]. This non-autonomous

mechanism of stem cell proliferation is hijacked by rapidly proliferating tumors to propagate at the expense of surrounding healthy wild type cells. For example, Notch tumors activate JNK signaling in surrounding ECs, which promotes tumor growth through cytokine production [35]. A similar non-autonomous role of JNK signaling is required for the growth of Sox21a [94] and Apc mutant [55] midgut tumors.

2.6 The Toll signaling pathway

2.6.1 Signaling components of the Toll signaling pathway

The Toll signaling pathway is an evolutionary conserved innate immune pathway, which along with the IMD pathway responds to pathogenic insults. Toll signaling specifically responds to Gram-positive bacteria and Fungi in flies [98].

The cell wall of Gram-positive bacteria, which contains Lys-type peptidoglycan, is recognized by Peptidoglycan Recognition Protein SA (PGRP-SA) and Gram-negative Bacteria Binding Protein 1 (GNBP1) [99, 100]. In contrast, the fungal cell wall is recognized by Gram-negative Bacteria Binding Protein 3 (GNBP3) [101]. The recognition signal is relayed to Spatzle Processing Enzyme (SPE) through a sequential protease cascade, which involves Modular Serine Protease (ModSP), Gram-positive Specific Serine Protease (Grass), and Spirit/Spheroide/Sphinx1/2 [102]. The activated SPE processes the full-length Spatzle (Spz) into its active form [103].

Activated Spz dimerizes and binds to the extracellular domain of the Toll (Tl) receptor [104, 105]. This binding induces the dimerization of the Tl receptors at the cell membrane [106]. The activated Tl dimers recruit the adaptor protein Myd88 to the intracellular TIR domain of the Tl receptor [107]. The interaction between Tl and Myd88 leads to the formation of a complex comprising of MyD88, the adaptor protein Tube (Tub), and kinase Pelle (Pll) [108]. This oligomeric Myd88-Tub-Pll complex phosphorylates the inhibitor Cactus (Cact), resulting in its degradation and release of the NF-κB transcription factor Dorsal-related immunity factor (Dif) and Dorsal (dl) [109]. The free Dif and dl translocate into the nucleus and transcribe target genes including anti-microbial peptides such as *Drosomycin (Drs)*, and *Defensin (def)* [110, 111, 112] **(Figure 6)**.

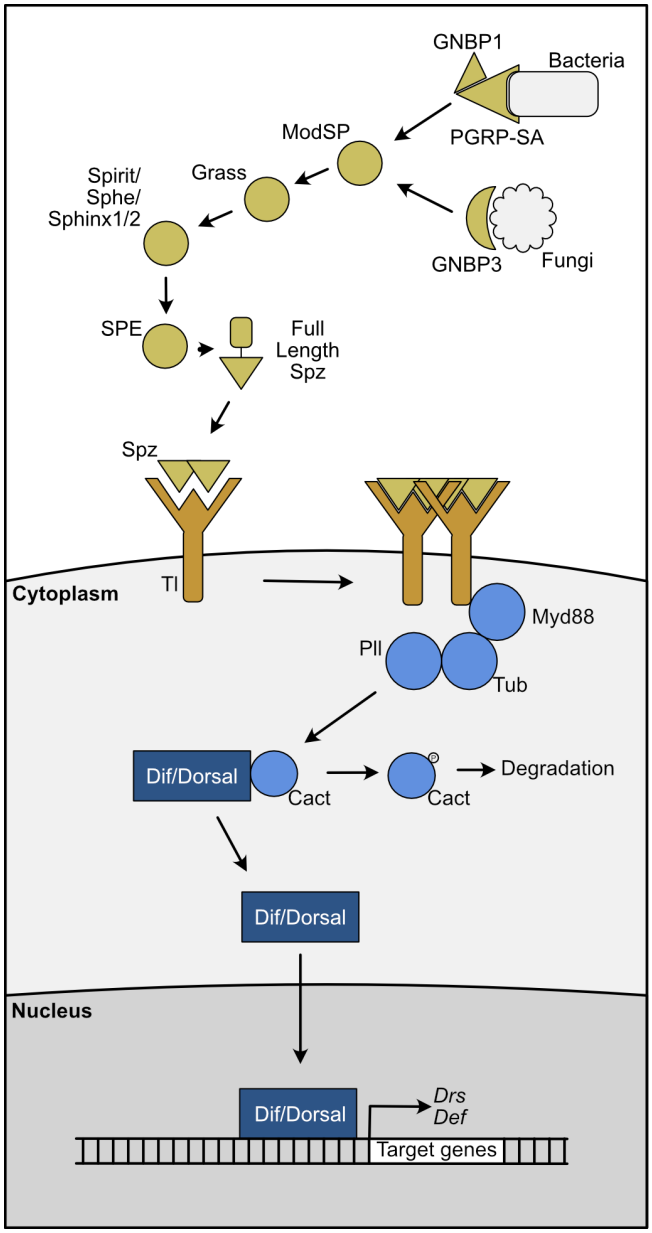

Figure 6: The *Drosophila* Toll Signaling Pathway: Extracellular components - Peptidoglycan Recognition Protein SA (PGRP-SA), Gram-negative Bacteria Binding Protein 1 (GNBP1), Gram-negative Bacteria Binding Protein 3 (GNBP3), Protease Cascade (ModSP, Grass, Sphinx1/2, Spirit, Spheroide), Spatzle Processing Enzyme (SPE) and Spatzle (Spz).
Transmembrane receptors - Toll (Tl).
Cytoplasmic proteins - Myd88, Tube (Tub), Pelle (Pll), Cactus (Cact).
Nuclear factors - Dorsal (Dl), and Dorsal related immunity factor (Dif).
Recognition of gram-positive bacteria by PGRP-SA/ GNBP1 and fungi by GNBP3 triggers signaling through a series of proteases: ModSP, Grass, Spirit/Sphe/ Sphinx1/2, and SPE. SPE processes full-length Spz into active Spz, which, as a dimer, binds to the Tl receptor. This leads to activation and dimerization of the Tl receptor at the plasma membrane, causing the recruitment and formation of the Myd88-Tub-Pll complex. Pll phosphorylates the inhibitor Cact resulting in its degradation and release of transcription factor Dif/ Dorsal. Dif/Dorsal then transcribes antimicrobial peptides such as *Drs*, and *Def* in the nucleus.

2.6.2 Toll signaling in stem cell homeostasis and tumorigenesis

The innate immune Toll and IMD pathways serve as a first line of defence in response to infection. Traditionally, these pathways have been characterized for their roles in pathogen recognition and immune response, but more recent studies have highlighted their involvement in regulating epithelial renewal. In the gut, IMD signaling regulates EC shedding in response to infection-induced damage, as well as tumorigenesis [113, 114]. However, the role of IMD signaling in stem cell proliferation has remained controversial, with some studies disproving its requirement [113], while others claim that it is necessary [115]. Although several studies have

tried to address the impact of IMD signaling in the fly midgut, the role of Toll signaling in midgut turnover remains largely unexplored.

Pioneering research on Toll signaling in larval hemocytes has revealed that Toll-active mutants develop melanotic tumors due to aberrant differentiation of hemocytes into lamellocytes [116]. Toll-7 is required for the proliferation of $Ras^{V12}/lgl^{-/-}$ tumors in the eye disc, and overexpression of Toll-7 is sufficient to promote tumorigenesis through JNK signaling [117]. Toll signaling also mediates cell competition in the wing disc. The Toll pathway ligand Spz induces Toll activation in loser cells, which is required for its elimination through the induction of pro-apoptotic genes such as Rpr and Hid [118, 119]. While Toll signaling is mainly associated with innate immune responses, its interaction with other signaling pathways, such as JNK signaling [120], and 4EBP/mTor signaling [121], makes it an interesting pathway to investigate in the context of midgut epithelial renewal.

2.7 Genetic tools used in *Drosophila melanogaster*

2.7.1 Binary expression systems: Gal4/UAS, LexA/LexAOP

The ability to manipulate gene expression with cellular and temporal control in complex tissues makes *Drosophila* a powerful and versatile model organism for genetic studies. This is largely attributed to the binary expression systems available in flies. The most commonly used binary system is the Gal4/UAS system, which was first discovered in yeast and later introduced into flies [122, 123]. In this system, the Gal4 transcription activator under the regulation of a tissue- or cell type-specific promoter, binds to the Upstream Activation Sequence (UAS) enhancer and transcribes genes downstream of it (eg knockdown, overexpression, or reporters). As a result, only those cells that contain both Gal4 and UAS sequences will express the construct controlled by UAS [123]. Gal80 is a regulatory protein that binds to Gal4 and represses its ability to transcribe UAS-tagged genes. The temperature-sensitive variant $Gal80^{ts}$ retains its repressive activity at 18°C, but loses its ability to bind to Gal4 and suppress its activity at 29°C [124]. Therefore, incubating flies at 29°C activates Gal4-dependent UAS gene expression, while incubating flies at 18°C prevents activation **(Figure 7A)**. In the *Drosophila* midgut progenitor cells, the *esg* promoter drives the expression of Gal4. In combination with the $Gal80^{ts}$ system and UAS-GFP expression, this generates a transgenic fly line that allows for temporally controlled expression of transgenes in midgut progenitor cells marked by GFP (hereafter

referred to as esg^{ts}).

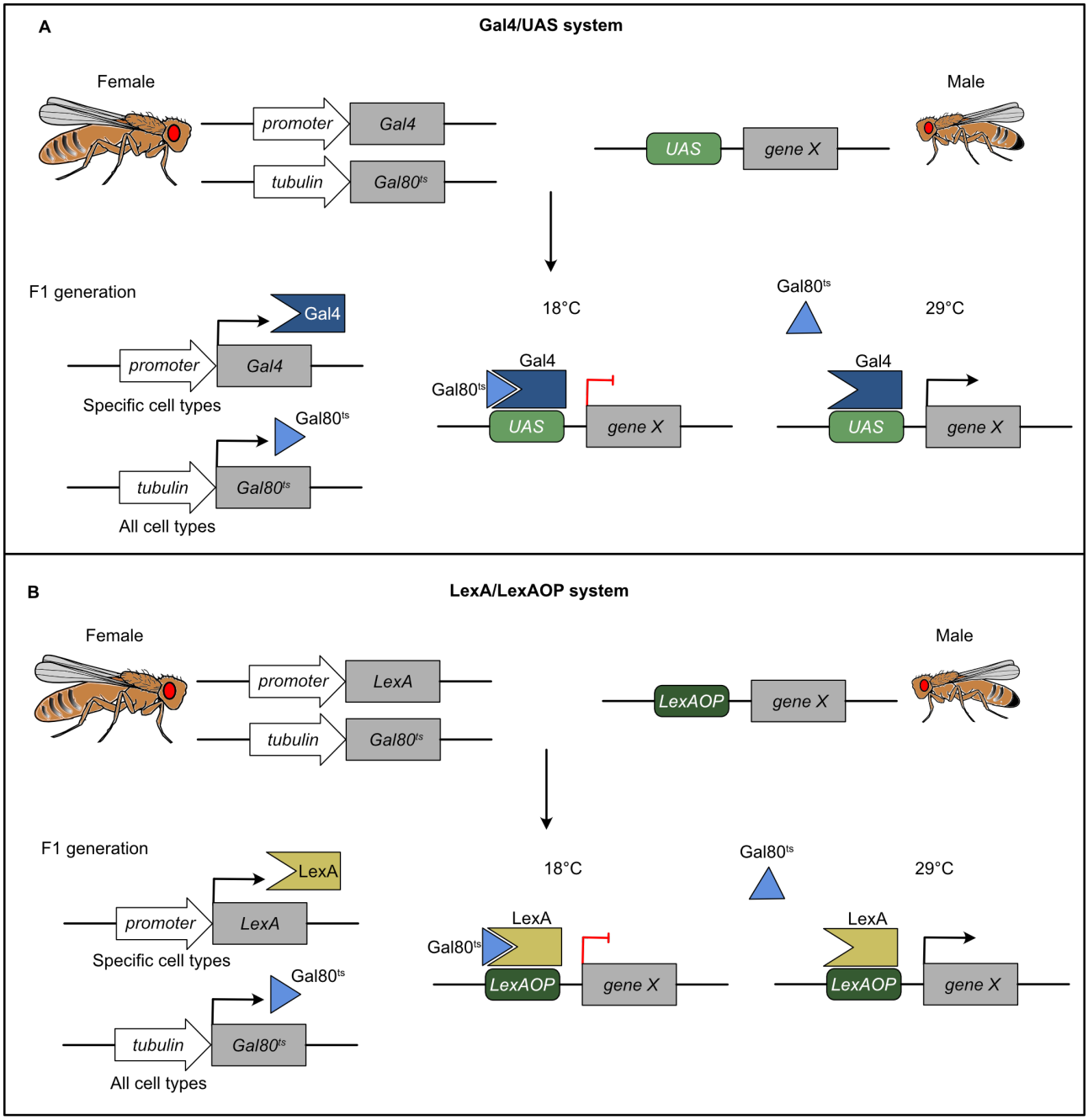

Figure 7: Binary system to regulate gene expression in *Drosophila melanogaster.*
(A) A schematic illustration of the Gal4/UAS binary expression system in Drosophila. Gal4 under the control of a specific cell-type promoter, binds to the UAS sequence and drives the transcription of the downstream gene of interest. Gal80^{ts} is expressed ubiquitously in the fly under the control of the *tubulin* promoter. At 18°C, Gal80^{ts} protein binds to Gal4 and suppressers its activity, preventing transcription of the downstream gene. However, at 29°C, Gal80^{ts} can no longer bind to Gal4, allowing Gal4-mediated transcription of the gene of interest downstream of it. **(B)** A schematic illustration of the LexA/LexAOP binary system. Similar to the Gal4/UAS system, LexA under the regulation of a cell-type specific promoter, binds to the LexAOP sequence and promotes the transcription of the downstream gene of interest. The activity of this system can also by regulated by the Gal80^{ts} system, as LexA is fused to the Gal4 activating domain (GAD).

Another binary system, LexA/LexAOP, operates on a principle similar to that of the Gal4/UAS system. The bacterial-derived DNA damage response repressor LexA, when expressed in specific cells using *Drosophila* enhancers, binds to the LexA operator-promoter (LexAOP) sequence and transcribes genes downstream of it. Temporal regulation of LexA activity was introduced by fusing it to the Gal4 activating domain (GAD), making it sensitive to $Gal80^{ts}$ [125] **(Figure 7B)**. Since the LexA/LexAOP and Gal4/UAS systems function independently to regulate gene expression, they can be used simultaneously to manipulate gene expression in two different cell populations.

2.7.2 Gene manipulation using RNAi and CRISPR/Cas9

Regulation of biological mechanisms relies on the orchestrated function of several genes, which can be studied by manipulating their activity. In flies, RNA interference (RNAi) has become a widely used tool to produce loss-of-function phenotypes, which have been employed to perform large-scale reverse genetic screens. RNAi-mediated gene silencing utilizes exogenous double-stranded RNA (dsRNA) to induce degradation of target mRNA transcripts, preventing translation and protein synthesis [126]. In flies, exogenous dsRNA associates with the ribonuclease III enzyme Dicer-2, which cleaves it into short 21 bp small interfering RNA (siRNA) fragments [127]. These siRNAs induce the formation of the RNA-induced silencer complex (RISC) complex, which unwinds the double-stranded fragments into single-stranded siRNAs, binds to complementary mRNA, induces its degradation, and silences gene expression [128, 129] **(Figure 8A)**. By incorporating the UAS sequence upstream of the dsRNA construct, genes can be knocked down in a cell-specific manner using the Gal4/UAS system.

Targeted mutagenesis of the genomic loci using the Clustered Regularly Interspersed Short Palindromic Repeats (CRISPR)—CRISPR-associated (Cas) system has become a very popular tool for functional genomics. Initially identified in bacteria as a mechanism of defence against viruses, CRISPR/Cas has been adapted for genome engineering applications in eukaryotes. The system comprises of two key components: Cas9 and guide-RNA (gRNA). Cas9 is a DNA endonuclease protein that induces double-stranded breaks (DSB) in DNA. It comprises of the recognition domain (REC), which binds to the guide-RNA, and the nuclease domain (NUC), which cuts the target DNA strand. The gRNA is made up of the CRISPR RNA (crRNA), which recognizes the target sequence, and the trans-activating CRISPR RNA, which helps Cas9 to

bind to the gRNA. In the host cell, Cas9 forms a complex with the programmed gRNA and confers an active state.

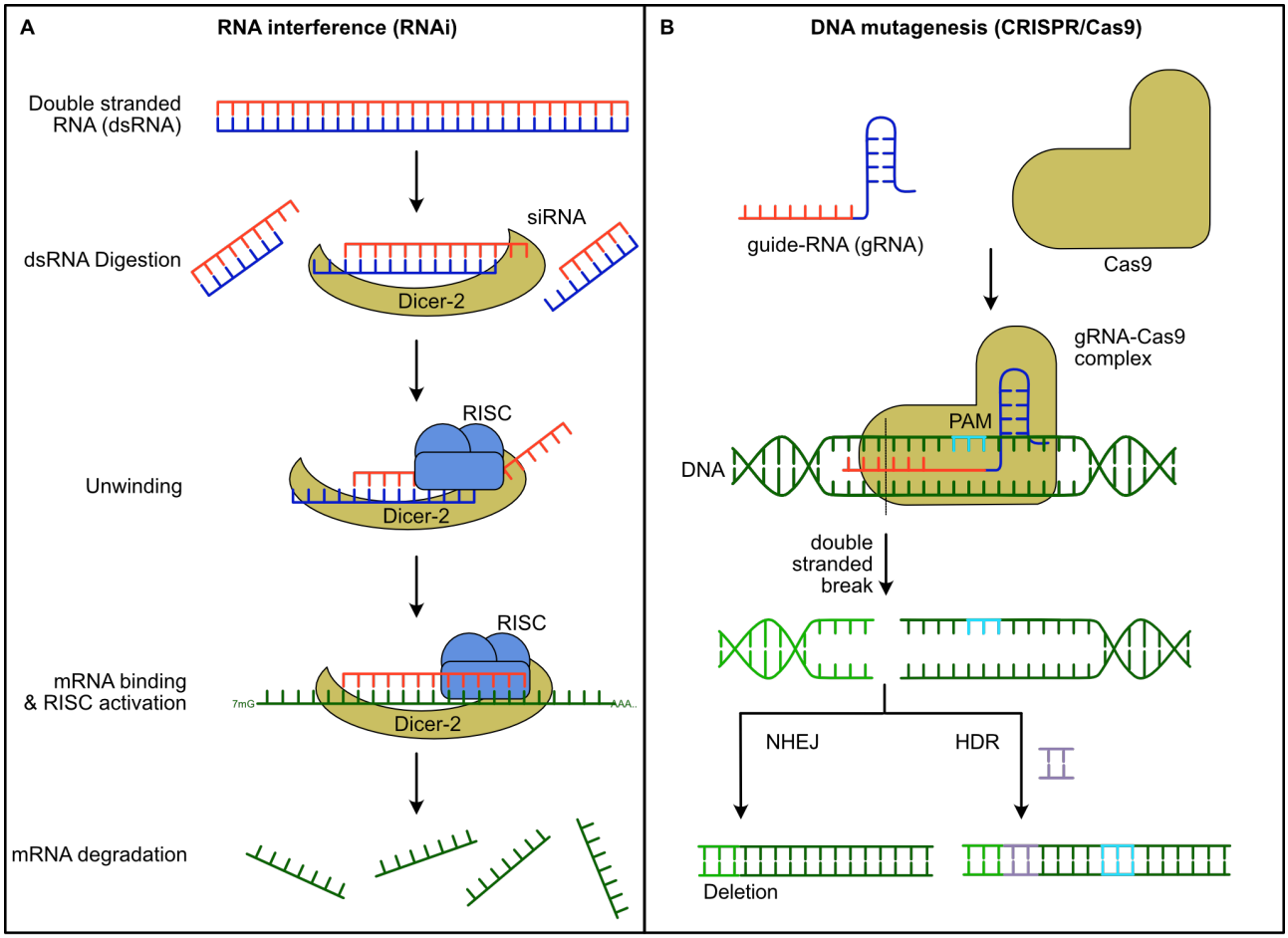

Figure 8: Tools *to* manipulate gene function in *Drosophila melanogaster.*
(A) A schematic representation of the mechanism of RNA interference (RNAi)-mediated gene silencing. Double-stranded RNA (dsRNA) containing a sequence complementary to the target mRNA of interest is introduced into the fly. Dicer-2 processes the dsRNA into short 21-nt siRNAs. These siRNAs, in association with the RNA-induced silencing complex (RISC), unwind and bind to the complementary mRNA, leading to its degradation.
(B) A schematic representation of Cas9-mediated DNA mutagenesis. The endonuclease Cas9 is directed to the target site by the guide-RNA. Here, Cas9 induces a double-stranded break three to four nucleotides upstream of the PAM sequence. This break is repaired by the host's DNA repair machinery through either Non-homologous end joining (NHEJ) or Homology-directed repair (HDR). NHEJ repairs the break by directly ligating the broken ends, often resulting in small indels at the cleavage site. In contrast, HDR uses a homologous DNA sequence to repair the break, restoring the original sequence.

The gRNA directs the Cas9 to the target site complementary to the crRNA sequence upstream of the Protospacer Adjacent Motif (PAM) sequence. Here, the NUC domain of Cas9 cuts double-stranded DNA, three nucleotides upstream of the PAM sequence to create a DSB. The cell repairs these DSBs via two major pathways: Non-homologous End Joining (NHEJ), which is error-prone and often results in insertions or deletions (indels) that can induce

frameshift mutations or premature stop codons, and Homology-Directed Repair (HDR), which is more accurate and often used for precise edits [130] **(Figure 8B)**. To increase the likelihood of gene knockout, multiplexed guides targeting the same gene has been developed in several organisms including the flies. Additionally, the Gal4/UAS binary system in flies has been employed to control Cas9 expression in a tissue-specific manner, enabling targeted mutagenesis [131, 132].

2.8 Aims and experimental goals of the thesis

The *Drosophila* midgut is under constant threat from external infections and toxins. To maintain midgut integrity, ISCs regenerate damaged cells through asymmetric division, replenishing both stem cells and differentiated cells. This process of division and differentiation is active throughout the life of the fly and is accelerated during a regenerative response. It is tightly regulated by signaling pathways such as Notch signaling, which promotes differentiation, Wnt and EGFR signaling, which regulate ISC proliferation, and JNK signaling, which activates regeneration in response to stress. These pathways interact with each other and several other genes to form a complex genetic network.

Oncogenic mutations or loss of tumor suppressors in the genetic network, drive rapid stem cell proliferation and abnormal differentiation, resulting in the formation of midgut tumors. Given the conservation of cellular architecture, function, and signaling pathways between the fly midgut and the human intestine, *Drosophila* serves as an excellent model for studying stem cell function and cancer. Additionally, the availability of a wide range of genetic tools for cell-specific gene manipulation makes flies a powerful *in-vivo* model for large-scale genetic screens and cancer mechanism research [133].

In my PhD project, I leverage the power of *Drosophila* genetics to model tumors in the midgut and malpighian tubules, aiming to identify novel genes that regulate stem cell function. The experimental plan is as follows:

1) **Generate Notch-loss-of-function midgut tumors:** Establish a protocol for generating CRISPR/Cas9-induced Notch loss-of-function tumors in the fly midgut.

2) **Single-cell RNA sequencing:** Perform single-cell RNA sequencing on midguts with Notch loss-of-function tumors to identify genetic changes associated with tumorigenesis.

3) ***In-vivo* genetic screen:** Conduct an *in-vivo* genetic screen of candidate genes to evaluate their role in Notch loss-of-function tumor formation.

4) **Stem cell function validation and mechanism:** Validate the role of positive hits in stem cell function using the Apc-Ras colorectal cancer fly model, infection-induced regenerative response, and during homeostasis.

Advanced single-cell sequencing techniques, combined with fly tumor models and large-scale genetic screening, provide a powerful approach to decode the complex genetic networks that regulate stem cell function. These findings can then be translated into higher model organisms, offering valuable insights into cancer biology and stem cell regulation.

3 Results

3.1 Identification of a novel regulator of stem cell function Nerfin-1 using the Notch loss-of-function tumor model

The *Drosophila melanogaster* midgut tumor model has commonly been used to understand intestinal stem cell dynamics and study the mechanisms regulating intestinal stem cell proliferation [133]. One such common midgut tumor model is the Notch loss-of-function tumor. Loss of the Notch receptor has previously been shown to cause a differentiation defect, leading to large tumorigenic clusters of rapidly dividing stem cells and the accumulation of secretory enteroendocrine cells [6]. This phenotype has been used to identify and study the role of genes in modulating tumorigenesis such as spi/EGFR signaling [35], and Upd/JAK-STAT signaling [134]. Given that novel gene regulators of stem cell proliferation and differentiation can be identified using the Notch loss-of-function midgut tumor, I decided to use this model in my study. In order to generate the Notch loss-of-function tumor model, I used the CRISPR/Cas9 system to knockout the *N* gene in the progenitor population of the midgut.

3.1.1 Generating intestinal tumors through conditional Cas9 expression

CRISPR/Cas9 has emerged as a powerful tool for performing targeted mutagenesis of genes at the genomic level and is commonly used in cancer biology to study functional genomics [135, 136]. In flies, controlled Cas9 expression in a tissue-specific manner has been achieved by combining the binary Gal4/UAS system with Cas9 expression [131, 132]. The first generated construct *UAS Cas9.P1* was toxic to cells because it expressed a large quantity of Cas9 proteins [131]. In order to reduce toxicity, another construct, *UAS Cas9.P2*, was generated, which expresses lower amounts of Cas9 as compared to *UAS Cas9.P1* and, together with multiplexed guide-RNA, is sufficient to induce targeted genetic mutations [132, 137].

In order to investigate if I could use the CRISPR/Cas9 system to perform conditional mutagenesis in the midgut, I first decided to express *UAS Cas9.P2* in progenitor cells using the *esg-Gal4, UAS GFP, tub-Gal80^{ts}* system hereafter referred to as *esg^{ts}*. To do this, I crossed virgin female flies carrying the *esg^{ts}* driver with male flies carrying the *UAS Cas9.P2* transgene. I collected adult progeny containing both transgenes and aged them for one week at 29°C

before dissection.

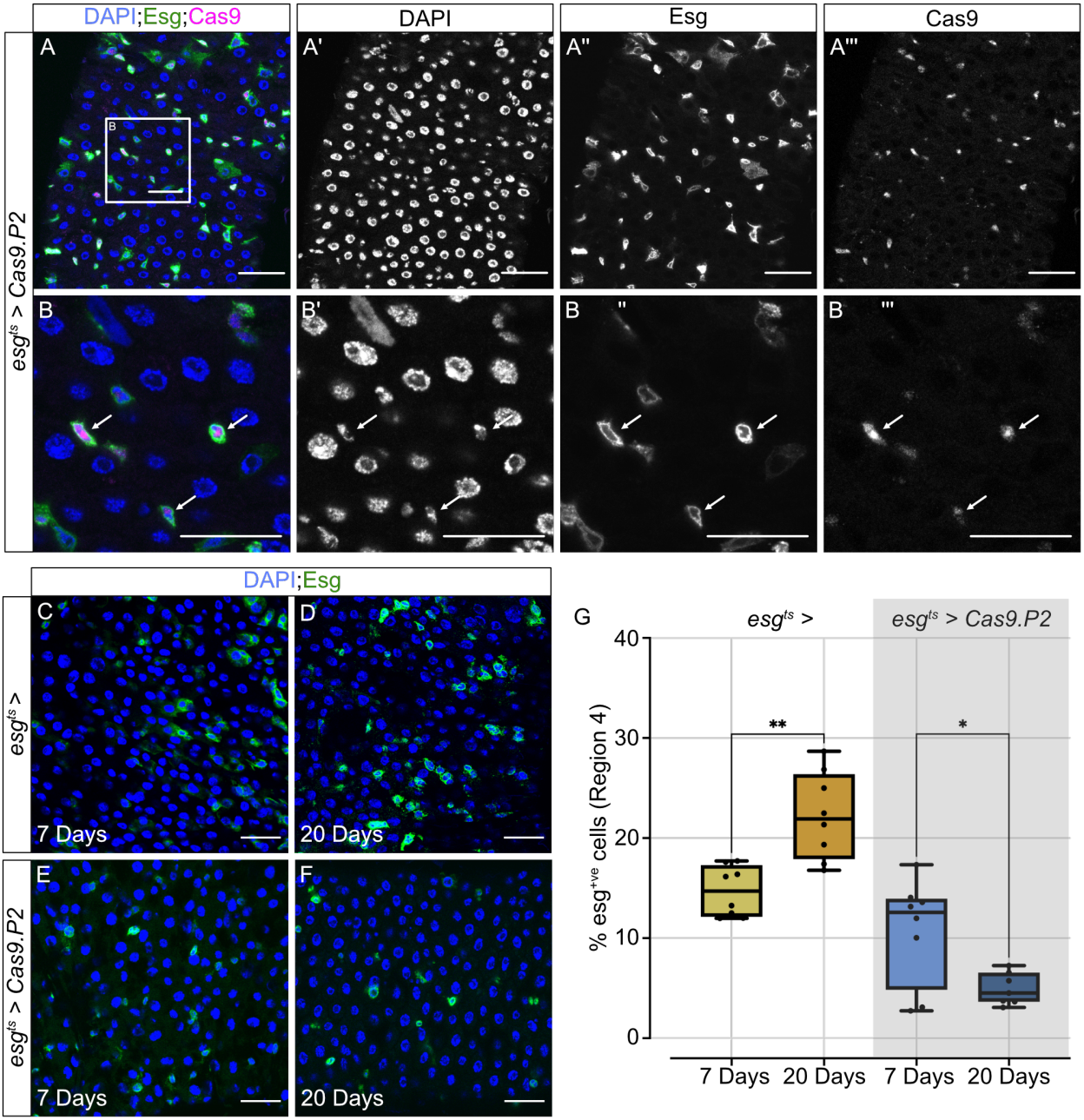

Figure 9 : Continuous Cas9 expression is deleterious to midgut progenitor cells. (A-B) Representative images of the posterior midgut of *esg^{ts} > Cas9.P2* flies stained with anti-Cas9 antibody. White arrows indicate esg-expressing progenitor cells that show Cas9 staining. **(C-D)** Representative images of the posterior midgut of 7-day-old **(C)** and 20-day-old **(D)** *esg^{ts} >* adult flies, and 7-day-old **(E)** and 20-day-old **(F)** *esg^{ts} > Cas9.P2* adult flies. **(G)** Quantification of the images shown in (C-F) and plotted as percentage GFP-positive ISC/EB cells in the posterior midgut (Region 4). The data shows an age-dependent increase in progenitor cells in *esg^{ts} >* flies, whereas a decrease in *esg^{ts} > Cas9.P2* flies is due to the toxic effect of Cas9. N = 7-8 flies; Significance values are marked by asterisks: *$P \leq 0.05$*, **$P < 0.01$*; Ordinary one-way ANOVA; Scale bar = 30μm **(A,C,D,E,F)**, 90μm in **(B)**.

Through antibody staining for Cas9 in the dissected midguts, I observed that Cas9 was

present only in Esg-positive cells, indicating that Cas9 is specifically expressed in progenitor cells **(Figure 9A,B)**. Therefore I confirmed that the *esg^{ts}* system can be used to drive the expression of Cas9 specifically in progenitor cells in the midgut.

High levels of Cas9 expression using the *UAS Cas9.P2* construct in wing disc was previously shown to be deleterious to cells [137]. To test whether Cas9 expression using the *UAS Cas9.P2* construct was also deleterious to progenitor cells in the midgut, I examined its effect on age-dependent intestinal stem cell proliferation. A previous study on aging in the fly midgut showed that older flies exhibit an increased number of progenitor cells as compared to younger flies [93]. I observed a similar phenotype, where I noticed that 20-day-old adult control *esg^{ts}* flies showed an increased number of Esg-positive progenitor cells in the midgut as compared to 7-day-old *esg^{ts}* control flies **(Figure 9C,D)**. Quantification of the percentage of Esg-positive progenitor cells also showed a consistent and significant age-dependent increase in progenitors in *esg^{ts}* flies **(Figure 9G)**. I then overexpressed Cas9 using the *UAS Cas9.P2* construct in progenitor cells for 7 days and 20 days. In contrast to control *esg^{ts}* flies, overexpression of Cas9 for 20 days resulted in a reduction of progenitors as compared to young 7-day-old Cas9 expressing flies **(Figure 9E,F)**. Quantification of the percentage of Esg-positive progenitor cells also showed a significant decline in the number of progenitors in flies overexpressing Cas9 using the *UAS Cas9.P2* construct **(Figure 9G)**. I, therefore, concluded that high levels of Cas9 protein expression using the *UAS Cas9.P2* construct is toxic to progenitor cells, even in the absence of a guide-RNA.

While high levels of Cas9 expression are deleterious to cells, only a small amount is sufficient to achieve an editing outcome [137]. Therefore, I decided to reduce toxicity by limiting Cas9 expression in progenitor cells using the *Gal80^{ts}* system. My experimental strategy referred to as the *Cas9.P2$^{ON/OFF}$* condition involves turning on the *esg^{ts}*-driven *UAS Cas9.P2* expression at 29°C for 10 days, followed by turning off the system at 18°C for 30 days, and turning on the system one final day to drive GFP expression for imagining progenitor cells. To first establish this system, I compared the *Cas9.P2$^{ON/OFF}$* condition to the *Cas9.P2^{ON}* condition, in which Cas9 expression was turned on continuously for 20 days **(Figure 10A)**. I implemented these experimental conditions in flies which have one copy of *esg^{ts}-driven UAS Cas9.P2* and one copy of guide-RNA against different genes known to regulate stem cell proliferation: *hep* (JNK signaling), *Mad* (BMP signaling), *neur* and *N* (Notch signaling).

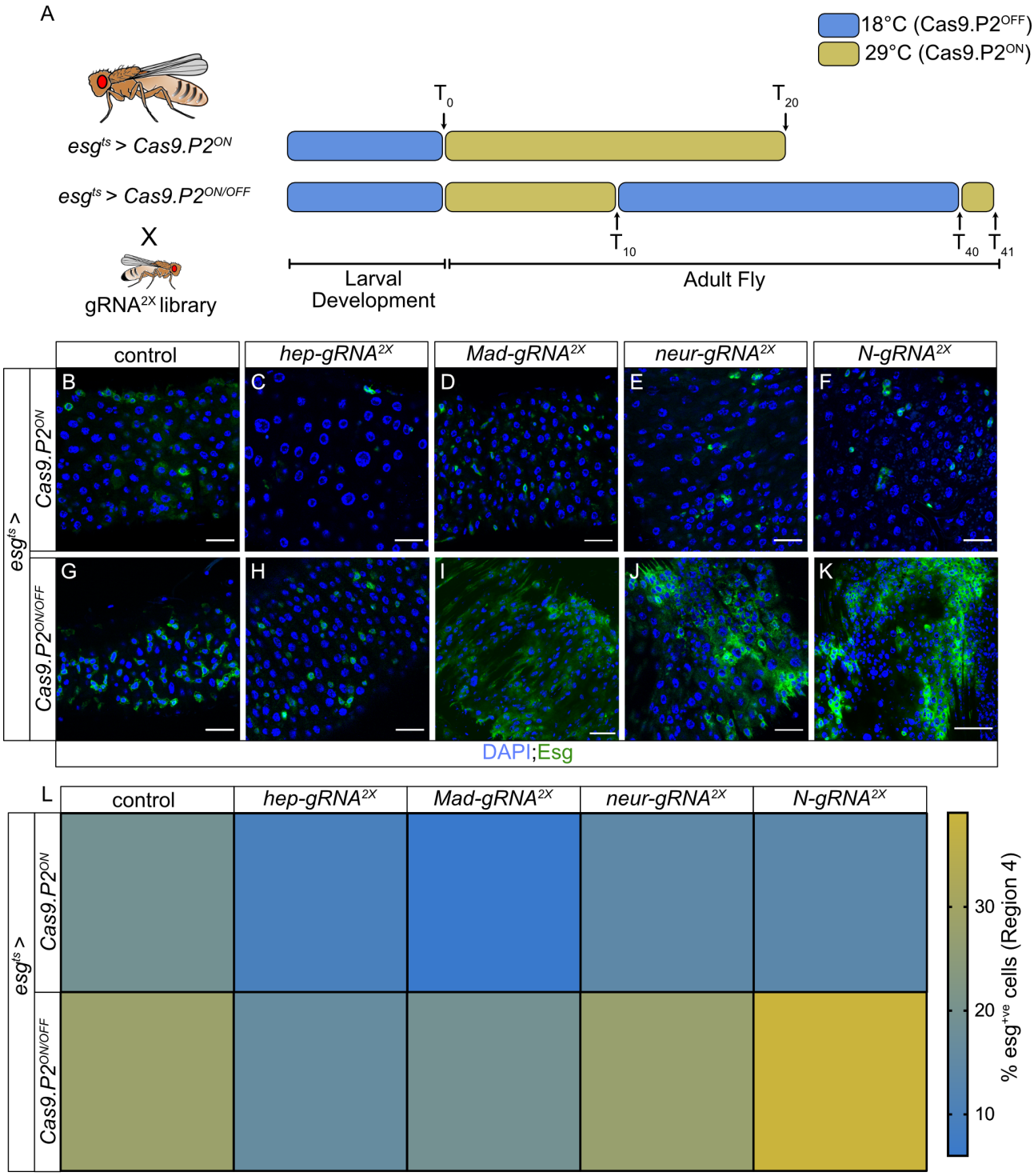

Figure 10 : Conditional expression of Cas9 is effective in inducing tumorigenic mutations in the midgut. **(A)** Experimental design to continuously (Cas9.P2^{ON}) or temporally (Cas9.P2$^{ON/OFF}$) express Cas9 in progenitor cells, along with guides targeting genes that regulate stem cell proliferation. **(B-F)** Representative images of the posterior midgut of *esg^{ts} > Cas9.P2^{ON}* driven control (*w^{1118}*) **(B)**, *hep-gRNA^{2X}* **(C)**, *Mad-gRNA^{2X}* **(D)**, *neur-gRNA^{2X}* **(E)**, and *N-gRNA^{2X}* flies **(F)**. **(G-K)** Representative images of the posterior midgut of *esg^{ts} > Cas9.P2$^{ON/OFF}$* driven control (*w^{1118}*) **(G)**, *hep-gRNA^{2X}* **(H)**, *Mad-gRNA^{2X}* **(I)**, *neur-gRNA^{2X}* **(J)**, and *N-gRNA^{2X}* flies **(K)**. **(L)** Heatmap indicating the percentage esg-positive progenitor cells in the posterior region (Region 4) of the adult midgut for both ON and ON/OFF regimen of the mentioned genotypes. N = 10-22 flies . Note that guides driven by *esg^{ts} > Cas9.P2^{ON}* do not lead to a stem cell phenotype, whereas guides driven by *esg^{ts} > Cas9.P2$^{ON/OFF}$* cause a phenotype. Scale bar = 30μm.

Loss of *hep* (JNK signaling) is known to reduce the number of progenitors [11], while loss of *Mad* (BMP signaling), *neur*, and *N* (Notch signaling) causes stem cell overproliferation [6, 138]. I found that continuous expression of Cas9 in the *Cas9.P2^{ON}* strategy resulted in a slight reduction in stem cell numbers across all perturbations **(Figure 10B-F)**. Quantification of the percentage of Esg-positive progenitor cells in the posterior region of the midgut also indicated a reduction in progenitors due to prolonged Cas9 expression, which is toxic to these cells **(Figure 10L)**. However, by restricting Cas9 expression through the *Cas9.P2$^{ON/OFF}$* strategy, I observed a decrease in progenitor cells following *hep* knockout and an increase in progenitor cells following *Mad*, *neur*, and *N* knockout in the adult midgut as compared to control **(Figure 10G-L)**. This suggests that restriction of Cas9 expression through temporal regulation can be used to introduce mutations that result in a midgut phenotype.

Altogether, I showed that continuous expression of Cas9 using the *Cas9.P2^{ON}* condition prevents the development of known stem cell phenotypes potentially due to the toxic effects of high Cas9 protein levels. However, by temporally regulating Cas9 expression through the *Cas9.P2$^{ON/OFF}$* system, I was able to mitigate its toxic effects on progenitor cells. I used this system to create a Notch loss-of-function midgut tumor model and identify its transcriptomic landscape in subsequent sections. This work, along with additional research on establishing the protocol to generate midgut tumors using CRISPR/Cas9, has been published in the Cells journal [139].

3.1.2 Notch loss-of-function midgut tumors have increased ISC and EE cells.

In the fly midgut, Notch signaling is essential for determining progenitor cell fate. High Notch signaling promotes EC differentiation, while low Notch signaling primes progenitors for EE differentiation [6]. Knockdown or expression of a mutant form of the Notch receptor in the midgut results in a differentiation defect, leading to an accumulation of rapidly dividing ISCs and secretory EEs [6]. To validate this phenotype, I first knocked down the Notch receptor in the midgut progenitor population using the *esg^{ts}* driver. I observed that knockdown of *N* (hereafter referred to as *N^{RNAi}*) in progenitor cells for 20 days resulted in a significant increase in both Esg-positive progenitor cells and Pros-positive EE cells **(Figure 11A,B)**. Moreover, this phenotype was also accompanied by a significant increase in mitosis, which I observed by staining the midgut for the mitotic marker phospho-Histone H3 (pH3) **(Figure 11E)**. I then tested

whether a similar phenotype could be observed upon Cas9-induced mutation of the *N* gene. To do this, I used the *Cas9.P2*$^{ON/OFF}$ system to express Cas9 in the progenitor population and target the *N* gene using the multiplexed guide RNA construct *N-gRNA*^{2X} in the midgut.

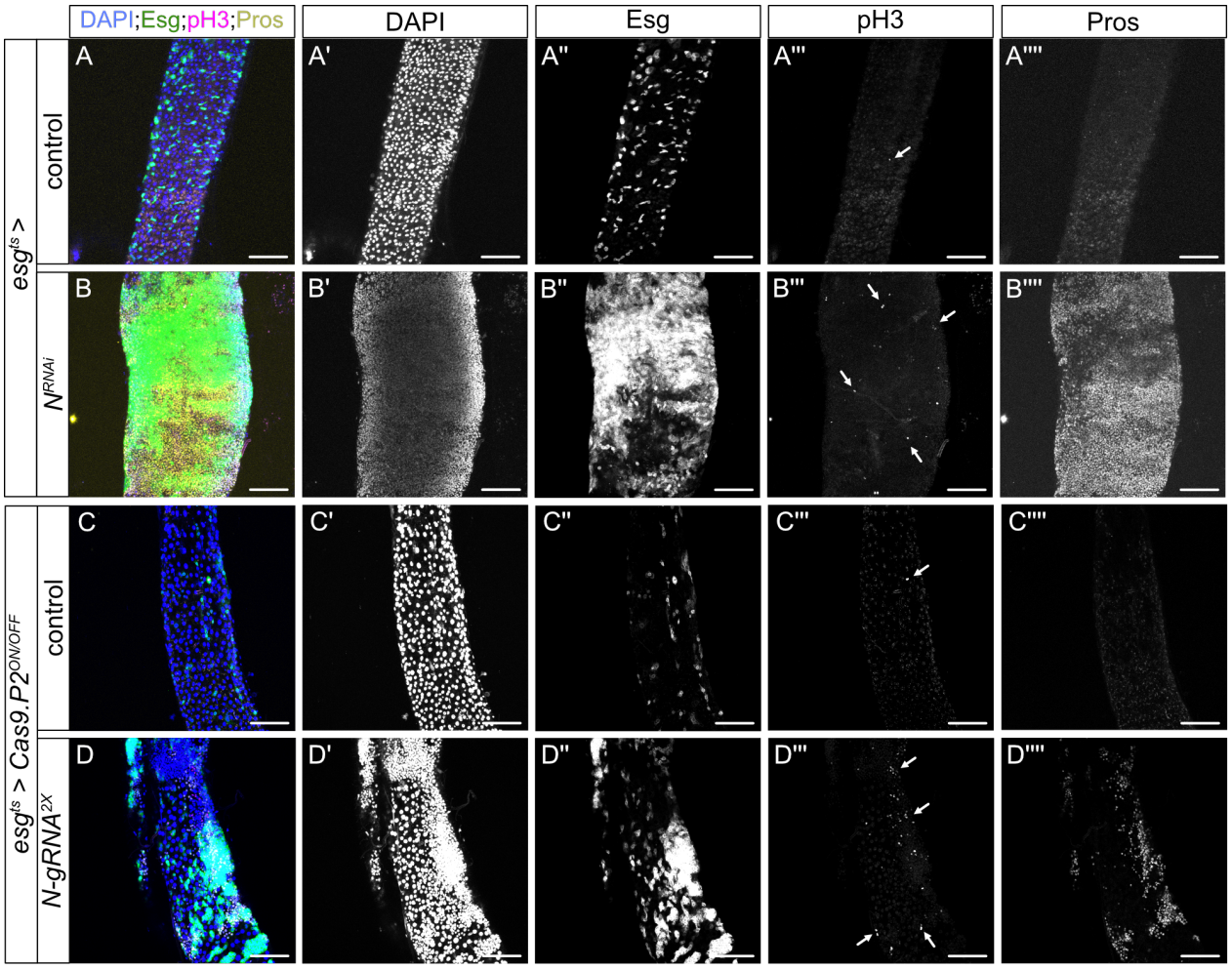

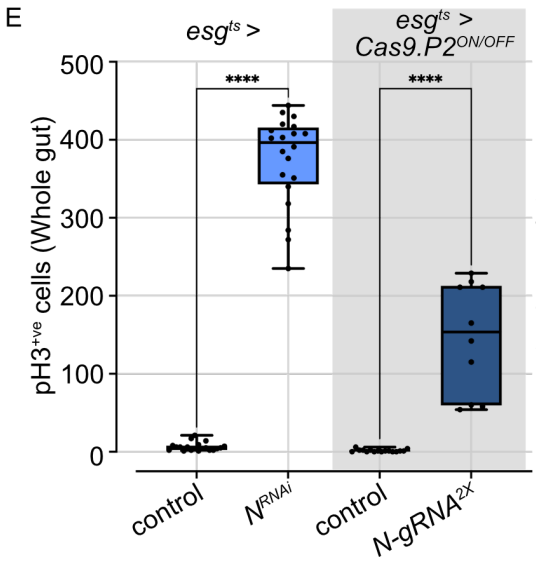

Figure 11 : Cas9-induced Notch mutation phenocopies knockdown-induced Notch midgut tumor phenotype. (A-D) Representative images of the posterior midgut of *esg*^{ts} > driven control (*w*^{1118}) **(A)** and *N*^{RNAi} **(B),** and *esg*^{ts} > *Cas9.P2*$^{ON/OFF}$ driven control (*sepia-gRNA*^{2X} or *w*^{1118}) **(C)** and *N-gRNA*^{2X} **(D)** flies stained with anti-pH3 (mitosis) and anti-Pros (EE cell) antibodies. White arrows indicate pH3-positive mitotic cells in the midgut. **(E)** Quantification of pH3-positive cells per midgut of the mentioned genotypes indicate that loss of the Notch receptor causes a significant increase in stem cell over-proliferation. N = 10-20 flies; Significance values are marked by asterisks: *****P < 0.0001*; Ordinary one-way ANOVA; Scale bar = 80*μ*m.

I noticed that similar to the knockdown phenotype, Cas9-induced Notch loss-of-function mutation also resulted in the accumulation of dividing progenitor cells and EE cells **(Figure 11C,D)**. Additionally, I saw an increase in the number of mitotic cells upon Cas9-induced *N* mutation in the midgut as compared to the control **(Figure 11E)**. In conclusion, I showed that similar to RNAi-mediated knockdown, introducing mutations in the *N* gene using Cas9-induced mutagenesis also results in a tumor phenotype characterized by increased stem cell mitosis and a high number of progenitor cells and EE cells.

After establishing the *Cas9.P2*$^{ON/OFF}$-driven Notch loss-of-function tumor model in the midgut, I wanted to identify regulatory genes involved in tumor formation. Transcriptomic studies using bulk RNA sequencing have been widely used to understand the functional characteristics of genes at the tissue level. However, recent advances in single-cell RNA sequencing (scRNA seq) technologies have enabled researchers to study genetic functions at a cellular level [140]. Since the *Drosophila* midgut comprises of multiple cell types, each with its unique genetic expression profiles, Together with Siamak Redhai from the Boutros lab (DKFZ, Heidelberg), I decided to perform scRNA seq on midguts carrying Cas9-induced Notch loss-of-function tumors to look at transcriptomic changes specifically in progenitor cells by comparing them to control midguts. I dissected midguts from *esg*^{ts}*;UAS Cas9.P2*$^{ON/OFF}$-driven control (*w*^{1118}) and *N-gRNA*^{2X} flies and subjected them to scRNA seq using the 10x Genomics platform. In collaboration with Nick Hirschmueller from the Huber lab (EMBL, Heidelberg), I analyzed the transcriptome of 13,453 cells from control (*w*^{1118}) **(Figure 12A)** and 16,289 cells from *N-gRNA*^{2X} midguts **(Figure 12B)**. Different cell types were identified in both genotypes using unique marker gene expression, such as *Delta* for ISCs, *esg*, *kay*, and *E(spl)mbeta-HLH* for EBs, and *pros* for EEs [141, 142].

First, I investigated changes in the cell type abundance upon Cas9-induced Notch loss-of-function mutation as compared to control midguts. Upon comparison, I noticed a significant increase in ISCs, EEPs, and EEs following *N* knockout **(Supplementary Figure S1A-C)**. The number of ECs was lower as compared to the control, while the number of EBs significantly declined in *N* knockout midguts **(Supplementary Figure S1D-E)**. This data aligns with my previous experimental results showing that Notch loss-of-function mutation results in a differentiation defect characterized by an increase in proliferative ISCs and EEs in the adult midgut **(Figure 11D)**.

Since I successfully captured cell composition changes upon introducing Cas9-induced Notch loss-of-function mutations in the midgut, I next looked at transcriptomic changes driving increased progenitor numbers in the *N* knockout midguts. Together with the help of Nick Hirschmueller from the Huber lab (EMBL, Heidelberg), I performed differential gene expression analysis on the progenitor population (ISC/EB/EEP) between *N-gRNA*^{2X} vs control and identified several differentially expressed genes, as shown in the volcano plot **(Figure 12C)**.

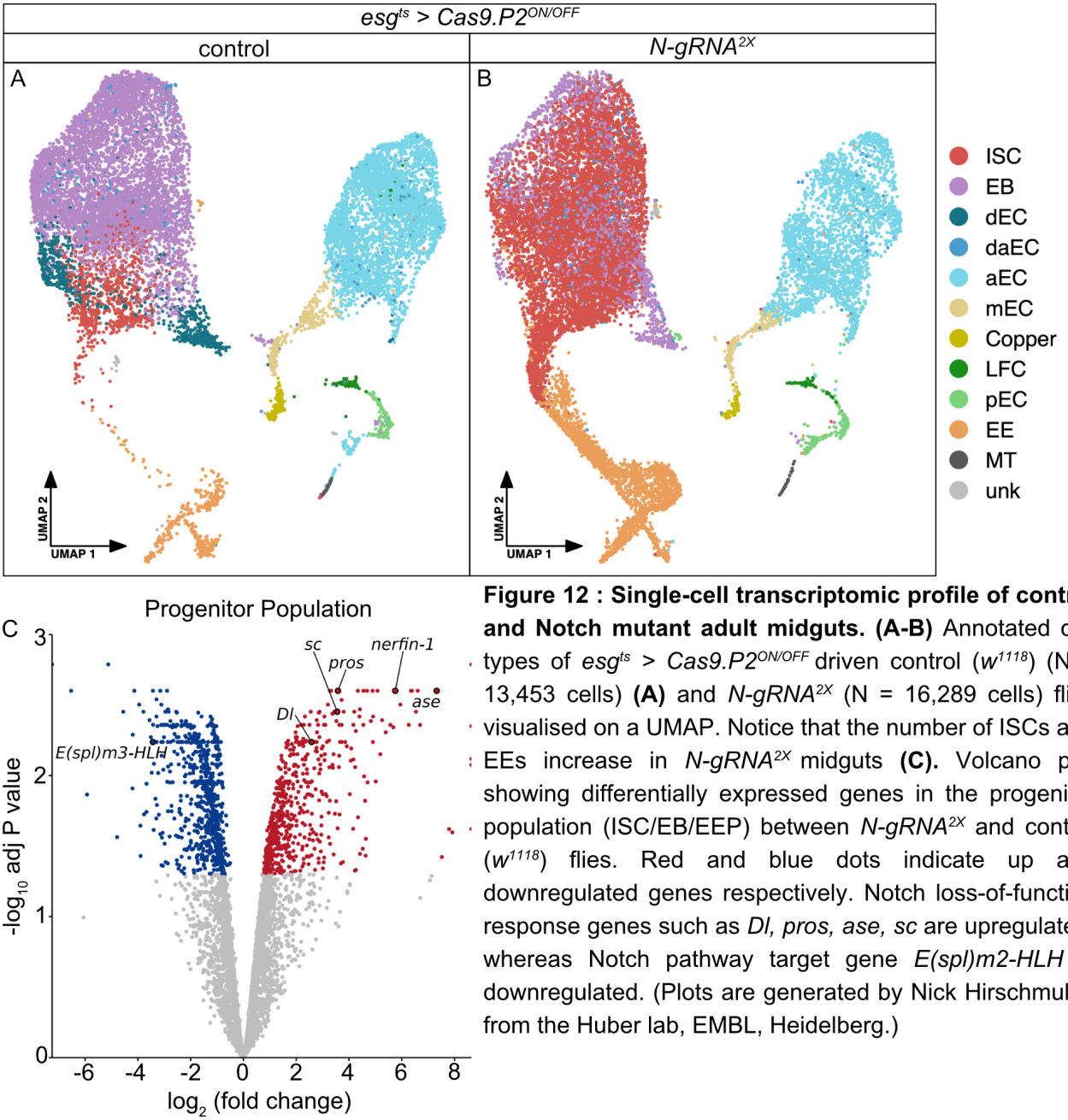

Figure 12 : Single-cell transcriptomic profile of control and Notch mutant adult midguts. (A-B) Annotated cell types of *esg*^{ts} > *Cas9.P2*$^{ON/OFF}$ driven control (*w*^{1118}) (N = 13,453 cells) **(A)** and *N-gRNA*^{2X} (N = 16,289 cells) flies visualised on a UMAP. Notice that the number of ISCs and EEs increase in *N-gRNA*^{2X} midguts **(C).** Volcano plot showing differentially expressed genes in the progenitor population (ISC/EB/EEP) between *N-gRNA*^{2X} and control (*w*^{1118}) flies. Red and blue dots indicate up and downregulated genes respectively. Notch loss-of-function response genes such as *Dl, pros, ase, sc* are upregulated, whereas Notch pathway target gene *E(spl)m2-HLH* is downregulated. (Plots are generated by Nick Hirschmuller from the Huber lab, EMBL, Heidelberg.)

Upon careful analysis of the list of differentially expressed genes, I found that the Notch pathway target genes *E(spl)m3-HLH*, *E(spl)malpha-BFM*, *E(spl)m6-BFM*, and *E(spl)mgamma-HLH* were

downregulated, whereas *Delta*, *sc*, *ase*, and *pros* were upregulated in the progenitor population of *N* knockout midguts as compared to control **(Figure 12C)**. This finding is consistent with previous literature, suggesting that the dataset successfully captured genes known to be affected by the loss of Notch signaling [33, 34, 143].

3.1.3 Nerfin-1 is required for the Notch loss-of-function midgut tumor formation.

To identify novel genes involved in mediating Notch loss-of-function tumor formation in the midgut, I decided to perform a genetic screen. I focused on the upregulated genes from the scRNA seq dataset of the progenitor population of *N-gRNA*^{2X} versus control midguts. I created a stable fly line, which consisted of both *esg*^{ts} and *N*^{RNAi} transgenes. For the genetic screen, I used the knockdown of *N* instead of Cas9-induced *N* mutation for two reasons: 1) the ease of creating a stable fly line with RNAi, and 2) the similar but stronger effect of *N*^{RNAi} as compared to Cas9-induced *N* mutation. In this stable line, activation of the Gal4/UAS system at 29°C, resulted in the development of tumors as a result of the knockdown of *N*. This stable fly can be crossed with any UAS-driven gene knockdown fly line to screen for genes that reduce Notch loss-of-function-induced tumors. As observed previously in **Figure 11E**, knockdown of *N* increased pH3-positive mitotic cells in the midgut **(Figure 13, Yellow bar)**. I, therefore, decided to use this increased mitosis phenotype as the readout for the screen by staining and quantifying pH3-positive cells in the midgut. Any genes whose knockdown led to a reduction of pH3-positive cells in the *N*^{RNAi} midgut background were selected as a positive hit.

Out of the 39 genes that I screened, knockdown of 28 genes resulted in a statistically significant reduction in *N*^{RNAi}-mediated mitosis **(Figure 13, Blue bars)**. One of the genes, Scute, served as a positive control for this screen. Scute is a transcription factor that is negatively regulated by Notch signaling. It is required for stem cell mitosis and EE fate specification in the midgut [33]. I observed that *scute* (*sc*) was upregulated in the progenitor population of Notch loss-of-function tumors in the scRNA seq dataset **(Figure 12C)**. Knockdown of *sc* suppressed both progenitor and EE cell numbers **(Supplementary Figure S2A,B)** as well as pH3-positive mitotic cells **(Figure 13, Purple bar)** in *N*^{RNAi} flies. Apart from *sc*, *spdo*, *insb*, and *nerfin-1* were other known regulators of Notch signaling pathway whose knockdown significantly rescued *N*^{RNAi} tumors. Among these genes, loss of *nerfin-1* resulted in the strongest rescue of mitosis in Notch loss-of-function tumors **(Figure 13, Green bar)**. I, therefore, chose to study the role of Nerfin-1 in mediating stem cell

function in the fly midgut.

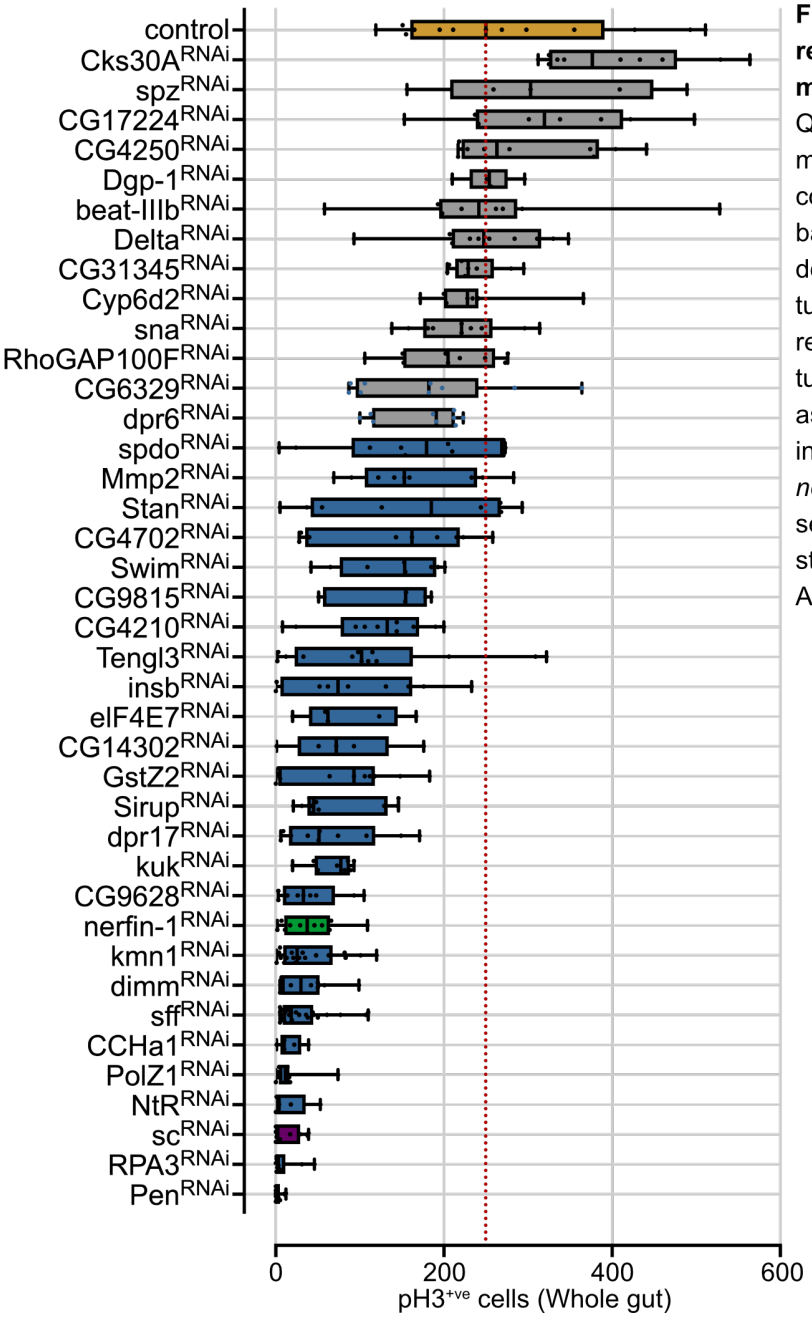

Figure 13 : Genetic screen to identify regulators of the Notch loss-of-function midgut tumor phenotype.
Quantification of pH3-positive cells in the midgut of the mentioned genotypes compared to *esg^{ts} > N^{RNAi}* (yellow bar). Grey bars represent genes whose knockdown does not affect the Notch loss-of-function tumor phenotype, while blue bars represent genes that significantly rescue tumor phenotype. Knockdown of *sc* serves as a positive control of the screen and is indicated by a purple bar. Knockdown of *nerfin-1* is indicated by a green bar and is selected as the candidate gene for further study. N = 5-24 flies; Ordinary one-way ANOVA.

Nervous fingers-1 (Nerfin-1) is a zinc finger transcription factor primarily expressed in the medullary neurons of the larval central nervous system (CNS) and is essential for maintaining their differentiated state. Loss of *nerfin-1* results in the de-differentiation of these neurons back into dividing neuroblasts (NB), a phenotype also observed upon activation of Notch signaling [144]. Loss of Nerfin-1 in neurons induces the upregulation of Notch pathway genes such as *N*, *Delta*, and *Su(H)*. Epistatic experiments showed that the de-differentiation defect in Nerfin-1

mutants can be reversed by inhibiting Notch signaling, indicating that Nerfin-1 negatively regulates Notch signaling and maintains the differentiated state of neurons [145]. While it is still unclear whether Notch signaling also regulates Nerfin-1 downstream of it, a negative epistatic relationship makes it an interesting gene to study in the midgut.

In our scRNA seq dataset, *nerfin-1* was upregulated in the progenitor population of *N-gRNA^{2X}* as compared to control **(Figure 12C)**. I confirmed this increased expression of *nerfin-1* in *N^{RNAi}* midguts through RT-qPCR **(Supplementary Figure S3B)**. Next, I asked if Nerfin-1 was required for the Notch loss-of-function-induced stem cell overproliferation and EE differentiation. I knocked down *nerfin-1* using two independent RNAis in the progenitor population of *N^{RNAi}* flies, and stained them with antibodies against pH3 and Pros to mark mitotic cells and EEs respectively. I found that loss of *nerfin-1* significantly reduced Esg-positive progenitor cells, Pros-positive EEs **(Figure 14A-D)**, and pH3-positive stem cell mitosis in *N^{RNAi}* midguts back to control levels **(Figure 14E)**. This indicated that *nerfin-1* is required for promoting stem cell proliferation and EE differentiation following loss of Notch signaling.

The accelerated proliferation of the stem cells due to inhibition of Notch signaling in the midgut negatively affects the overall lifespan of the fly [35]. I confirmed that *N^{RNAi}* in the midgut resulted in a reduction in the lifespan as compared to control flies **(Figure 15, red curve)**. This is primarily due to accelerated stem cell proliferation and tumor formation. Reduction of Notch loss-of-function mediated tumor formation through *nerfin-1* knockdown using two independent RNAis restored the lifespan of the flies to the control levels **(Figure 15, green and blue curves)**. This indicates that loss of Nerfin-1 restricts *N^{RNAi}* mediated tumorigenesis and thereby prevents the shortening of the lifespan.

In summary, I conclude that Notch signaling negatively regulates *nerfin-1* levels in the midgut, thereby keeping stem cell proliferation and differentiation in check. However in the absence of Notch signaling, *nerfin-1* is upregulated, which mediates stem cell overproliferation, EE accumulation, and reduces the fly lifespan.

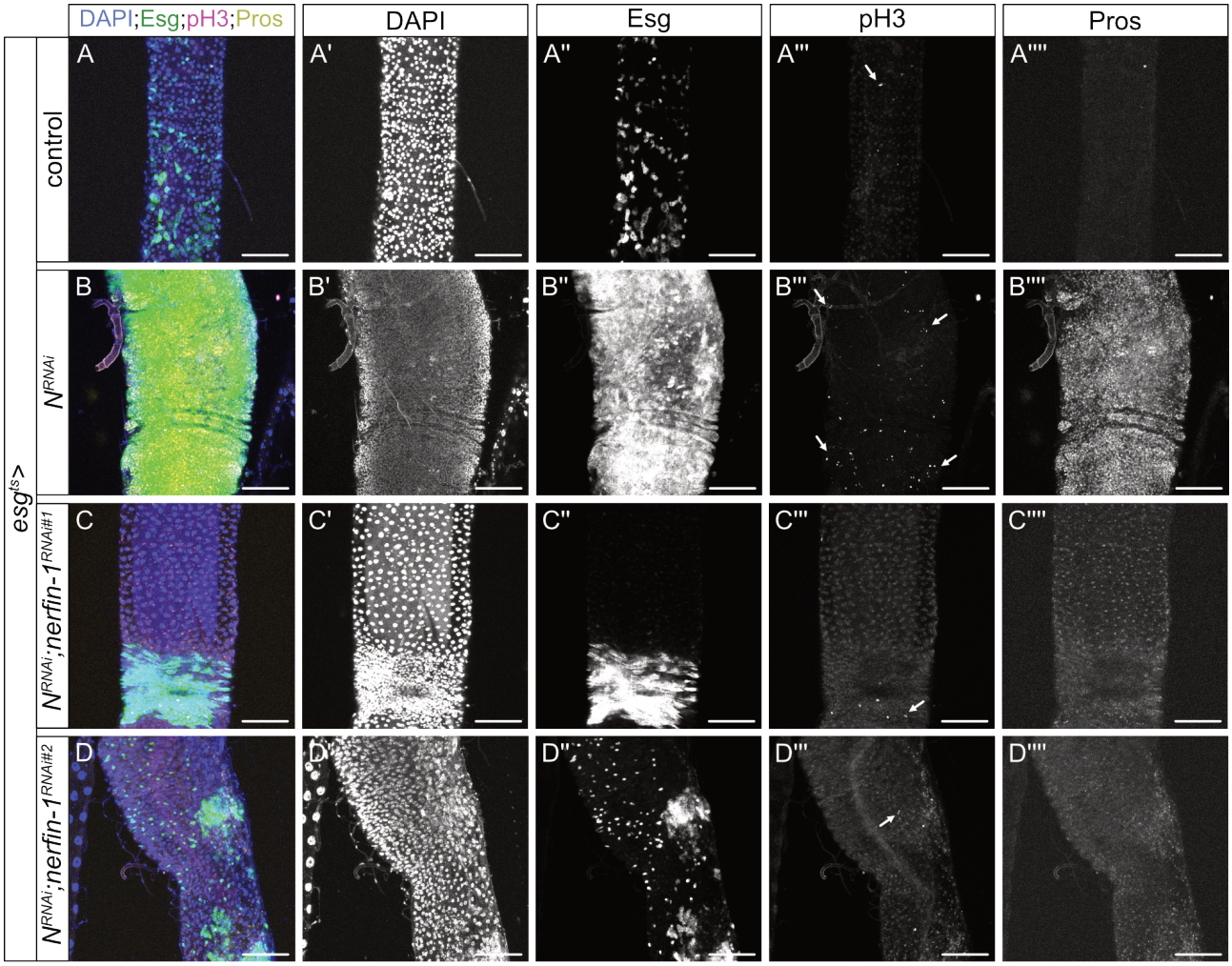

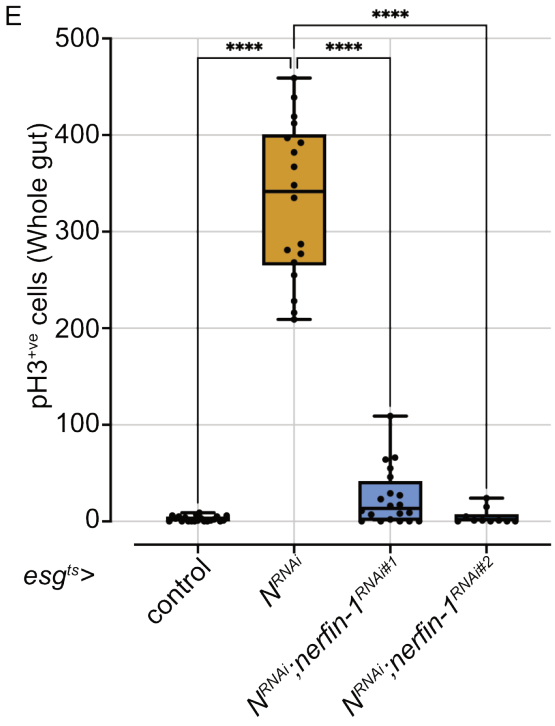

Figure 14 : Nerfin-1 is required for the Notch loss-of-function midgut tumor phenotype. (A-D) Representative images of the posterior midgut of *esg*^{ts} > driven control (*w*^{1118}) **(A)**, *N*^{RNAi} **(B)** *N*^{RNAi};*nerfin-1*$^{RNAi\#1}$ **(C)**, and *N*^{RNAi};*nerfin-1*$^{RNAi\#2}$ **(D)** flies stained with anti-pH3 and anti-Pros antibodies. White arrows indicate pH3-positive mitotic cells in the midgut. **(E)** Quantification of pH3-positive cells per midgut of the mentioned genotypes. Note that loss of *nerfin-1* can reduce Notch loss-of-function stem cell overproliferation and EE differentiation phenotype. N = 10-20 flies; Significance values are marked by asterisks: ****$P < 0.0001$; Ordinary one-way ANOVA; Scale bar = 80μm.

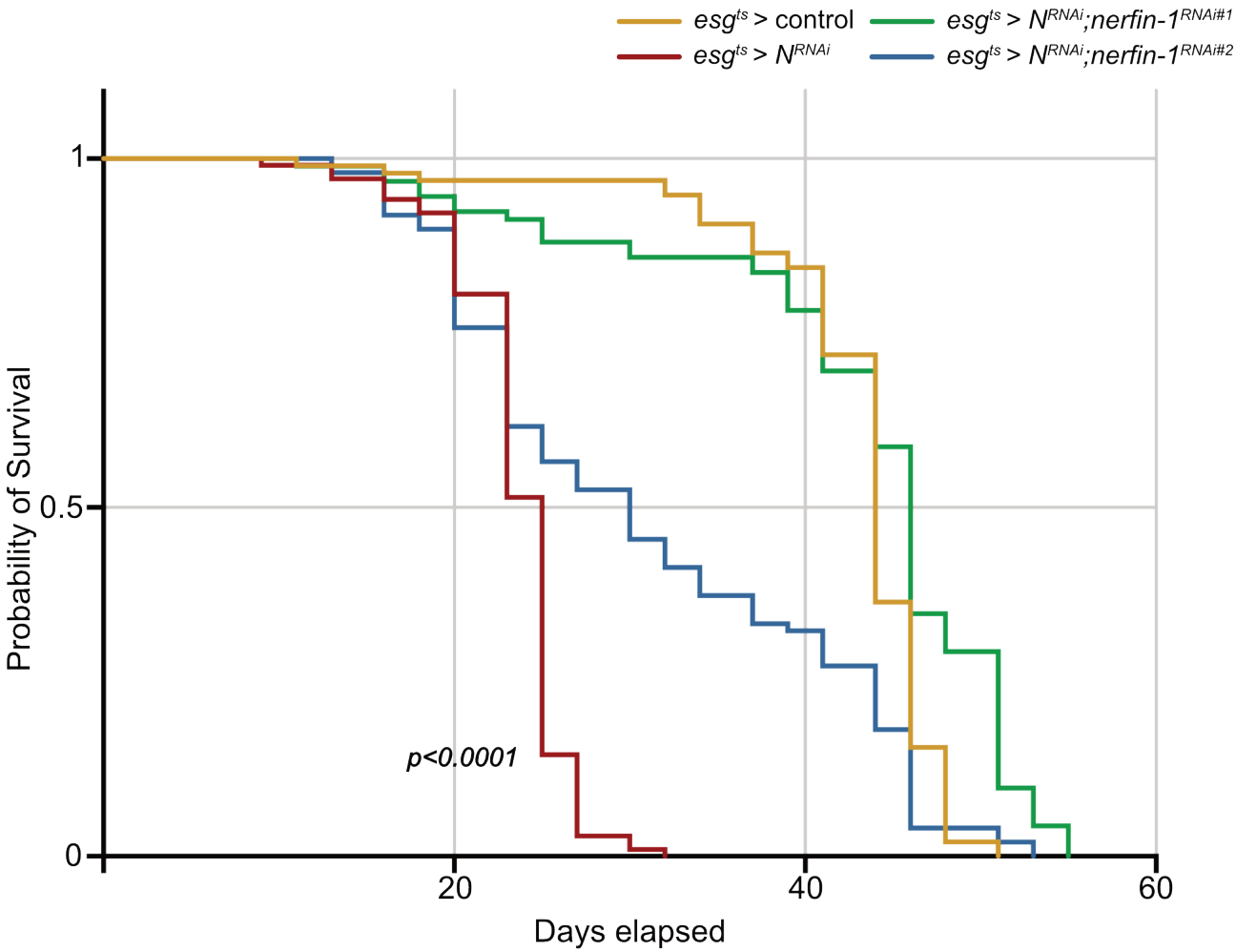

Figure 15 : Loss of Nerfin-1 can rescue lifespan shortening of the Notch loss-of-function adult flies. Lifespan curves of female esg^{ts} > driven control (w^{1118}) (N = 96) (yellow), N^{RNAi} (N = 103) (red), N^{RNAi};$nerfin\text{-}1^{RNAi\#1}$ (N = 92) (green), and N^{RNAi};$nerfin\text{-}1^{RNAi\#2}$ (N = 99) (blue) flies at 29°C; Log-rank p value <0.0001.

3.1.4 Nerfin-1 mediates tumorigenesis in the fly colorectal cancer model.

Colorectal cancer (CRC) remains a leading cause of cancer-related deaths worldwide, largely due to the accumulation of mutations that drive tumorigenesis through a complex genetic network. The most common genetic mutation observed in CRC patients is the loss-of-function mutation in the tumor suppressor gene *APC*, which activates Wnt signaling and serves as an initial trigger for the formation of adenomas [146, 147]. These adenomas subsequently transform into malignant carcinomas due to oncogenic activation of *KRAS* gene as a result of a mutation at codon 12 from glycine to valine (G12V or V12) [148, 149].

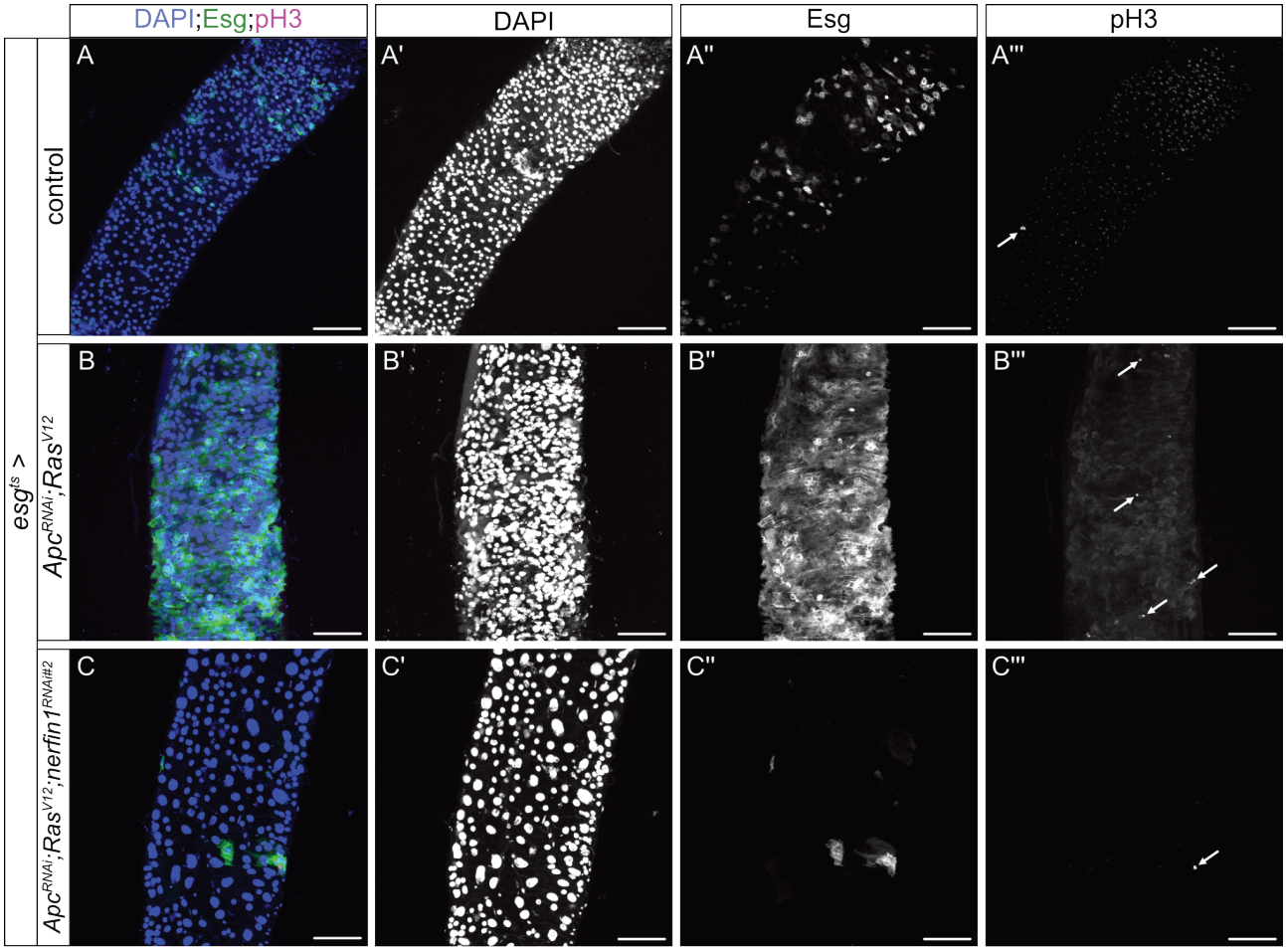

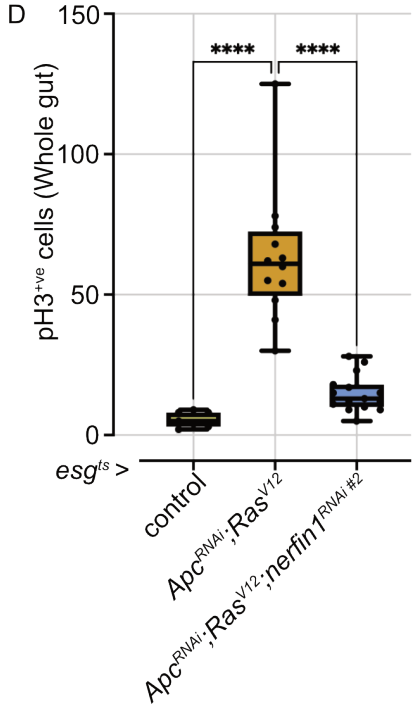

Figure 16 : Nerfin-1 is required for *Apc^{RNAi};Ras^{V12}*-induced midgut tumorigenesis. (A-C) Representative images of the posterior midgut of *esg^{ts}* > driven control **(A),** *Apc^{RNAi};Ras^{V12}* **(B),** *Apc^{RNAi};Ras^{V12};nerfin1$^{RNAi\ \#2}$* **(C)** flies stained with anti-pH3 antibody. White arrows indicate pH3-positive mitotic cells in the midgut. **(D)** Quantification of pH3-positive cells per midgut of the mentioned genotypes; N = 7-15 flies; Significance values are marked by asterisks: *****P < 0.0001*; Ordinary one-way ANOVA; Scale bar = 80µm.

I generated a CRC fly model by introducing simultaneous knockdown of *Apc* (*APC^{RNAi}*) and overexpression of *Ras^{V12}* in the progenitor population (*esg^{ts}*) of the midgut (hereafter referred to

as *Apc*^{RNAi};*Ras*^{V12}). Midguts of this fly showed a significant increase in the number of Esg-positive progenitor cells **(Figure 16A,B)** and pH3-positive stem cell mitosis **(Figure 16D)**. This aligns with the phenotype observed in mice carrying loss-of-function Apc mutation and overexpression of *Ras*^{V12} [150]. Through bulk RNA sequencing, I noticed that flies expressing *Apc*^{RNAi};*Ras*^{V12} showed increased expression of *nerfin-1* in the midgut as compared to controls **(Supplementary Figure S4)**. In order to test if *nerfin-1* plays a critical role in *Apc*^{RNAi};*Ras*^{V12} mediated midgut tumorigenesis, I knocked down *nerfin-1* in flies carrying *Apc*^{RNAi};*Ras*^{V12} in the progenitor population of the midgut. I observed that the knockdown of *nerfin-1* resulted in a significant reduction of Esg-positive progenitor cells **(Figure 16C)** and pH3-positive stem cell mitosis **(Figure 16D)**. This result indicates that Nerfin-1 is required for *Apc*^{RNAi};*Ras*^{V12}-mediated stem cell overproliferation. It would be interesting to test if the human ortholog of Nerfin-1: INSM1 might also have a mechanistic role in regulating the formation of *APC-KRAS*^{V12}-driven CRC tumors in higher organisms such as mouse or humans.

3.1.5 Nerfin-1 is required but not sufficient for stem cell proliferation and differentiation in the midgut.

The *Drosophila* midgut is a regenerative organ capable of undergoing rapid epithelial turnover in response to stress in the form of pathogenic bacterial infection [79]. This process is characterized by accelerated ISC proliferation and their subsequent differentiation to replace damaged or lost epithelial cells, thereby maintaining gut integrity and organismal homeostasis [79]. Enteric infection of the midgut by ingestion of pathogen *Erwinia carotovora carotovora 15* (*Ecc15*) has been shown to initiate a regenerative response by increasing stem cell proliferation in the midgut [151]. Given that *Ecc15* infection-induced stem cell proliferation has been used to study the effects of various genes on stem cell proliferation [79, 152], I decided to investigate if Nerfin-1 is required for this infection-induced increased stem cell proliferation. Consistent with previous studies, I observed that infection of *esg*^{ts} flies with *Ecc15* resulted in a significant increase in Esg-positive progenitor cells **(Figure 17A, B)** and pH3-positive mitotic cells **(Figure 17E)** in the midgut, as compared to uninfected control flies. However, knockdown of *nerfin-1* using two independent RNAis significantly reduced *Ecc15*-induced increase in progenitor cells **(Figure 17B-D)** and pH3-positive stem cell mitosis **(Figure 17E)** back to uninfected control levels. This indicates that Nerfin-1 is required for stem cell proliferation during the infection-induced regenerative response.

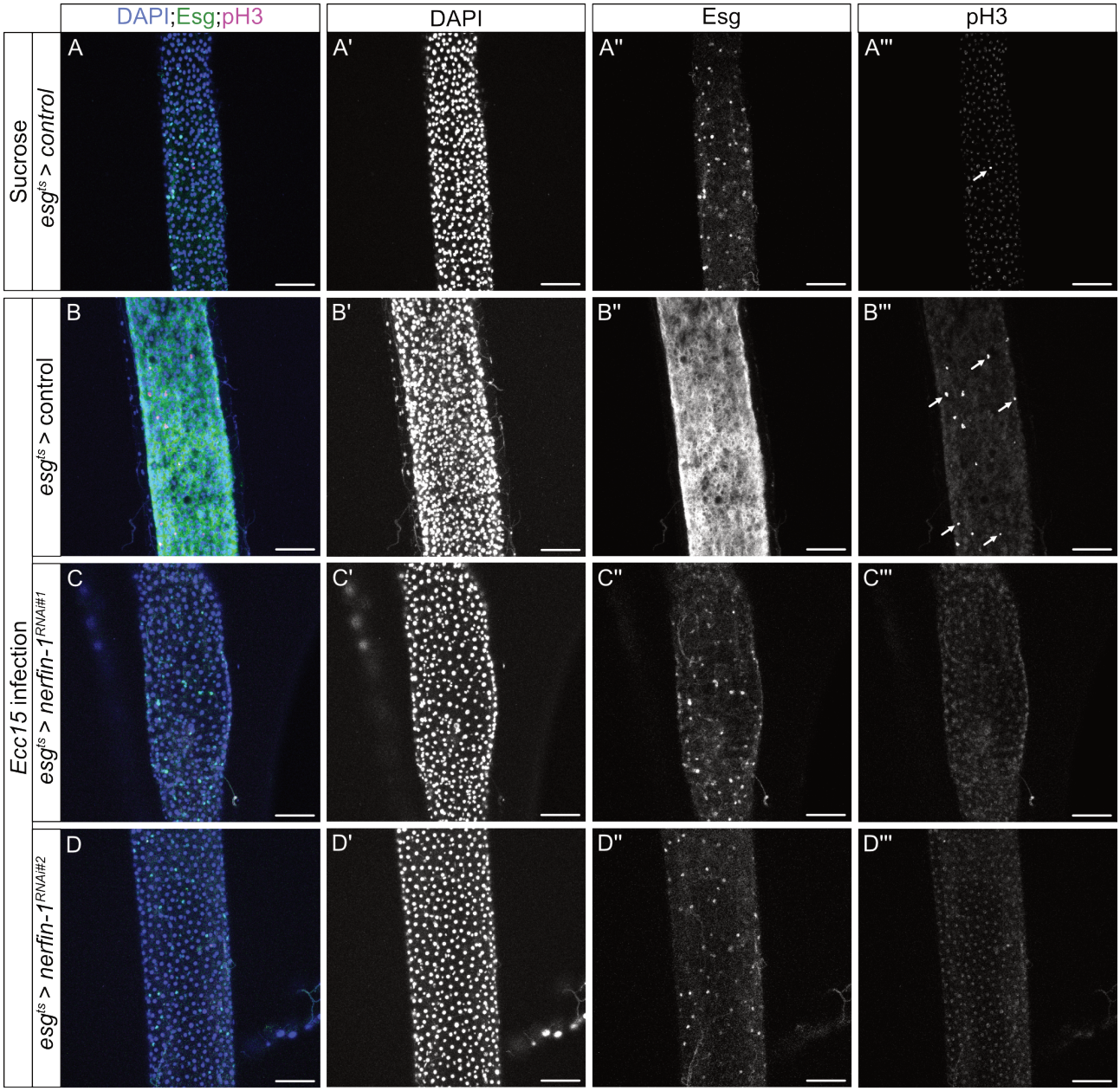

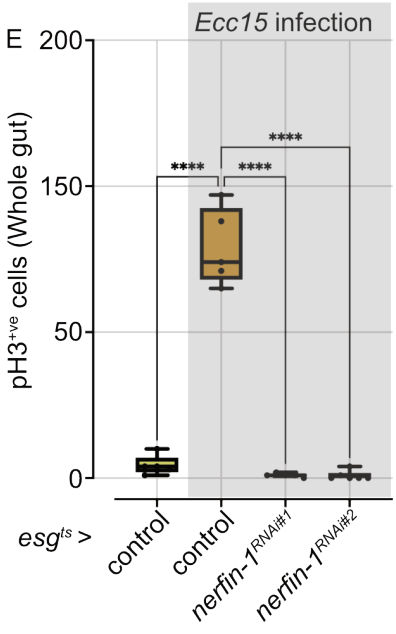

Figure 17 : Nerfin-1 is required for stem cell proliferation during infection-induced regeneration in the midgut. (A-D) Representative images of the posterior midgut of *esg*^{ts} > driven uninfected control (*w*^{1118}) **(A)**, and *Ecc15* infected control (*w*^{1118}) **(B)**, *nerfin-1*$^{RNAi\#1}$ **(C),** and *nerfin-1*$^{RNAi\#2}$ **(D)** flies stained with anti-pH3 antibody. White arrows indicate pH3-positive mitotic cells in the midgut. **(E)** Quantification of pH3-positive cells per midgut of the mentioned uninfected and *Ecc15* infected genotypes. Loss of *nerfin-1* suppresses infection induced increase in stem cell overproliferation phenotype. N = 13-14 flies. Significance values are marked by asterisks: *****P < 0.0001*; Ordinary one-way ANOVA; Scale bar = 80*μ*m.

Given that Nerfin-1 regulates the proliferation of stem cells during tumorigenesis and following infection-induced regenerative response, I investigated if Nerfin-1 is also required for stem cell proliferation during homeostasis. To test this, I knocked down *nerfin-1* in the progenitor cells of the midgut and observed a reduction in Esg-positive progenitor cells **(Figure 18A-C)**, and a significant decline in pH3-positive mitotic cells **(Figure 18D)** in the midgut. This suggests that Nerfin-1 is essential for mediating stem cell proliferation in the midgut during homeostasis. However, while the knockdown of *nerfin-1* significantly reduced stem cell proliferation during homeostasis, it had no significant effect on the lifespan of the fly **(Supplementary Figure S5)**. This might be because during homeostasis, the demand to regenerate is low, and therefore, flies might be able to tolerate a small reduction in progenitor proliferation without affecting their lifespan. From this data, I conclude that Nerfin-1 is required for stem cell proliferation during homeostasis and infection-induced regenerative response in the midgut.

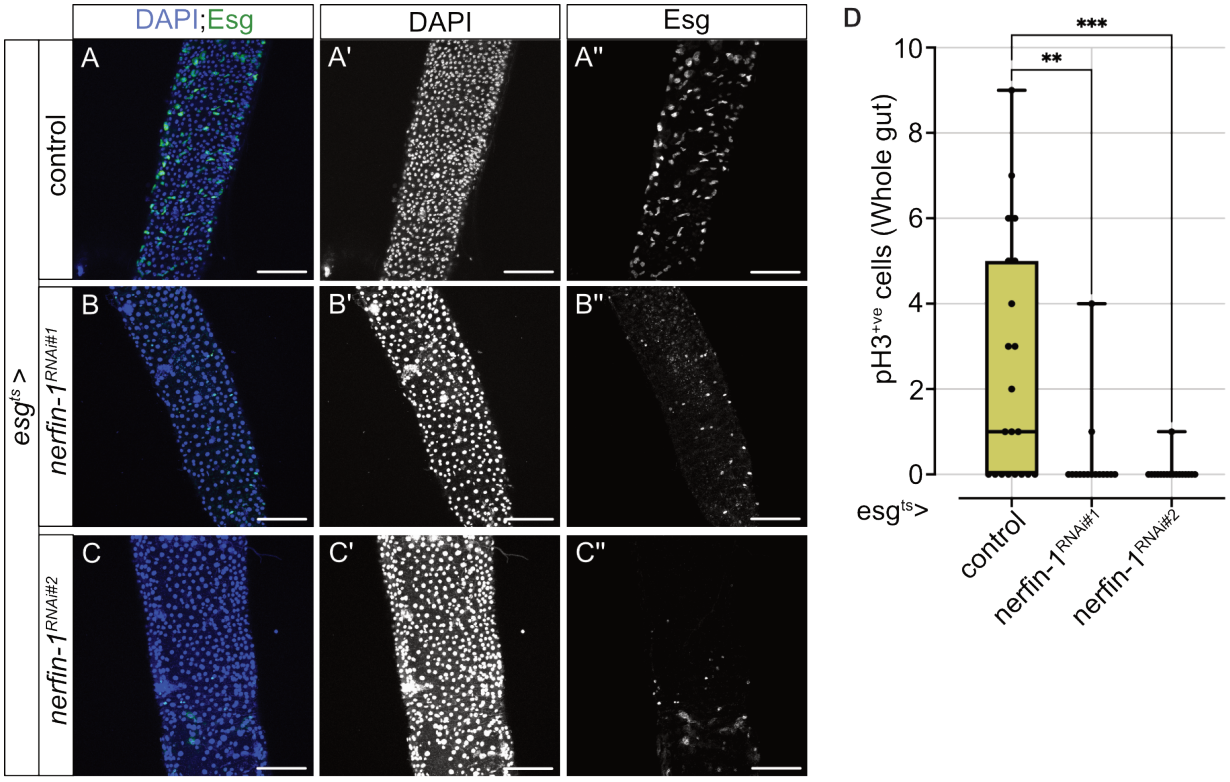

Figure 18 : Loss of *nerfin-1* reduces the number of progenitor cells and stem cell proliferation during homeostasis. (A-C) Representative images of the posterior midgut of esg^{ts} > driven *control* (w^{1118}) **(A)**, *nerfin-1*$^{RNAi\#1}$ **(B)**, and *nerfin-1*$^{RNAi\#2}$ **(C)** flies. **(D)** Quantification of pH3-positive cells per midgut of the mentioned genotypes; N = 15-20 flies. Significance values are marked by asterisks: ***P ≤ 0.01, ***P ≤ 0.001*; Ordinary one-way ANOVA; Scale bar = 80μm.

Since the knockdown of Nerfin-1 also reduced the number of EEs in Notch loss-of-function tumors **(Figure 14C,D)**, I decided to investigate if Nerfin-1 is also required for progenitor cell differentiation. To test this, I used a lineage tracing method called the flipout system (F/O). In this system, the *esg* promoter drives the expression of the *UAS Flp* recombinase in the progenitor population of the midgut. The Flp recombinase excises the inhibitory CD2 cassette from Act>CD2>Gal4, thereby enabling the expression of the ubiquitous *Actin-Gal4* driver. By this method, progenitors and their subsequent lineage inherit *Actin-Gal4*, which drives the expression of UAS constructs such as *UAS GFP*, thereby marking the entire stem cell lineage with GFP fluorescence [7]. In control flies, $esg^{ts}F/O$ marks almost all cells with GFP within 2-3 weeks of flipout system induction, indicating normal and complete midgut epithelial turnover during homeostasis **(Supplementary Figure S6A)**. However, knockdown of *nerfin-1* using this $esg^{ts}F/O$ system resulted in a significant reduction in the number of stem cell clones as well as their size **(Supplementary Figure S6B,C)**. Moreover, most of the GFP-positive clones were large nucleated cells, indicating that loss of *nerfin-1* forces the small diploid progenitor cells to differentiate into ECs **(Supplementary Figure S6A-C, Red arrows)**. These experiments suggest that Nerfin-1 is required for regulating progenitor cell fate decisions by preventing their differentiation to ECs.

While I showed that Nerfin-1 is required for the proliferation and differentiation of progenitor cells, I wanted to test if Nerfin-1 is sufficient to regulate these functions. To investigate this, I overexpressed *nerfin-1* in the progenitor population of the midgut. I observed that overexpression of *nerfin-1* did not affect the number of progenitor cells, EEs or stem cell mitosis as compared to control midguts **(Supplementary Figure S7A,B)**. Altogether, I conclude that Nerfin-1 is required, but not sufficient, for regulating stem cell proliferation and differentiation in the midgut. I propose that Nerfin-1 regulates these processes together with other interacting proteins.

3.2 Innate immune Toll pathway regulates stem cell proliferation in the adult midgut

In flies, the innate immune Toll and IMD signaling pathways defend the host against pathogenic infections. These pathways detect pathogenic bacteria and activate a signaling cascade that produces antimicrobial peptides (AMPs), which are toxic to the pathogens [153]. The IMD signaling pathway, which specifically responds to and eliminates gram-negative bacteria, has been described in regulating stem cell proliferation and EC shedding in the midgut [113, 114, 115]. While the role of the IMD pathway in epithelial renewal has been well established, the Toll pathway's involvement in mediating the midgut's epithelial turnover remains poorly understood.

3.2.1 Notch loss-of-function tumors require the Toll signaling pathway for proliferation

I chose to study the role of the Toll pathway in the context of intestinal stem cell proliferation because I observed that the Toll pathway ligand Spatzle (Spz) was upregulated in the progenitor population of *N-gRNA^{2X}* tumors as compared to control midguts in our scRNA seq dataset **(Figure 12C, Supplementary Figure S8A,B)**. Spz is an extracellular ligand which binds to the Toll receptor and activates the Toll pathway [106]. Activated Toll pathway subsequently transcribes *spz* thereby creating a positive feedback loop [154]. Since *spz* was upregulated in the progenitor population of *N-gRNA^{2X}* midguts and is a target gene of the Toll pathway, I asked if Notch loss-of-function driven tumorigenesis can activate the Toll pathway in the midgut.

To test this, I first looked at the expression levels of the Toll pathway target gene *spz*, as well as AMPs *Drosomycin* (*Drs*), and *Defensin* (*Def*) [112, 154]. To do this, I suppressed Notch signaling by expressing *N^{RNAi}* in progenitor cells and performed RT-qPCR of *spz*, *Drs*, and *Def*. I found that expression of the Toll pathway target genes *spz*, *Drs*, and *Def* were significantly upregulated in *N^{RNAi}* midguts as compared to controls **(Figure 19A-C)**. This indicated that the Toll pathway was active in midguts carrying *N^{RNAi}* driven tumors.

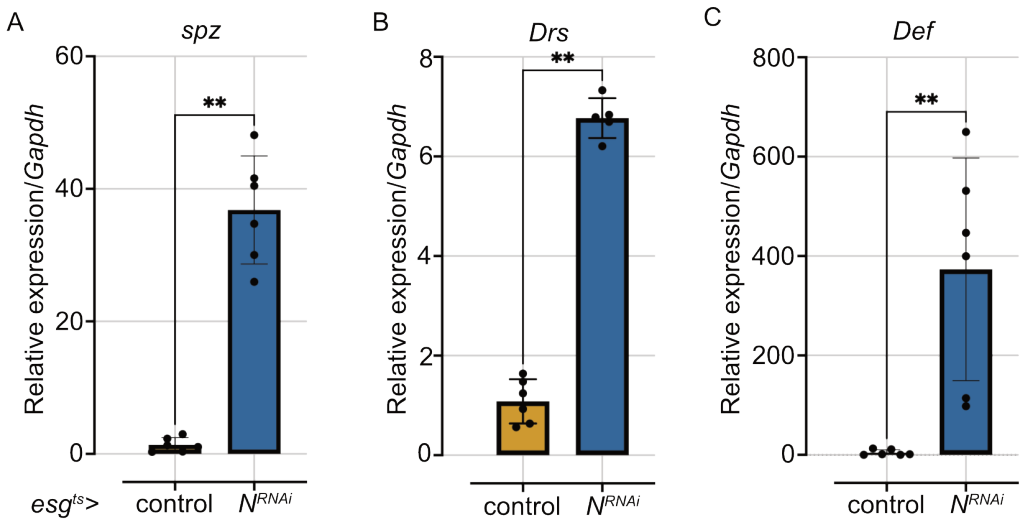

Figure 19 : Loss of Notch signaling upregulates target genes of the Toll signaling pathway. (A-C) RT-qPCR analysis showing the upregulation of the Toll pathway target genes *spz* **(A)**, *Drs* **(B)**, and *Def* **(C)** relative to *Gapdh* expression in esg^{ts} > driven N^{RNAi} vs control (w^{1118}) flies. All experiments were performed in technical duplicates, with 3 independent biological replicates; Mann-Whitney t-test; Significance values are marked by asterisks: $^{**}P < 0.01$.

Next, I tested whether activation of the Toll pathway in N^{RNAi} is required for midgut tumorigenesis. To investigate this, I knocked down intracellular components of the Toll pathway: Toll receptor (Tl), Dif, and Dorsal (dl) in the progenitor cells of N^{RNAi} flies. I observed that inhibition of the Toll pathway by knocking down *Tl*, *Dif*, and *dl* significantly reduced both Esg-positive progenitor cells and Pros-positive EE accumulation in N^{RNAi} midguts **(Figure 20A-D)**. This was also accompanied by a significant decrease in pH3-positive mitotic cells **(Figure 20E)**. Additionally, knockdown of *Myd88* and *pll* also reduced the number of progenitor cells, EEs, and mitotic cells in N^{RNAi} midgut **(Supplementary Figure S9A-D)**. Altogether, I conclude that Notch loss-of-function activates the Toll signaling pathway in the midgut which is required for tumorigenesis.

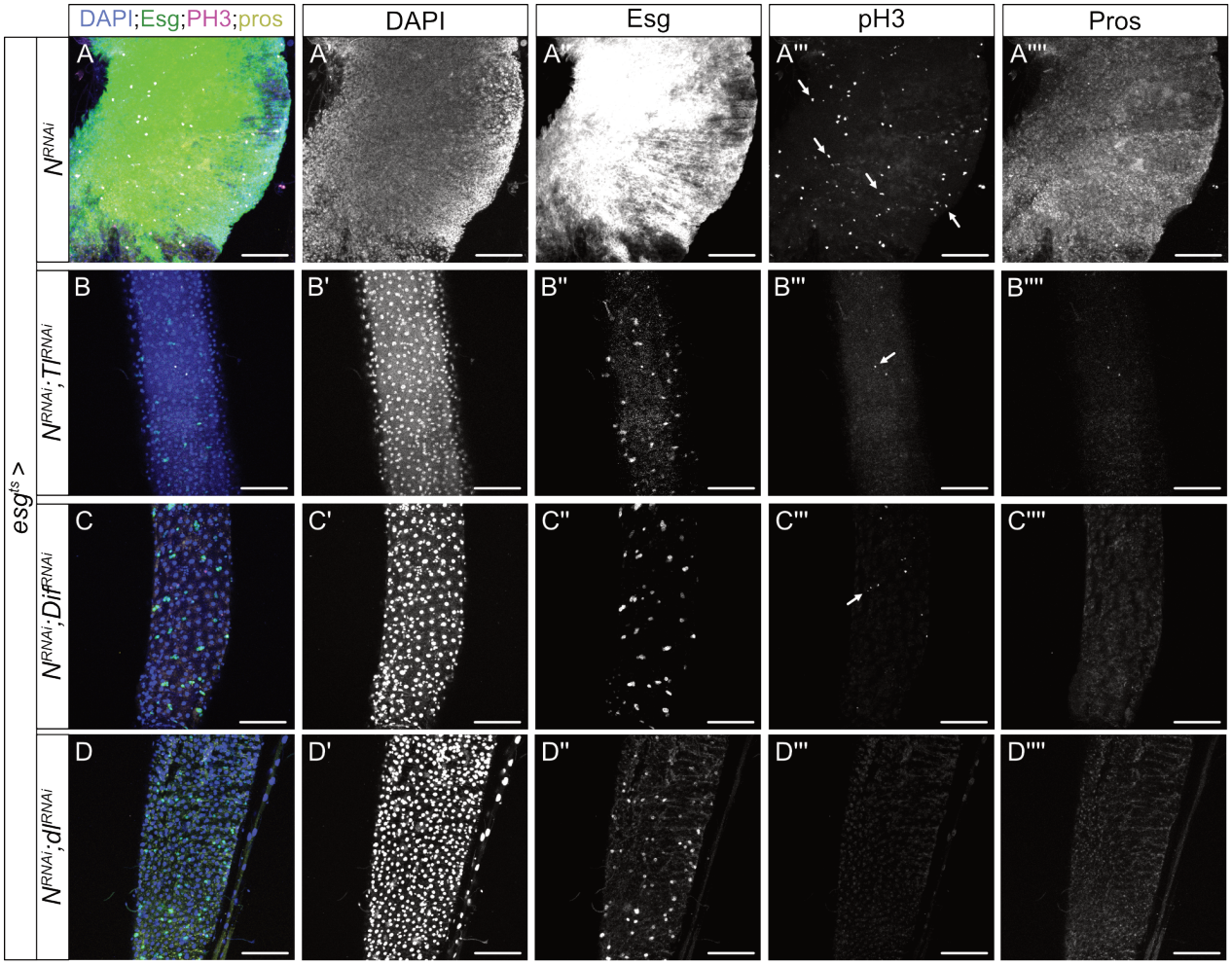

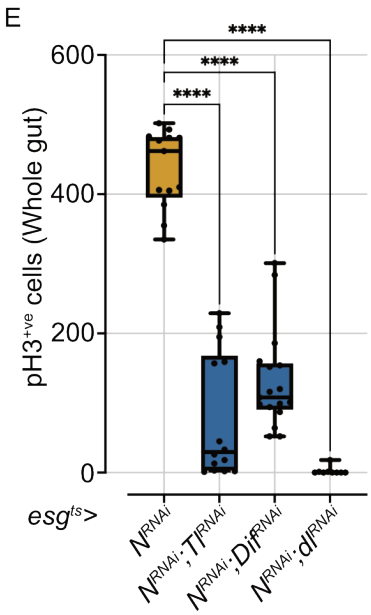

Figure 20 : Toll signaling pathway regulates the Notch loss-of-function midgut tumor phenotype. (A-D) Representative images of the posterior midgut of *esg*^{ts} > driven N^{RNAi} **(A)**, N^{RNAi};Tl^{RNAi} **(B)**, N^{RNAi};Dif^{RNAi} **(C)**, and N^{RNAi};dl^{RNAi} **(D)** flies stained with anti-pH3 and anti-Pros antibodies. White arrows indicate pH3-positive mitotic cells in the midgut. **(E)** Quantification of pH3-positive cells per midgut of the mentioned genotypes. Note that loss of *Tl*, *Dif,* and *dl* suppresses N^{RNAi} midgut tumor formation. N = 13-17 flies; Significance values are marked by asterisks: ****P < *0.0001*; Ordinary one-way ANOVA; Scale bar = 80μm.

3.2.2 Active Toll pathway mediates tumorigenesis in the fly colorectal cancer model.

Given that suppression of the Toll signaling pathway significantly reduced stem cell mitosis in Notch loss-of-function tumor midguts, I tested whether the Toll signaling pathway is also required for tumor formation in the CRC fly model. To investigate this, I checked if Apc^{RNAi};Ras^{V12} midguts activate the Toll signaling pathway. Bulk RNA sequencing data revealed that the Toll pathway target genes *spz*, *Drs*, and *Def* were all significantly upregulated in Apc^{RNAi};Ras^{V12} midguts as compared to controls, indicating that the Toll signaling pathway was activated in tumor-bearing midguts **(Supplementary Figure S10A-C)**. Next, I knocked down *Tl*, *Dif*, and *dl* in the progenitor population of Apc^{RNAi};Ras^{V12} expressing midguts. I observed that knockdown of *Tl* **(Figure 21B)** and *dl* **(Figure 21D)** significantly reduced Esg-positive progenitor cells and pH3-positive midgut mitosis **(Figure 21E)**. Suppression of *Dif* also reduced the tumor phenotype, albeit non-significantly **(Figure 21C)**. These findings suggest that *Tl* and *dl*, and to some extent *Dif*, are required for Apc^{RNAi};Ras^{V12}-mediated stem cell overproliferation in the midgut.

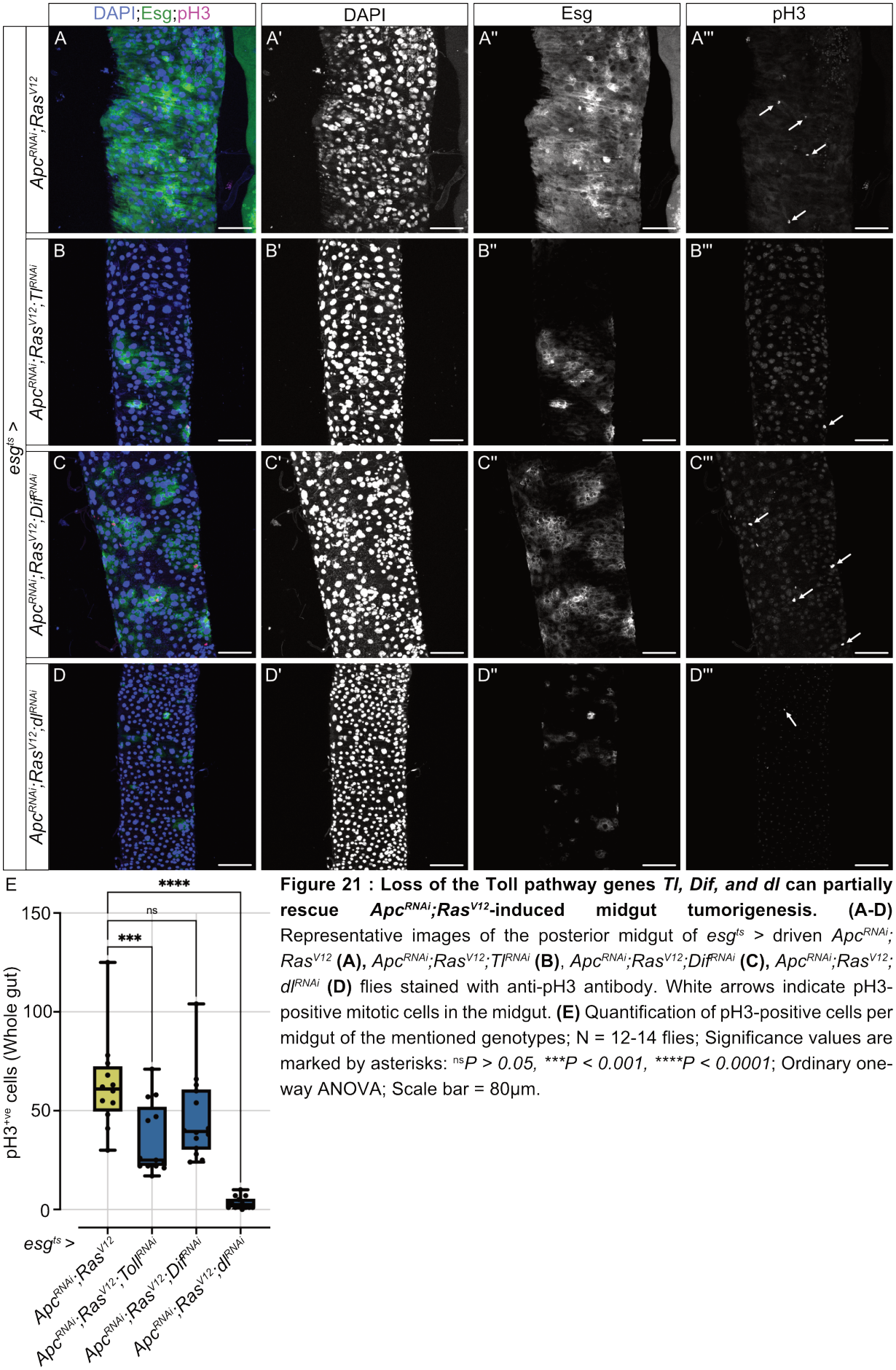

Figure 21 : Loss of the Toll pathway genes *Tl, Dif, and dl* can partially rescue *Apc^{RNAi};Ras^{V12}*-induced midgut tumorigenesis. (A-D) Representative images of the posterior midgut of *esg^{ts}* > driven *Apc^{RNAi};Ras^{V12}* **(A),** *Apc^{RNAi};Ras^{V12};Tl^{RNAi}* **(B)**, *Apc^{RNAi};Ras^{V12};Dif^{RNAi}* **(C),** *Apc^{RNAi};Ras^{V12};dl^{RNAi}* **(D)** flies stained with anti-pH3 antibody. White arrows indicate pH3-positive mitotic cells in the midgut. **(E)** Quantification of pH3-positive cells per midgut of the mentioned genotypes; N = 12-14 flies; Significance values are marked by asterisks: $^{ns}P > 0.05$, $^{***}P < 0.001$, $^{****}P < 0.0001$; Ordinary one-way ANOVA; Scale bar = 80µm.

3.2.3 Toll pathway is both required and sufficient for maintaining the proliferative capacity of intestinal stem cells

Since I demonstrated that active Toll signaling is required for both Notch loss-of-function and *Apc*^{RNAi};*Ras*^{V12}-mediated tumorigenesis, I next asked whether the Toll signaling pathway also regulates stem cell proliferation during infection-induced regeneration. To test this, I infected adult flies of different genotypes with *Ecc15* and stained their midguts for stem cell mitosis marker pH3. As expected, infection of control flies with *Ecc15* triggered rapid intestinal regeneration, characterised by a significant increase in progenitor cells **(Figure 22A,B)** and stem cell mitosis **(Supplementary Figure S11)** as compared to uninfected control flies. I then infected flies carrying knockdown of *Tl*, *Dif*, and *dl* in progenitor cells and observed a significant reduction in Esg-positive progenitor cells **(Figure 22C-E)** and pH3-positive stem cell mitosis back to uninfected control levels **(Supplementary Figure S11)**. This suggests that the Toll signaling pathway is required for accelerating stem cell proliferation during infection-induced midgut regeneration.

Given that inhibition of the Toll signaling pathway suppressed both tumor formation and infection-induced regeneration, I next examined whether activation of Toll signaling is sufficient to promote stem cell proliferation during homeostasis. To investigate this, I overexpressed an active form of the Toll receptor (Tl^{10b}) in progenitor cells using two independent *UAS Tl*^{10b} constructs. Tl^{10b} is a mutant form of the Toll receptor that contains a C781Y amino acid substitution in its extracellular domain, rendering it constitutively active. This mutation allows Tl^{10b} to activate Toll signaling without the need for ligand binding [155, 156]. Overexpression of two independent *Tl*^{10b} overexpression constructs resulted in a significant increase in Esg-positive progenitor cells **(Figure 23A-C)** and pH3-positive stem cell mitosis **(Figure 23D)** as compared to controls. I also overexpressed a similar effect following the overexpression of Dif **(Supplementary Figure S12A-C)**, further supporting the hypothesis that activation of Toll signaling is sufficient for promoting stem cell proliferation in the midgut.

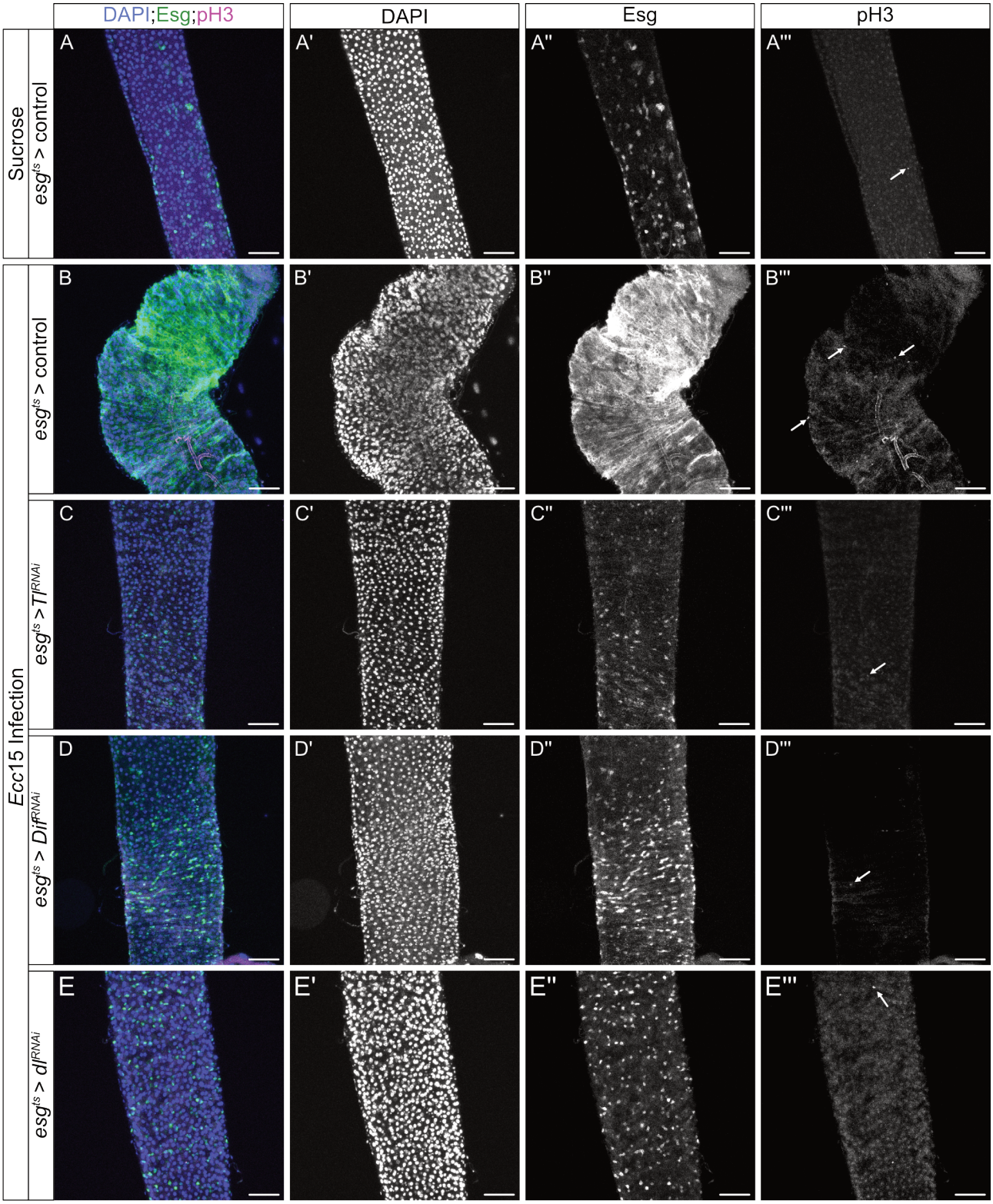

Figure 22 : Toll signaling pathway is required for infection-induced regenerative response in the midgut. (A-E) Representative images of the posterior midgut of esg^{ts} > driven uninfected control (w^{1118}) **(A)**, and *Ecc*15 infected control (w^{1118}) **(B)**, Tl^{RNAi} **(C)**, Dif^{RNAi} **(D)**, and dl^{RNAi} **(E)** flies stained with anti-pH3 antibody. White arrows indicate pH3-positive mitotic cells in the midgut. Loss of *Tl*, *Dif,* and *dl* suppresses infection-induced increase in stem cell proliferation. Scale bar = 80μm.

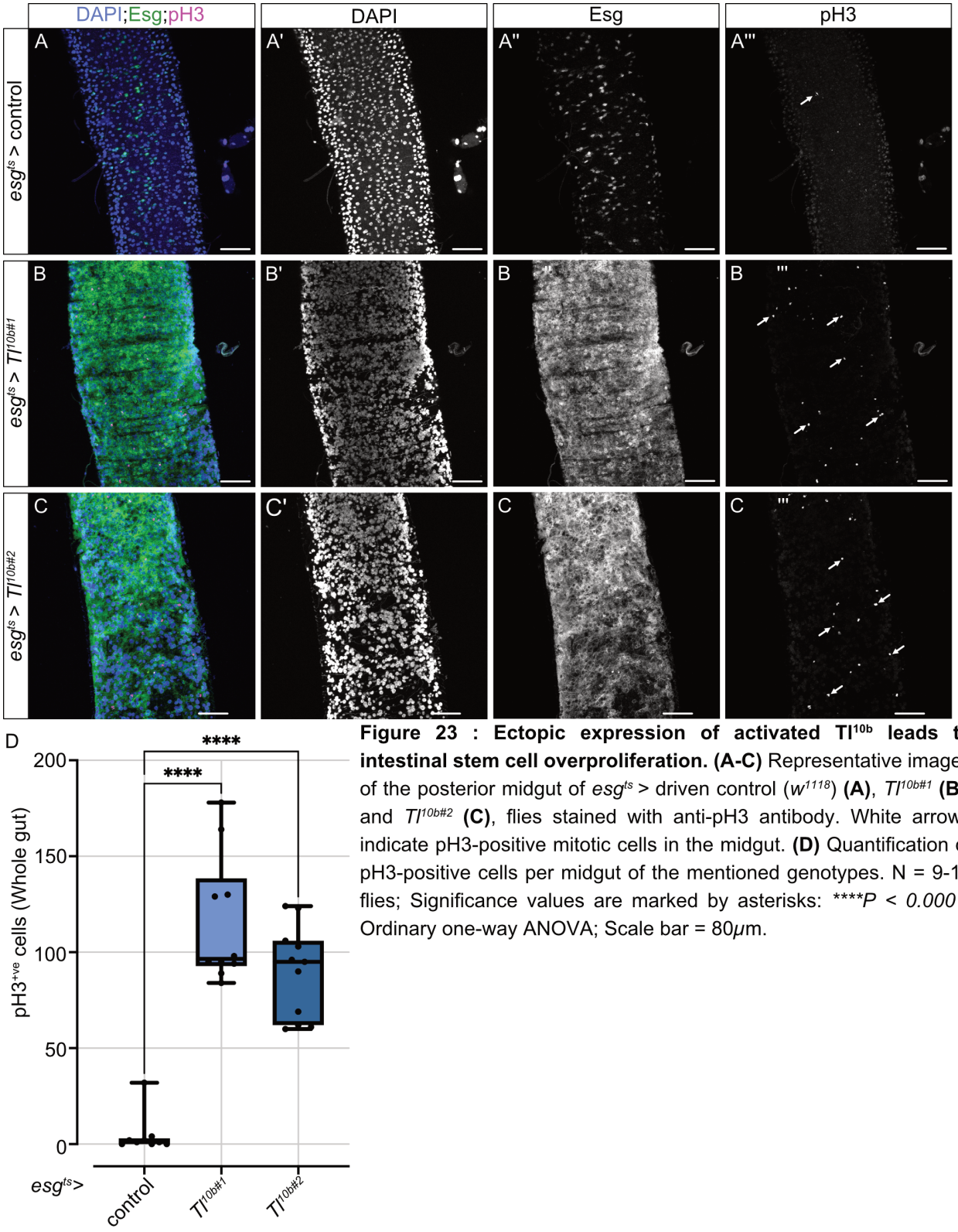

Figure 23 : Ectopic expression of activated Tl^{10b} leads to intestinal stem cell overproliferation. (A-C) Representative images of the posterior midgut of *esg^{ts}* > driven control (*w^{1118}*) **(A)**, *Tl$^{10b\#1}$* **(B)**, and *Tl$^{10b\#2}$* **(C)**, flies stained with anti-pH3 antibody. White arrows indicate pH3-positive mitotic cells in the midgut. **(D)** Quantification of pH3-positive cells per midgut of the mentioned genotypes. N = 9-11 flies; Significance values are marked by asterisks: ****$P < 0.0001$; Ordinary one-way ANOVA; Scale bar = 80μm.

Although the Toll pathway signals through the transcription factors Dif and Dorsal, and the IMD pathway signals through the transcription factor Relish, these transcription factors can form homo- and hetero-dimers, working together to simultaneously regulate the expression of target

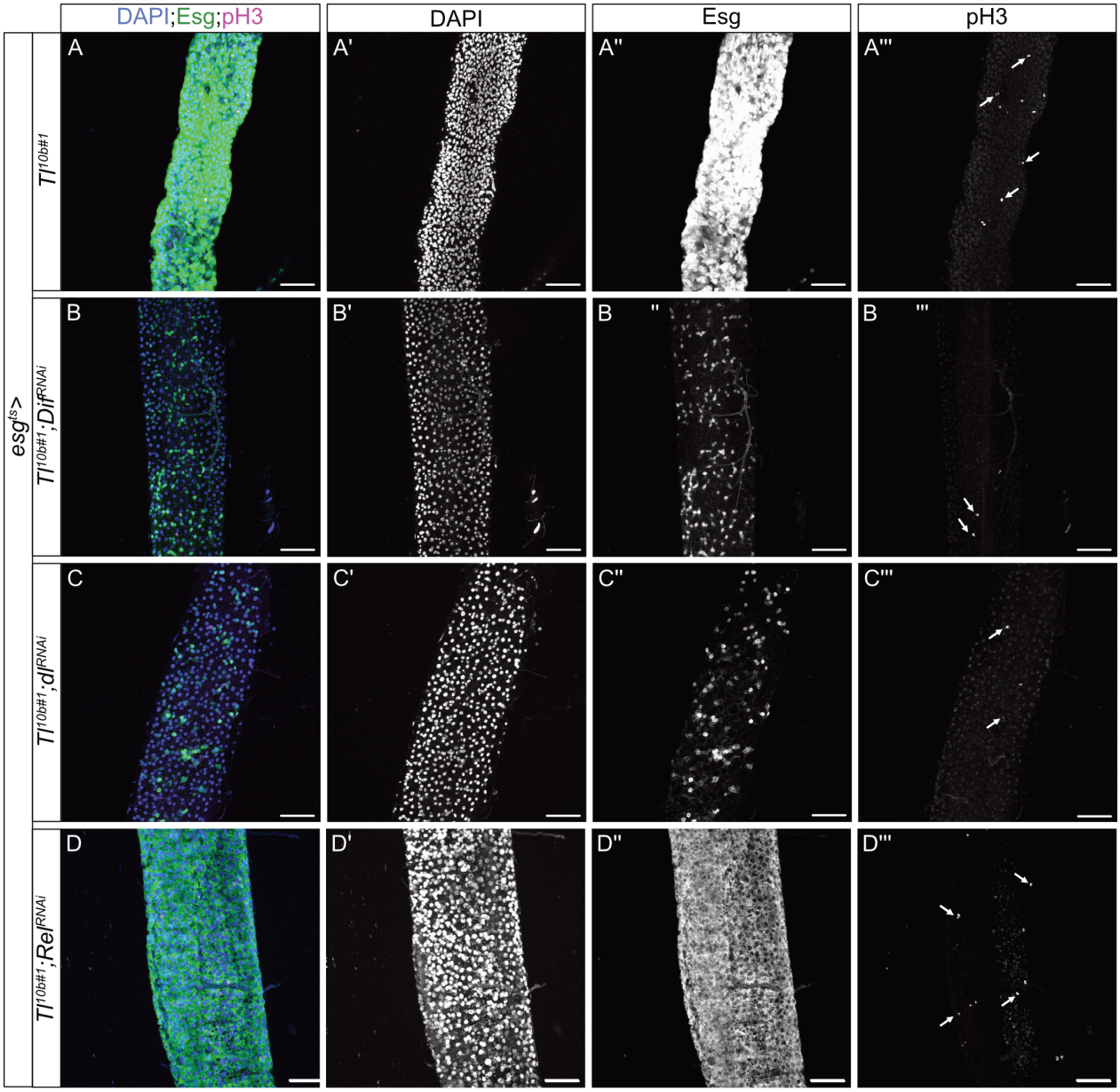

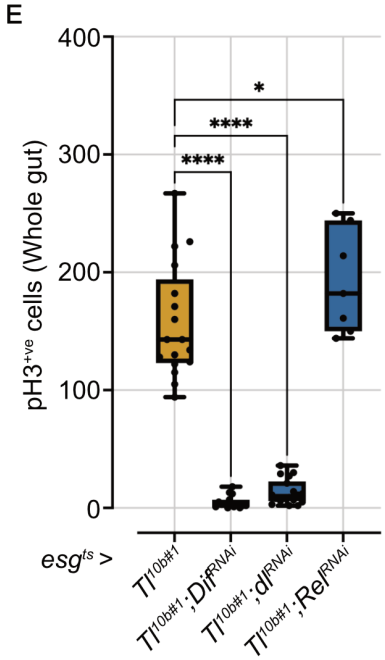

Figure 24 : Tl^{10b}-induced stem cell phenotype requires the Toll pathway transcription factors Dif and Dorsal. (A-C) Representative images of the posterior midgut of *esg^{ts}* > driven *Tl$^{10b\#1}$* **(A)**, *Tl$^{10b\#1}$;Dif^{RNAi}* **(B)**, *Tl$^{10b\#1}$;dl^{RNAi}* **(C)**, and *Tl$^{10b\#1}$;Rel^{RNAi}* **(D)** flies stained with anti-pH3 antibody. White arrows indicate pH3-positive mitotic cells in the midgut. **(E)** Quantification of pH3-positive cells per midgut of the mentioned genotypes. Note that loss of *Dif* and *dl* but not *Rel* rescuex *Tl^{10b}*-induced stem cell overproliferation phenotype. N = 7-17 flies; Significance values are marked by asterisks: ****$P < 0.0001$; Ordinary one-way ANOVA; Scale bar = 80μm.

genes from both pathways [157]. To determine which pathway is involved in *Tl*^{10b}-mediated effects on stem cell proliferation, I knocked down *Dif*, *dl*, and *Rel* in progenitor cells of *Tl*^{10b}-overexpressing flies. I observed that knockdown of *Dif* and *dl*, but not *Rel* reduced the number of Esg-positive progenitor cells **(Figure 24A-D)** and pH3-positive mitotic cells **(Figure 24E)** in *Tl*^{10b} midguts .

In summary, I conclude that the Toll pathway is required for infection-induced intestinal stem cell overproliferation and that overexpression of an activated form of Toll receptor (Tl^{10b}) can sufficiently promote intestinal stem cell overproliferation during homeostasis through the transcription factors Dif and Dorsal but not Relish.

3.2.4 Toll pathway regulates intestinal stem cell proliferation through JNK signaling

In a previous study by *Buchon et al.*, it was shown that enteric infection with *Ecc15* activated JNK signaling in both ISCs and ECs in the midgut. Moreover, they demonstrated that suppressing JNK signaling in the midgut reduced infection-induced stem cell overproliferation [11]. Since I showed that the Toll pathway is also required for infection-induced stem cell overproliferation in the midgut, I investigated whether JNK signaling interacts with the activated Toll pathway to mediate this process in the midgut.

I first asked if activation of the Toll pathway affects JNK signaling in the midgut. To test this, I overexpressed *Tl*^{10b} in progenitor cells and stained the midguts for the JNK signaling reporter Puc-LacZ. Immunostaining revealed that JNK signaling was active in Esg-positive progenitor cells and ECs in the control midguts albeit at low levels **(Figure 25A)**. However, overexpression of *Tl*^{10b} induced a strong and widespread Puc-LacZ expression in these cell types **(Figure 25B,C)**, indicating a significant activation of JNK signaling. In addition to these results, my collaborator Aiswarya Udayakumar (Ligoxygakis lab, University of Oxford) also observed an upregulation of JNK pathway genes *drk*, *p38c*, and *hep* in *Tl*^{10b} overexpressing midguts (data not shown), confirming that the Toll signaling pathway positively regulates JNK signaling in the midgut.

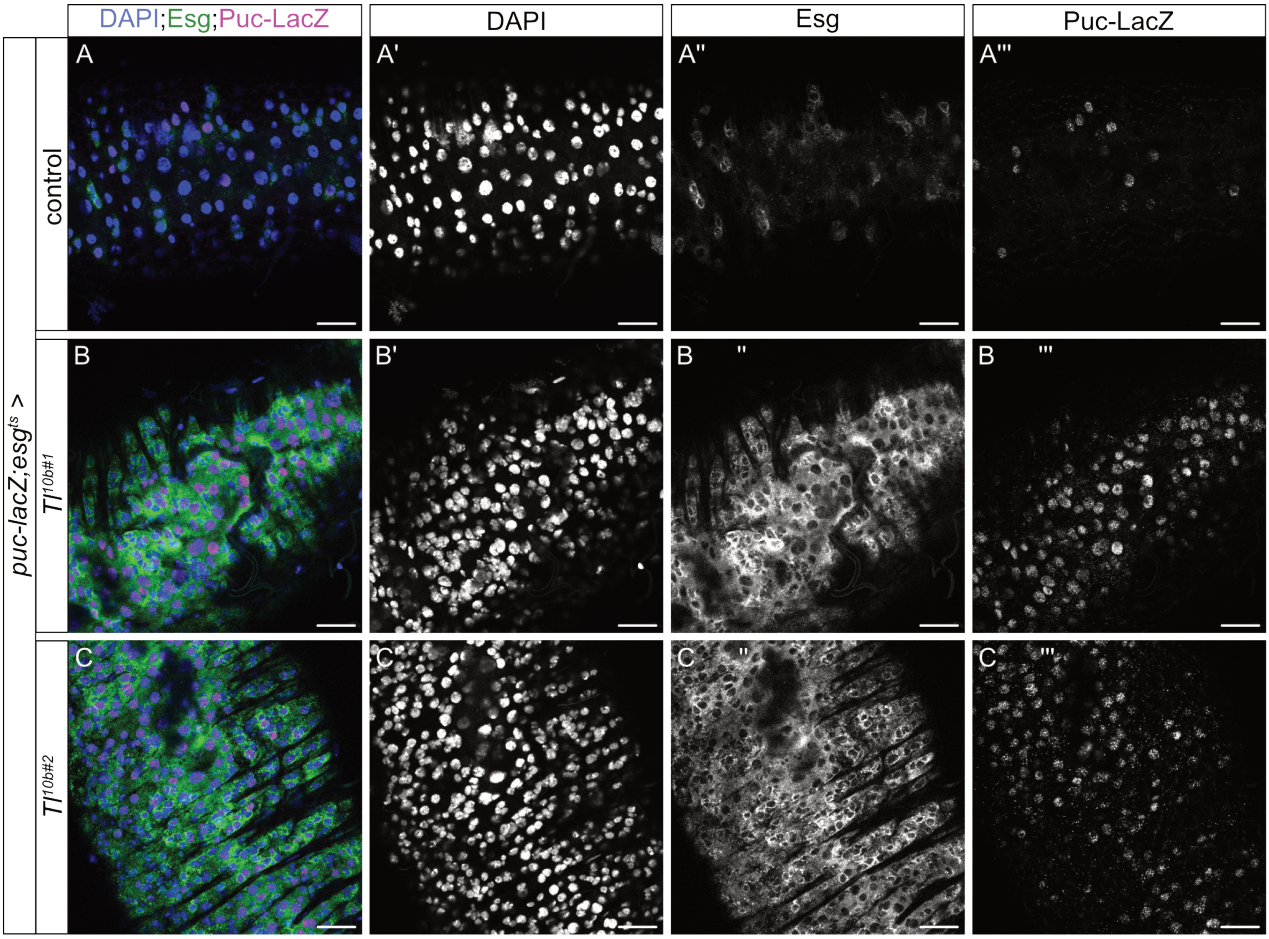

Figure 25 : Tl^{10b} activates the JNK signaling pathway in the adult midgut. (A-C) Representative images of the JNK pathway reporter Puc-LacZ expression in the posterior midgut of *puc-LacZ;esg*^{ts} > driven control (w^{1118}) **(A)**, $Tl^{10b\#1}$ **(B)**, and $Tl^{10b\#2}$ **(C)** flies stained with anti-β-Galactosidase antibody. Note that the overexpression of Tl^{10b} significantly increases JNK activation as seen by increased Puc-LacZ staining. Scale bar = 30μm.

Given that the Toll pathway activates JNK signaling in the midgut, I next investigated whether JNK signaling acts downstream of the Toll pathway to regulate stem cell proliferation. To test this, I blocked JNK signaling by overexpressing a dominant-negative form of *bsk* (bsk^{DN}) in progenitor cells. Overexpression of Tl^{10b} caused an increase in the number of Esg-positive progenitor cells and pH3-positive mitotic cells as compared to controls **(Figure 26A,B, and D)**. However, inhibition of JNK signaling significantly reduced both progenitor cell numbers and stem cell mitosis to control levels **(Figure 26C,D)**. Altogether, I conclude that active Toll signaling induces JNK signaling, which is required for accelerated stem cell proliferation in the midgut.

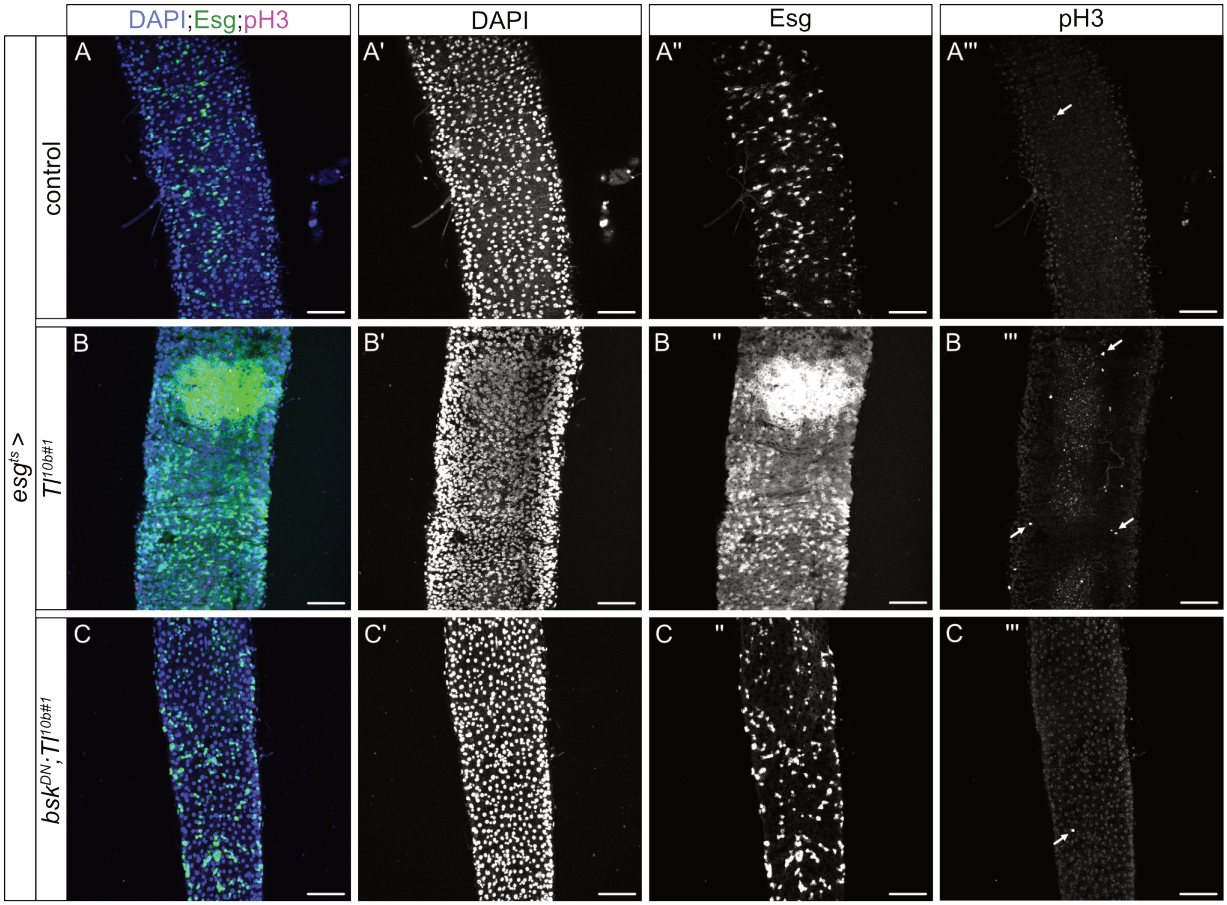

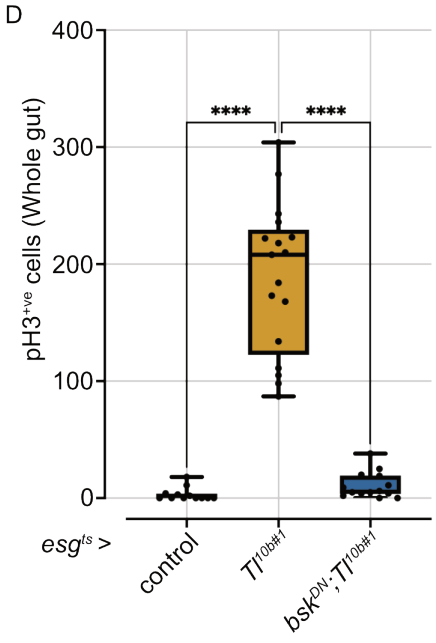

Figure 26 : JNK signaling is required for Tl^{10b}-induced intestinal stem cell phenotype. (A-C) Representative images of the posterior midgut of *esg^{ts}* > driven control (*w^{1118}*) **(A)**, *Tl$^{10b\#1}$* **(B)**, and *bsk^{DN};Tl$^{10b\#1}$* **(C)**, flies stained with anti-pH3 antibody. White arrows indicate pH3-positive mitotic cells in the midgut. **(D)** Quantification of pH3-positive cells per midgut of the mentioned genotypes. Suppression of JNK signaling through overexpression of a dominant negative form of *bsk* rescues *Tl^{10b}*-mediated stem cell overproliferation phenotype. N = 12-17 flies; Significance values are marked by asterisks: *****P < 0.0001*; Ordinary one-way ANOVA; Scale bar = 80μm.

3.2.5 Toll signaling pathway can non-autonomously promote stem cell proliferation in the midgut

While stem cells can autonomously regulate their proliferation, niche cells can also influence stem cell proliferation through non-autonomous signaling mechanisms [158]. For example, Notch loss-of-function-induced tumorigenesis triggers JNK signaling in the surrounding epithelial cells, which, through the production of cytokines, non-autonomously promote tumor growth [35]. The non-autonomous role of the Toll pathway has previously been described in mediating the elimination of 'loser cells' by 'winner cells' in the wing disc cell competition model [119]. In this model, Myc expressing 'winner cells' in the wing disc rapidly proliferate and expand at the expense of their surrounding wild-type 'loser cells'. Winner cells boost Spz production, which activates the Toll pathway in the loser cells. The activated Toll pathway promotes the expression of pro-apoptotic genes *Hid* and *rpr*, which subsequently mediates apoptosis of loser cells and promotes winner cell outgrowth [119]. These experiments motivated me to ask if the Toll pathway also non-autonomously influences stem cell proliferation in the midgut.

To explore this, I overexpressed Tl^{10b} in enterocytes (ECs) using the *Myosin31DF-Gal4, UAS GFP, tub-Gal80*^{ts} (*Myo1A*^{ts}) driver and measured stem cell mitosis through pH3 immunostaining. I observed that overexpression of Tl^{10b} in ECs using two independent overexpression fly lines resulted in the reduction of Myo1A-positive ECs **(Figure 27A-C)**, and a significant increase in pH3-positive mitotic cells as compared to controls **(Figure 27D)**. This suggests that activation of Toll signaling in ECs leads to EC loss and accelerates stem cell proliferation through non-autonomous signaling mechanisms in the midgut.

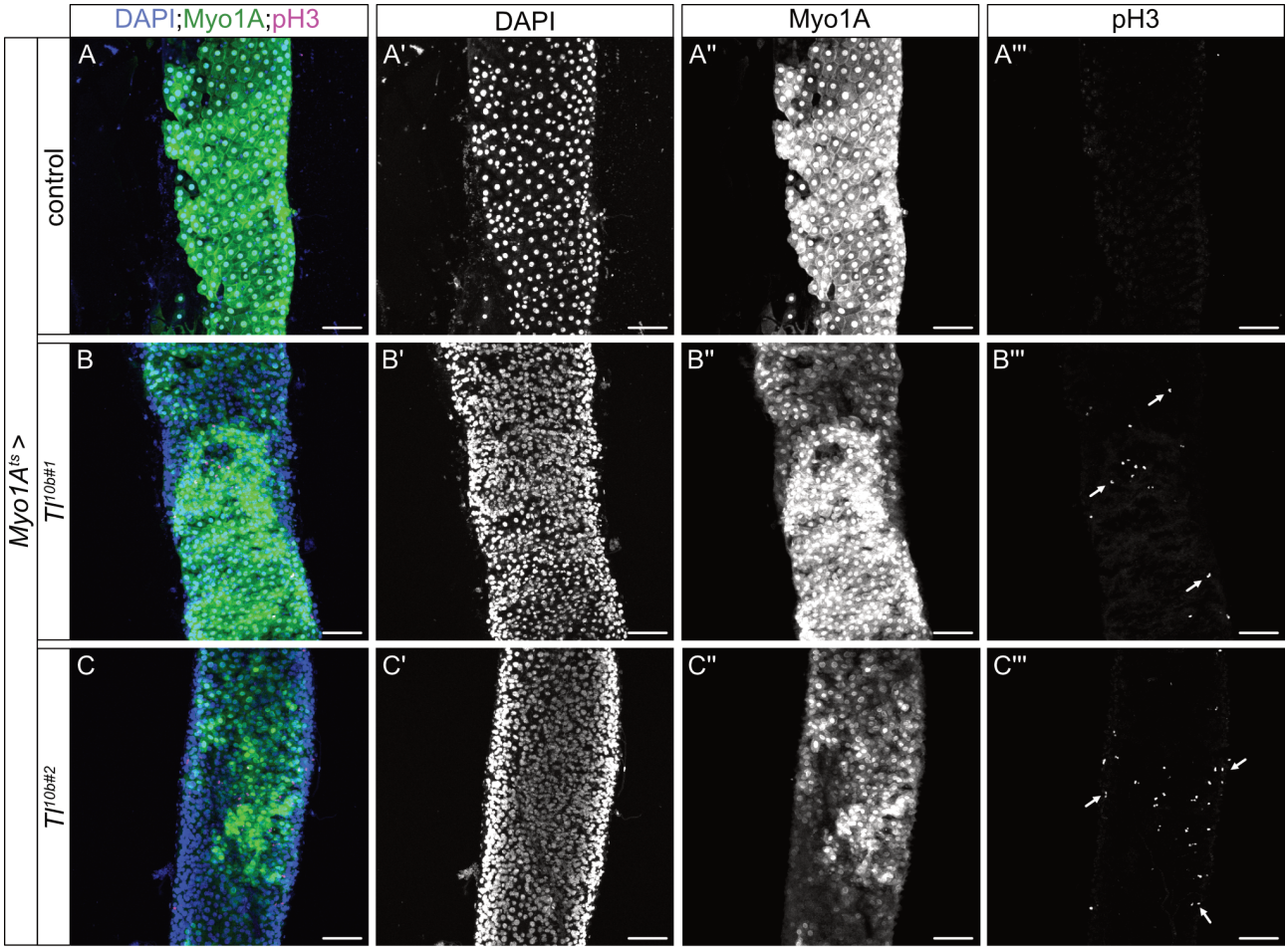

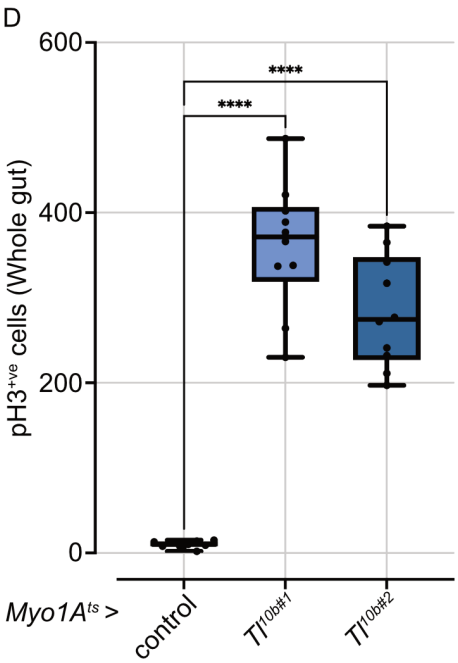

Figure 27 : Ectopic expression of Tl^{10b} in enterocytes induces non-autonomous overproliferation of stem cells in the adult midgut. (A-C) Representative images of the posterior midgut of *Myo1A^{ts}* > driven control (*w^{1118}*) **(A)**, *Tl$^{10b\#1}$* **(B)**, and *Tl$^{10b\#2}$* **(C)**, flies stained with anti-pH3 antibody. White arrows indicate pH3-positive mitotic cells in the midgut. **(D)** Quantification of pH3-positive cells per midgut of the mentioned genotypes. N = 9-10 flies; Significance values are marked by asterisks: *****P < 0.0001*; Ordinary one-way ANOVA; Scale bar = 80μm.

3.3 Modeling Renal cell carcinoma in the fly Malpighian Tubules.

Drosophila melanogaster has been a model organism of choice to decode genetic mechanisms involved in stem cell proliferation. Since several organs in flies have functional and genetic similarities to humans, they are commonly used to model tumors at the organ level including brain, prostate, and intestinal cancer [133]. For instance, several studies including the one I have presented in this thesis, have used fly midgut tumors to model human intestinal cancer and uncover novel genetic mechanisms regulating intestinal stem cell proliferation.

Another important regenerative organ that has not been extensively explored is the *Drosophila* Malpighian Tubules (MTs). MTs are an important excretory organ for toxin removal, ion exchange, and fluid transport. These functions are primarily carried out by two specialized differentiated cells namely principal cells and stellate cells [159]. Additionally, MTs contain renal stem cells (RSCs), located at the stem cell zone (ureter and lower tubule) that are formed during metamorphosis from the same group of adult midgut progenitors that give rise to adult ISCs [13, 14]. As a result, RSCs share many genetic similarities with ISCs, including the the expression of stem cell genes such as *esg* and *Delta* [160]. However, unlike ISCs, RSCs are mostly quiescent and divide slowly during homeostasis. Upon injury, RSCs exit quiescence and proliferate symmetrically to regenerate lost principal cells locally in the stem cell zone. This ability is regulated by JNK, EGFR, JAK/STAT, and Yki pathways [15]. Given that MTs share functional similarities with the mammalian kidney, such as fluid transport, stone formation, and neuroendocrine regulation, they have been commonly used to model human renal diseases, including kidney stones and ion transport malfunctions like Bartter syndrome [161]. However, very few studies have focused on modelling Renal cell carcinoma (RCC) in the fly MT.

RCC is one of the 10 most common cancers worldwide and has several subtypes. The most common subtype is clear cell Renal Cell Carcinoma (ccRCC), which constitutes about 75-80% of all RCC cases. Within ccRCC, the majority of the patients carry a biallelic loss of *Von Hippel–lindau (VHL)* gene. VHL is a component of the E3 ubiquitin ligase complex that triggers proteasomal degradation through ubiquitination of HIF1α and HIF2α [162]. This is followed by other prevalent mutations in chromatin/histone modifier tumor suppressor genes *Polybromo 1* (*PBRM1*: 40%), *SET domain containing 2* (*SETD2*: 15%) and *BRCA1 associated protein-1* (*BAP1*: 10%) [163, 164]. Flies contain orthologs of these commonly mutated ccRCC genes:

Vhl, *polybromo*, *Set2*, and *caly* **(Figure 28A)**.

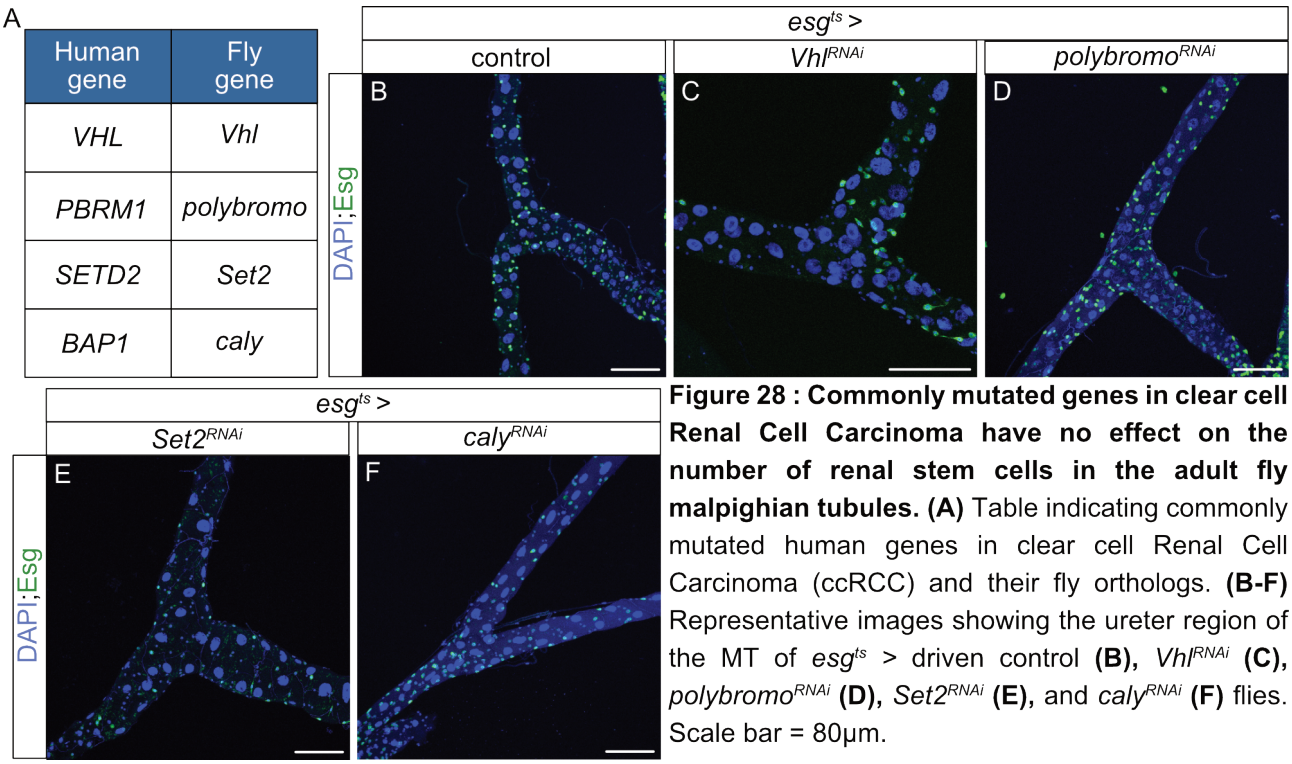

Figure 28 : Commonly mutated genes in clear cell Renal Cell Carcinoma have no effect on the number of renal stem cells in the adult fly malpighian tubules. (A) Table indicating commonly mutated human genes in clear cell Renal Cell Carcinoma (ccRCC) and their fly orthologs. **(B-F)** Representative images showing the ureter region of the MT of esg^{ts} > driven control **(B),** Vhl^{RNAi} **(C),** $polybromo^{RNAi}$ **(D),** $Set2^{RNAi}$ **(E),** and $caly^{RNAi}$ **(F)** flies. Scale bar = 80µm.

I, therefore, decided to investigate whether the knockdown of these tumor suppressor genes have any effect on RSC proliferation in the fly MT. Given that RSCs express Esg, I used the esg^{ts} driver to perform experiments in the MTs. I observed that knocking down *Vhl*, *polybromo*, *Set2*, and *caly* in fly RSCs did not affect RSC numbers as compared to control **(Figure 28B-F)**. This suggests that the knockdown of these tumor suppressor genes alone is not sufficient to promote RSC proliferation in the fly MTs.

3.3.1 Apc^{RNAi};Ras^{V12} promotes RSC proliferation in the adult malpighian tubules.

In humans, the development and growth of RCC are regulated by four major signaling pathways: Wnt, Pi3K/Akt/mTor, HGF/Met, and HIF signaling [165]. A study done in the mouse renal epithelium showed that combined activation of Pi3K/Akt/mTor and Wnt signaling through the conditional expression of *K-rasV12* and loss of *Apc* ($AhCre^{+/T}$,$K\text{-}ras^{+/LSLV12}$, $Apc^{fl/fl}$) resulted in the formation of renal carcinoma [150]. In order to test if the combined activation of Pi3K/Akt/mTor and Wnt signaling affects RSC proliferation of the fly MTs, I decided to overexpress the active form of *Ras* (Ras^{V12}) together with the knockdown of *Apc* (Apc^{RNAi}) in fly RSCs. I observed that expression of Apc^{RNAi};Ras^{V12} resulted in a significant increase in Esg

positive RSCs in the stem cell zone of the MTs as compared to control **(Figure 29A,B)**. This was associated with an increase in mitotic pH3 positive cells **(Figure 29C)** and a disruption of the renal epithelium as indicated by mislocalized Dlg staining **(Supplementary Figure S13A,B)**. Together this data indicated that expression of *Apc*^{RNAi};*Ras*^{V12} results in the formation of large MT tumors similar to those observed in the mouse renal epithelium.

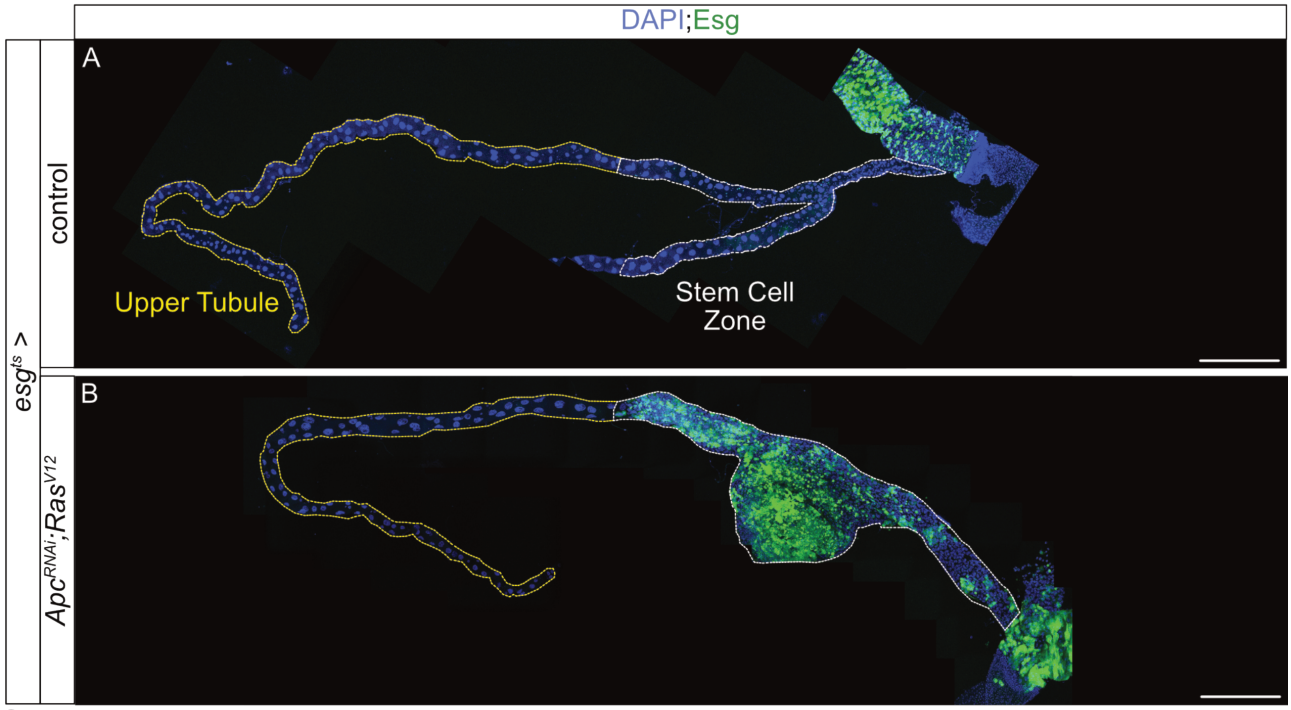

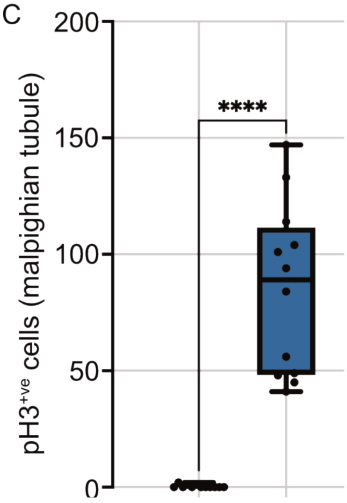

Figure 29 : Ectopic expression of *Ras*^{V12} ,together with loss of *Apc,* drives stem cell overproliferation in the adult malpighian tubules. (A-D) Representative images of the whole Malpighian tubule of *esg*^{ts} > driven control (*w*^{1118}) **(A)**, and *Apc*^{RNAi};*Ras*^{V12} **(B)** flies. **(C)** Quantification of pH3-positive cells per Malpighain tubule of the mentioned genotypes. N = 12 flies; Significance values are marked by asterisks: ****$P < 0.0001$; Mann-Whitney T-test; Scale bar = 350µm.

3.3.2 Activated Wnt signaling is necessary for *Apc^{RNAi};Ras^{V12}*-mediated MT tumorigenesis.

Activation of Wnt signaling has been implicated in several types of cancers including RCC. In RCC patients, cytoplasmic β-catenin has been associated with advanced-stage cancer [166]. Furthermore, several studies have reported an increased mRNA expression of Wnt ligands (*Wnt1* and *Wnt10*) and Fzd receptors (*Fz5* and *Fz8*), alongside a decrease in the expression of negative regulators of Wnt signaling such as *WIF1* and *sFRP1* in RCC samples [167, 168, 169, 170, 171]. Studies on the tumor suppressor gene *APC* in RCC patients have shown a reduced protein expression, loss of heterozygosity and promoter methylation, all indicative of Wnt signaling activation [172, 173, 174].

Introduction of the mutant allele of *APC* in the mouse renal epithelium resulted in the nuclear localization of β-catenin, which was further enhanced upon expression of *K-ras^{V12}* indicating Wnt signaling activation [150, 175]. I, therefore, decided to test if the expression of *Apc^{RNAi};Ras^{V12}* in fly RSCs would also result in the activation of Wnt signaling in the fly MTs. To do this, I stained the MTs expressing *Apc^{RNAi};Ras^{V12}* for the fly β-catenin, Armadillo (Arm). I observed that similar to the fly midgut, Arm is located at the cell membrane of RSCs in control MTs **(Figure 30A)**. However, upon expression of *Apc^{RNAi};Ras^{V12}* in RSCs, I observed the relocalization of Arm to the cytoplasm, which indicates an activation of Wnt signaling in the MTs **(Figure 30B, White arrows)**.

In flies, Wnt signaling regulates the expression of downstream target genes such as *fz3*. Several studies have used the Fz3-RFP reporter fly line to assess Wnt activity in the midgut [176, 177]. To determine whether *Apc^{RNAi};Ras^{V12}* expressing RSCs activate Wnt signaling in the MT, I utilized this reporter construct. While there was no Fz3-RFP expression in the control MTs, *Apc^{RNAi};Ras^{V12}* MTs exhibited increased Fz3-RFP expression **(Figure 30C,D)**. Through RNA sequencing of the fly MT, I also observed an increase in *fz3* mRNA levels in *Apc^{RNAi};Ras^{V12}* MTs as compared to controls (log2 Fold Change = 2.23, Padj = 1.02E-0.7) **(Supplementary Figure S14)**. Altogether I conclude that the expression of *Apc^{RNAi};Ras^{V12}* in RSCs leads to the activation of Wnt signaling, as indicated by the cytoplasmic localization of Arm, increased Fz3-RFP reporter expression, and elevated *fz3* mRNA levels.

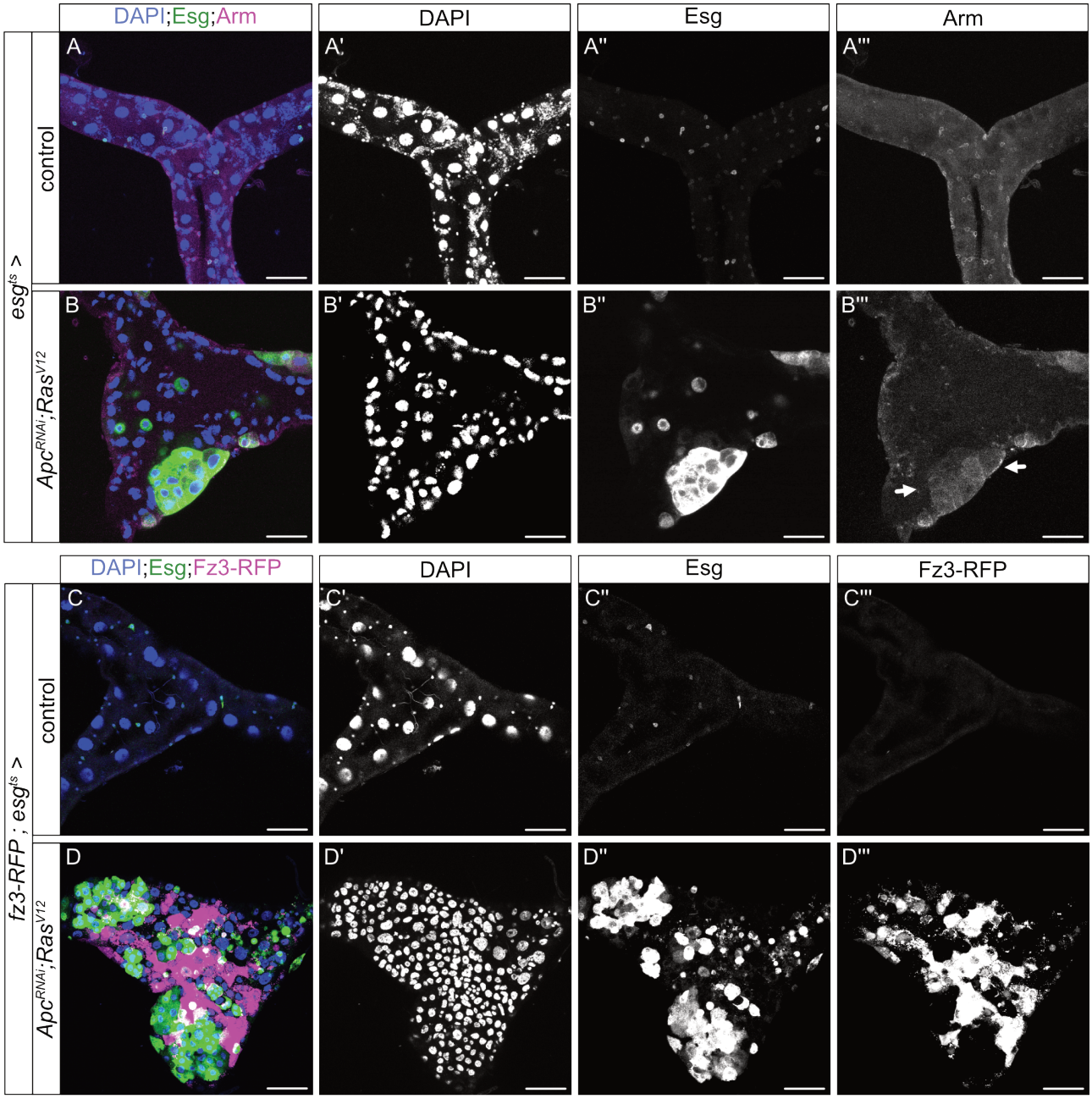

Figure 30 : *Apc*^{RNAi}*;Ras*^{V12} activates Wnt signaling in the adult malpighian tubules. (A-B) Representative images of the ureter of *esg*^{ts} > driven control *(w*^{1118}*)* **(A)** and *Apc*^{RNAi}*;Ras*^{V12} **(B)** flies stained with anti-Arm antibody. White arrows indicate staining of cytoplasmic Arm which can only be seen in *Apc*^{RNAi}*;Ras*^{V12} malpighian tubule as compared to control, where Arm localizes on the cell membrane. **(C-D)** Representative images of the ureter of *fz3-RFP;esg*^{ts} > driven control *(w*^{1118}*)* **(C)** and *Apc*^{RNAi}*;Ras*^{V12} **(D)** flies. Note that only *Apc*^{RNAi}*;Ras*^{V12} activates Fz3-RFP expression in the ureter of the malpighian tubule as compared to control. Scale bar = 80µm.

Given that the expression of *Apc*^{RNAi}*;Ras*^{V12} in RSCs result in a strong activation of Wnt signaling in the MT, I decided to investigate if activated Wnt signaling is required for RSC overproliferation. To address this, I chose to suppress Wnt signaling upstream and downstream of *Apc* by knocking down *wg* (*wg*^{RNAi}) or overexpressing the dominant negative form of *pan*

(*pan*^{DN}) respectively. In line with previous observations, expression of *Apc*^{RNAi};*Ras*^{V12} resulted in an increase in Esg-positive RSCs and activation of Fz3-RFP-positive Wnt signaling in the MTs **(Figure 31A)**. However, I noticed that loss of *pan*, but not *wg* reduced RSC overproliferation, as well as Wnt activation in *Apc*^{RNAi};*Ras*^{V12} expressing MTs **(Figure 31B,C)**. This suggests that Wnt signaling, downstream of Apc, is required for *Apc*^{RNAi};*Ras*^{V12}-mediated MT tumorigenesis.

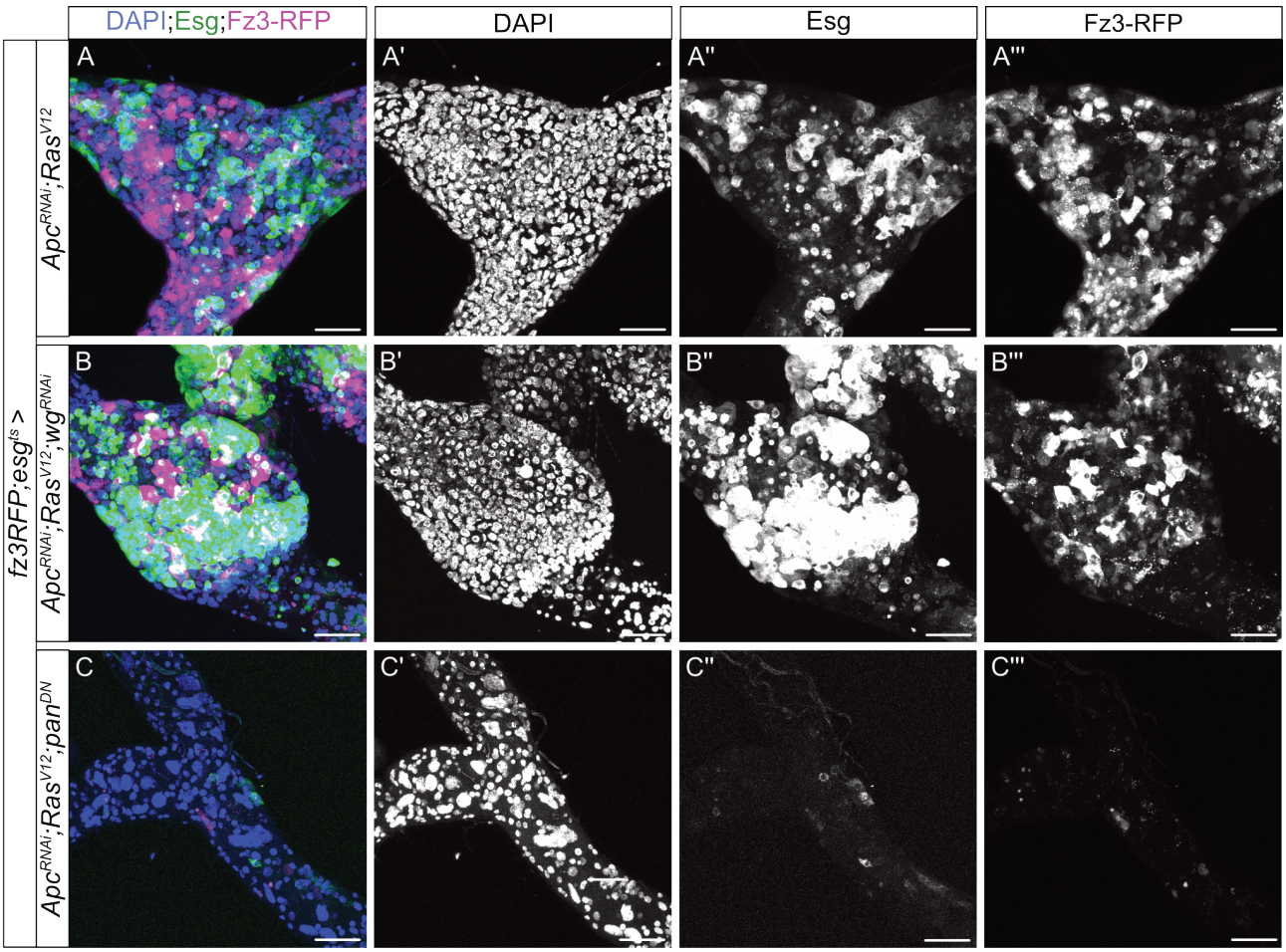

Figure 31 : Pan is required for *Apc*^{RNAi};*Ras*^{V12}-mediated tumorigenesis in the adult malpighian tubules. **(A-C)** Representative images of the ureter of *fz3-RFP;esg*^{ts} > driven *Apc*^{RNAi};*Ras*^{V12} **(A)**, *Apc*^{RNAi};*Ras*^{V12};*wg*^{RNAi} **(B)**, and *Apc*^{RNAi};*Ras*^{V12};*pan*^{DN} **(C)** flies. Note that suppression of *pan* (downstream of *Apc*) but not *wg* (upstream of *Apc*) rescues *Apc*^{RNAi};*Ras*^{V12}-mediated tumorigenesis and Wnt activation (Fz3-RFP) in the malpighian tubules. Scale bar = 45μm.

3.3.3 Activated Pi3K/Akt/mTor signaling is necessary for *Apc*^{RNAi};*Ras*^{V12}-mediated MT tumorigenesis.

EGFR signaling, which regulates both the Pi3K/Akt/mTor and Raf/MEK/ERK pathways through the activity of the oncogene K-ras, is required for the proliferation of various cancers [178, 179]. In RCC patients, activation of the Pi3K/AKT/mTor signalling pathway is frequently associated

with aggressive renal tumors and poor survival rate [180, 181]. Furthermore, mutations in negative regulators such as *PTEN* and *TSC1/2* have been identified in RCC patients, leading to the activation of Pi3K/AKT/mTor signaling pathway [182].

Sansom *et al.* demonstrated that *AhCre*$^{+/T}$,*K-ras*$^{+/LSLV12}$, *Apc*$^{fl/fl}$ mice with renal carcinoma exhibited an activation of the Pi3K/Akt/mTor signaling pathway in the renal epithelium [150]. In order to test if the expression of *Apc*^{RNAi};*Ras*^{V12} in fly RSCs would activate Pi3K/AKT/mTor signalling, I performed immunostaining of the MT for the Pi3K/AKT/mTor signaling reporter p4EBP. While I did not observe any p4EBP staining in the control MT, I detected p4EBP in MT expressing *Apc*^{RNAi};*Ras*^{V12} **(Figure 32A,B)**. This indicates that the expression of *Apc*^{RNAi};*Ras*^{V12} in RSCs of the fly MT activates the Pi3K/Akt/mTor signaling pathway.

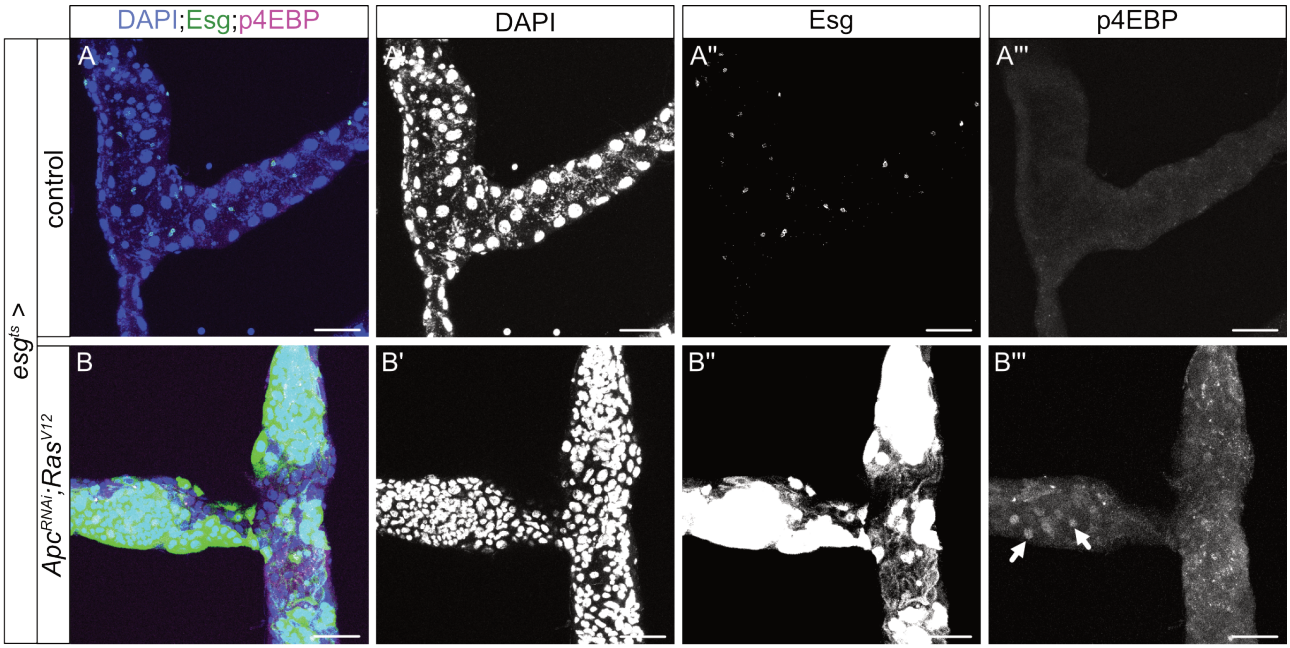

Figure 32 : *Apc*^{RNAi};*Ras*^{V12} activates Pi3K/Akt/mTor signaling in the adult malpighian tubules. (A-B) Representative images of the ureter of *esg*^{ts} > driven control *(w*^{1118}*)* **(A)** and *Apc*^{RNAi};*Ras*^{V12} **(B)** flies stained with anti-p4EBP antibody. White arrows indicate staining of p4EBP, which can only be seen in *Apc*^{RNAi};*Ras*^{V12} malpighian tubules. Scale bar = 45µm.

I next asked whether activated Pi3K/Akt/mTor signaling is required for RSC overproliferation in *Apc*^{RNAi};*Ras*^{V12} MT. To examine this, I chose to suppress Pi3K/Akt/mTor signaling upstream and downstream of *Ras* by knocking down *Egfr* (*Egfr*^{RNAi}) and *Akt* (*Akt*^{RNAi}) respectively. I noticed that knockdown of *Akt* but not *Egfr* reduced RSC overproliferation, as well as Wnt activation in *Apc*^{RNAi};*Ras*^{V12} expressing MT **(Figure 33A-C)**. Therefore, this data suggests that Pi3K/Akt/mTor signaling, downstream of Ras, is required for *Apc*^{RNAi};*Ras*^{V12}-mediated MT tumorigenesis.

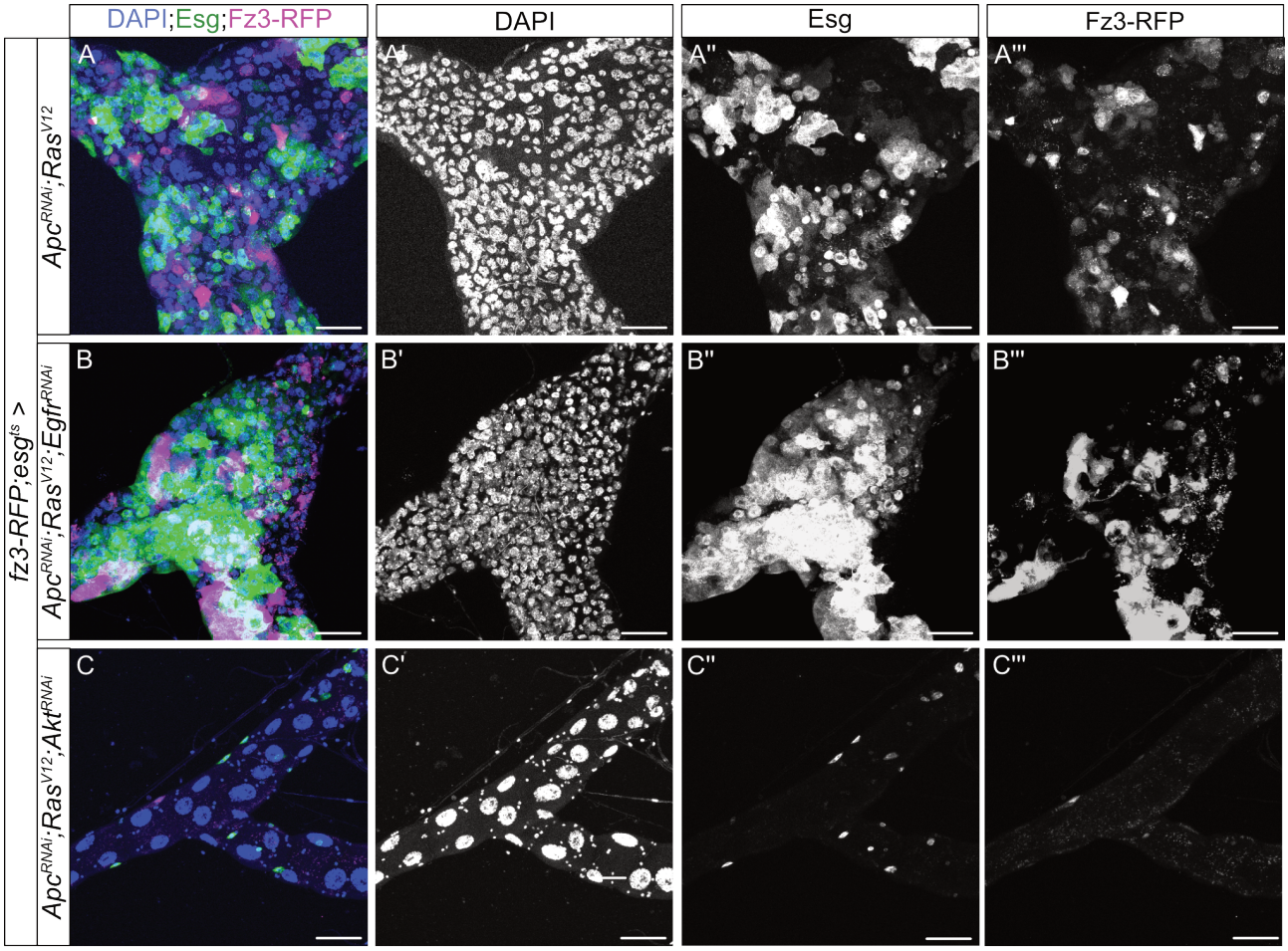

Figure 33 : Akt is required for *Apc^{RNAi};Ras^{V12}*-mediated tumorigenesis in the adult malpighian tubules. **(A-C)** Representative images of the ureter of *fz3-RFP;esg^{ts}* > driven *Apc^{RNAi};Ras^{V12}* **(A)**, *Apc^{RNAi};Ras^{V12};Egfr^{RNAi}* **(B)**, and *Apc^{RNAi};Ras^{V12};Akt^{RNAi}* **(C)** flies. Note that suppression of *Akt* (downstream of *Ras*) but not *Egfr* (upstream of *Ras*) rescues *Apc^{RNAi};Ras^{V12}*-mediated tumorigenesis and Wnt activation (Fz3-RFP) in the malpighian tubules. Scale bar = 45μm.

Sansom *et al.* also demonstrated that *AhCre$^{+/T}$,K-ras$^{+/LSLV12}$, Apc$^{fl/fl}$* renal tumor mice displayed activation of the Raf/MEK/ERK signaling pathway in the renal epithelium [150]. To test if this is also true in the fly MT, I looked at the expression of Raf/MEK/ERK target genes *CycE*, *Ets21C*, and *stg* [183]. Expression of *Apc^{RNAi};Ras^{V12}* led to a significant increase in transcript levels *CycE* (log2 Fold Change = 0.815, Padj = 0.0000784), *Ets21C* (log2 Fold Change = 4.268, Padj = 6.4E-28), and *stg* (log2 Fold Change = 6.675, Padj = 9.83E-29) as compared to control MT **(Figure 34A-C)**. This confirms that similar to the mouse renal epithelium, expression of *Apc^{RNAi};Ras^{V12}* in RSCs result in the activation of the Raf/MEK/ERK signaling pathway in the fly MT.

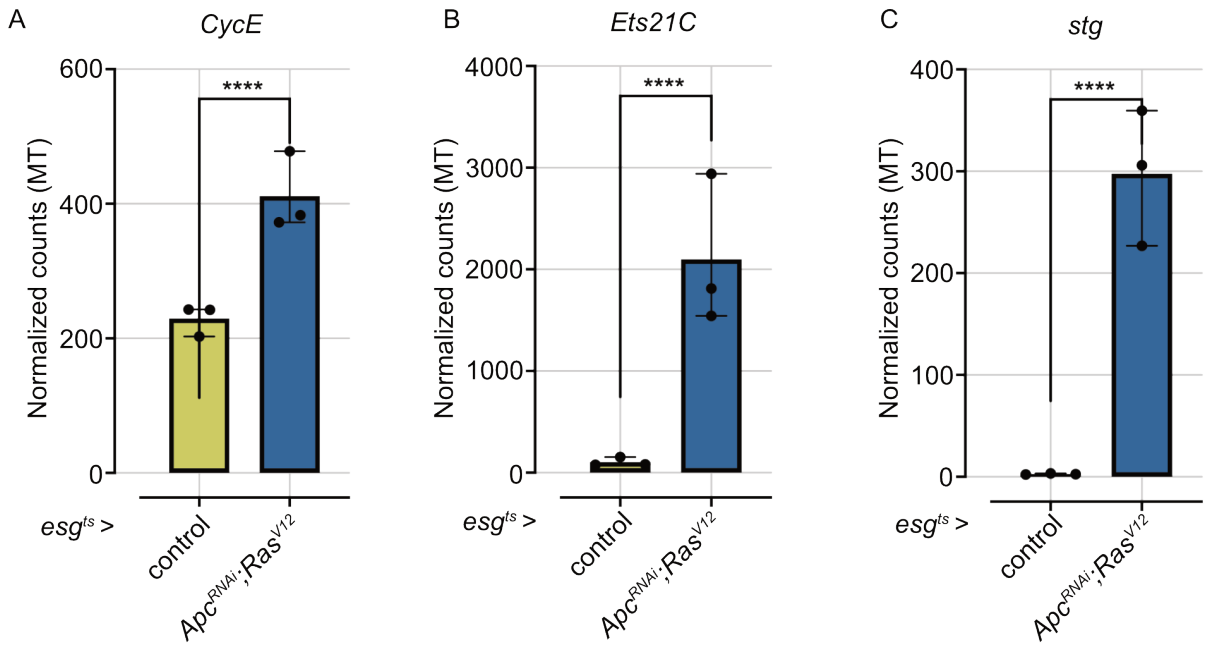

Figure 34 : *Apc^{RNAi};Ras^{V12}* activates Raf/MEK/ERK signaling in the adult malpighian tubules. Normalized counts of Raf/MEK/ERK target genes *CycE* **(A),** *Ets21C* **(B),** and *stg* **(C)** from bulk RNA sequencing of MT of *esg^{ts}* > driven control and *Apc^{RNAi};Ras^{V12}* flies; Wald test and benjamini hochberg correction to obtain adj p-value; Significance values are marked by asterisks: *****P < 0.0001*.

I next decided to investigate whether active Raf/MEK/ERK signaling is required for *Apc^{RNAi};Ras^{V12}*-mediated MT tumorigenesis. To test this, I knocked down *Dsor1*, which lies downstream of *Ras* in the Raf/MEK/ERK axis. Suppression of *Dsor1* resulted in the reduction of *Apc^{RNAi};Ras^{V12}*-mediated RSC overproliferation as well as Wnt activation **(Figure 35A,B)**, suggesting that the Raf/MEK/ERK signaling pathway, downstream of Ras, is also essential for *Apc^{RNAi};Ras^{V12}*-mediated MT tumorigenesis.

Altogether, I conclude that the expression of *Apc^{RNAi};Ras^{V12}* in RSCs of the fly MT leads to the activation of both the Pi3K/Akt/mTor and Raf/MEK/ERK signaling pathways, which are required for tumorigenesis in the MT.

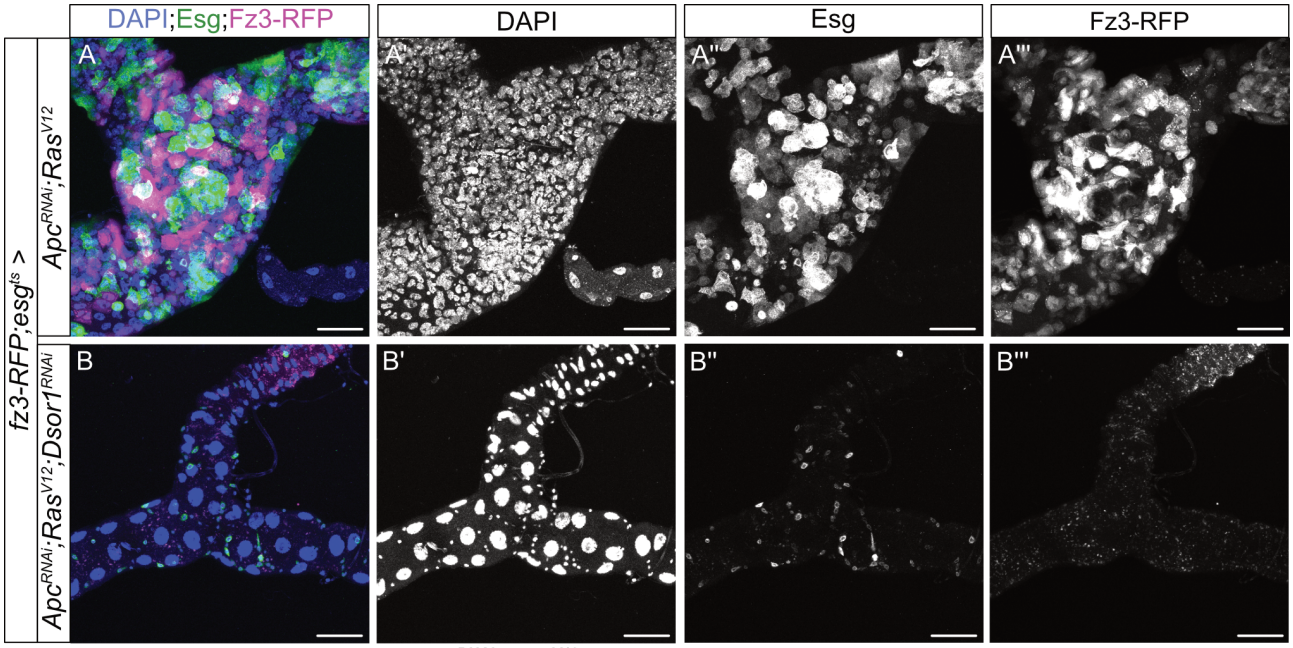

Figure 35 : Dsor1 is required for *Apc^{RNAi};Ras^{V12}*-mediated tumorigenesis in the adult malpighian tubules. **(A-B)** Representative images of the ureter of *fz3-RFP;esg^{ts}* > driven *Apc^{RNAi};Ras^{V12}* **(A)**, and *Apc^{RNAi};Ras^{V12};Dsor1^{RNAi}* **(B)** flies**.** Note that suppression of *Dsor1* (downstream of *Ras*) can rescue *Apc^{RNAi};Ras^{V12}*-mediated tumorigenesis and Wnt activation (Fz3-RFP) in the malpighian tubules. Scale bar = 45μm**.**

3.3.4 Functional characterization of genes required for RCC using the fly MT *Apc^{RNAi};Ras^{V12}* tumor model

In the previous sections, I demonstrated that the expression of *Apc^{RNAi};Ras^{V12}* in RSCs of the fly MT leads to the formation of rapidly proliferating renal tumors, driven by the activation of Wnt, Pi3K/Akt/mTor, and Raf/MEK/ERK signaling pathways. Given that similar mechanisms are also reported in the renal epithelium of *AhCre$^{+/T}$,K-ras$^{+/LSLV12}$, Apc$^{fl/fl}$* mice, I conclude that *Apc^{RNAi};Ras^{V12}* flies can be used for studying mammalian RCC and identifying novel genes required for cancer growth and progression.

In order to identify novel genes essential for tumor growth in RCC, I first aimed to identify human genes that are overexpressed in RCC patients. In collaboration with Erica Valentini from the Boutros lab (DKFZ, Heidelberg), I extracted a list of genes overexpressed in ccRCC patients from the publicly available Kidney Renal Clear Cell Carcinoma (TCGA, PanCancer Atlas) database [184, 185]. From a database of 512 ccRCC patients (kirc), 1764 human genes were overexpressed, with a median Z-score greater than 2. Among these, 319 genes had homologs in the fly genome. I selected 15 fly genes at random **(Figure 36A)** and performed a reverse

genetic screen by knocking down each gene individually in the fly *Apc*^{RNAi};*Ras*^{V12} MT tumor model.

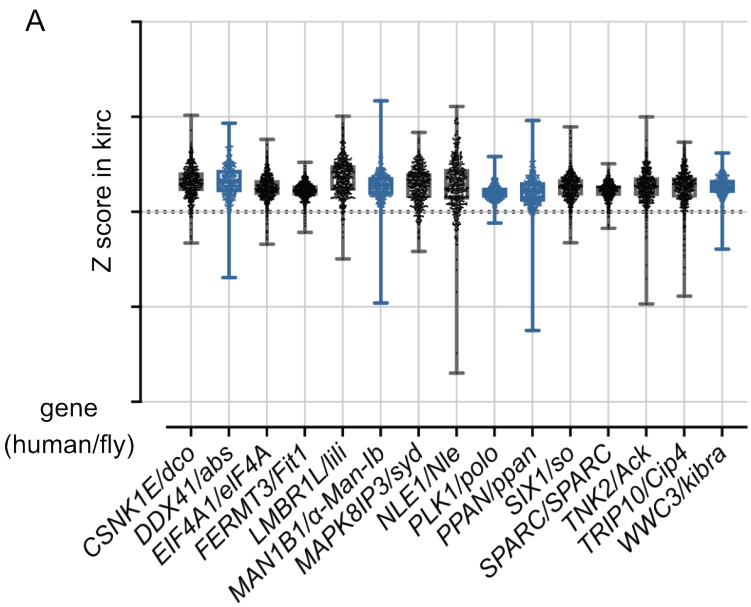

Figure 36 : *Apc*^{RNAi};*Ras*^{V12} MT tumors can be used to study human gene function in renal cancer . (A) Z-scores of the upregulated human genes in Kidney Renal Clear Cell Carcinoma samples (kirc) and their fly orthologs. **(B-G)** Representative images of the ureter of *fz3-RFP;esg*^{ts} > driven *Apc*^{RNAi};*Ras*^{V12} **(B)**, *Apc*^{RNAi};*Ras*^{V12};*abs*^{RNAi} **(C)**, *Apc*^{RNAi};*Ras*^{V12};*α-Man-Ib*^{RNAi} **(D)**, *Apc*^{RNAi};*Ras*^{V12};*polo*^{RNAi} **(E)**, *Apc*^{RNAi};*Ras*^{V12};*ppan*^{RNAi} **(F)**, *and Apc*^{RNAi};*Ras*^{V12};*kibra*^{RNAi} **(G)** flies. Blue bars represent genes whose knockdown reduces MT tumor phenotype in the adult fly. Scale bar = 80*μ*m.

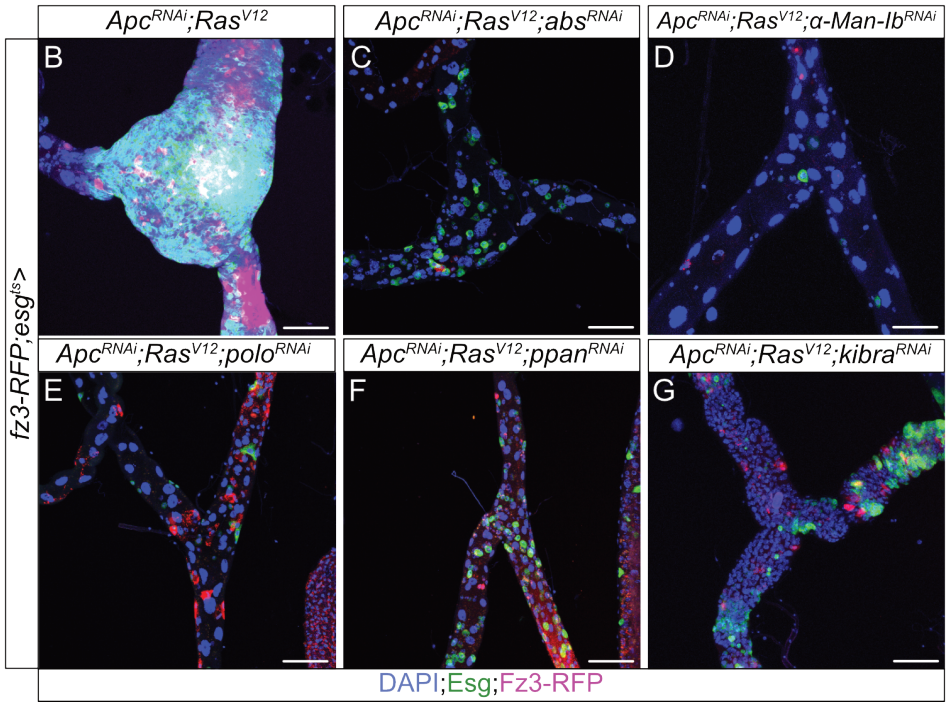

I observed that knockdown of 5 genes: *abs*, *α-Man-Ib*, *polo*, *ppan*, and *kibra* reduced *Apc*^{RNAi};*Ras*^{V12}-mediated RSC overproliferation and Wnt activation **(Figure 36B-G)**. Experimental evidence have shown that human homologs of *abs* and *polo*, DDX41 and PLK1 respectively are upregulated in RCC patients, however the molecular mechanism by which they drive RCC proliferation and growth is unknown [186, 187]. Using the *Apc*^{RNAi};*Ras*^{V12} MT tumor

model, additional genes involved in tumor growth can be identified, and their underlying genetic mechanisms can be studied. These findings can then be validated in higher mammalian models.

4 Discussion

Regenerative organs such as the *Drosophila* midgut and malpighian tubules, are constantly exposed to threats from harmful toxins and pathogenic microbes, which can disrupt their epithelial architecture. A group of dividing stem cells in these organs is responsible for replacing damaged cells with new, differentiated cells, while maintaining their own pool of progenitors. This process of epithelial regeneration is tightly regulated by a complex genetic network, the disruption of which leads to uncontrolled proliferation and mis-differentiation. In my thesis, I used the *Drosophila melanogaster* model to identify previously uncharacterized genes required for regulating stem cell function in the midgut and malpighian tubules.

4.1 CRISPR/Cas9 to generate midgut tumors in flies

Drosophila melanogaster is a widely used *in-vivo* model organism for studying gene function through genetic manipulation. One of the most common methods for this is RNA interference (RNAi) using dsRNA, which silences genes post-transcriptionally by degrading target mRNA, thereby preventing its translation. Since the expression of dsRNA is transient and relies on the Gal4/UAS system, the effects of RNAi do not persist in daughter cells that do not express Gal4. Therefore, only those cells that continuously express dsRNA will exhibit a gene knockdown. In contrast, DNA mutations are passed down through cellular lineages, leading to the accumulation of large populations of mutant cells, a phenomenon frequently observed in cancer. Using CRISPR/Cas9, researchers can introduce DNA mutations into any gene in flies, including tumor suppressor genes, effectively mimicking cancer development in this model organism [139].

Since a large-scale CRISPR fly library targeting various fly genes has recently been created, my first aim was to establish a method to generate a fly midgut tumor model using CRISPR/Cas9 [137]. To achieve this, I expressed Cas9 specifically in the progenitor population of the midgut using the esg enhancer-driven Gal4. I noticed that in the midguts where I continuously expressed *UAS Cas9.P2*, the expected age-dependent increase in progenitor cells was suppressed **(Figure 9C-G)**. This could be due to high levels of Cas9 in the progenitor cells, which may be deleterious to their function in the midgut. The toxic effects of Cas9 have been reported in other *in-vitro* and *in-vivo* systems including flies, where high levels of Cas9 in wing discs induced cellular apoptosis even in the absence of a guide RNA [137, 188, 189]. Port *et al.* demonstrated that reducing

the amount of Cas9 prevented such toxic effects on cells [137]. Therefore, I decided to use the Gal80^{ts} system to temporally limit Gal4/UAS-dependent Cas9 expression. At lower temperatures (18°C), Gal80^{ts} restricts the activity of Gal4, preventing Cas9 expression. However, at higher temperatures (29°C), Gal80^{ts} can no longer bind to Gal4, allowing Gal4-dependent transcription of Cas9. By placing the flies at different temperatures, I devised an ON/OFF strategy to control Cas9 expression specifically in the adult midgut progenitor cells. Using this method, I successfully generated midgut tumors by targeting tumor suppressor genes *N*, *neur*, and *Mad* **(Figure 10G-L)**.

While the *Cas9.P2$^{ON/OFF}$* method can be used to limit Cas9 toxicity and generate midgut tumors, it has two major limitations. First, this method relies on the Gal80^{ts} system, which requires changing the incubation temperature to restrict Gal4 activity. Temperature has been shown to influence the development and lifespan of the fly, which can, in turn, alter the aging process [190]. Aging can impact stem cell function and midgut homeostasis, both of which are important for organismal health [191]. Second, it takes 40 days for the limited expression of Cas9 to develop into a tumor phenotype in the adult fly as compared to just 15-20 days for the RNAi.

To address both these limitations, Port *et al.* developed a system to fine-tune the expression of Cas9, independent of the Gal4 enhancer strength. This system operates on the biological principle of ribosomal reinitiation and employs an upstream open reading frame (uORF) to reduce the translation of the downstream Cas9 sequence. In eukaryotes, ribosomes scan mRNA and initiate translation at the first AUG initiator codon. However, when the AUG codon is followed closely by a stop codon, post-termination ribosomes may continue scanning and reinitiate the translation of a downstream sequence that contains a start codon. The length of the uORF influences the extent of this reinitiation of ribosomal translation. Short-length uORF allows for more reinitiation of ribosomes, leading to increased translation events, whereas longer uORFs allow for fewer reinitiation events, causing reduced translation [192]. Port *et al.* introduced uORFs of varying lengths, from 30bp to 714bp upstream of the Cas9 sequence, and found that a 114bp uORF (*UAS-uMCas9*) prevented Cas9-mediated toxicity, while still maintaining gene-editing capability [137]. I showed that prolonged expression of *UAS-uMCas9* was non-toxic to progenitor cells as indicated by the age-dependent increase in stem cell phenotype. Additionally, targeting the tumor suppressor genes *N*, *neur* and *Mad* with prolonged *UAS-uMCas9* expression resulted in the formation of midgut tumors. This was not the case

when Cas9 was expressed for the same duration with *UAS Cas9.P2*, indicating that the addition of uORF can effectively titrate Cas9 levels and produce genetic mutations without toxic effects [139].

For my thesis, I chose to use the Notch loss-of-function midgut tumor model to identify unknown genes required for the regulation of stem cell function [6]. In the fly midgut, Notch signaling acts as a genetic switch that regulates the differentiation fate of progenitor cells. ISCs express *Delta*, which binds to the Notch receptor and activates Notch signaling in EBs. High Notch signaling in EBs facilitates their differentiation into ECs, while reduced Delta levels lead to low Notch activity, committing ISCs to differentiate into EEs. Genetic disruption of Notch signaling prevents EB differentiation, resulting in the accumulation of dividing ISCs and differentiated EEs in the fly midgut [6]. I confirmed that knockout of the Notch receptor using *Cas9.P2*$^{ON/OFF}$-mediated mutagenesis resulted in the formation of clusters of dividing stem cells and differentiated EEs. However, the effect of Cas9-mediated Notch receptor knockout was significantly weaker than RNAi-mediated knock-down of the *Notch* receptor (N^{RNAi}) **(Figure 11)**. This could be due to the limitations of the CRISPR/Cas9 system, such as low efficiency of the Notch guide-RNA in editing the Notch gene, error-free repair of Cas9-induced breaks by homology-directed repair (HDR), or the introduction of silent mutations in the *Notch* gene. Additionally, some clones that fail to mutate the *Notch* gene proliferate normally, while those that successfully mutate the *Notch* gene develop tumors. This would dilute the overall phenotypic effect of CRISPR/Cas9-mediated mutagenesis in the fly midgut. In contrast, the knockdown of the *Notch* transcript by N^{RNAi} depends largely on the efficiency of the RNAi targeting the gene. Since N^{RNAi} effectively targets the *Notch* transcript in all progenitor cells, it results in the formation of a stronger phenotype across the midgut.

One potential solution to improve the phenotypic outcome of the CRISPR/Cas system can be through introducing larger mutations or increasing the probability of mutations by multiplexing more than two guides targeting the same gene. In flies, CRISPR/Cas12a system has been shown to facilitate easier multiplexing of multiple guides in a single CRISPR RNA (crRNA) array compared to the Cas9 system [193]. This is because Cas12a has endogenous RNase activity, which can process single crRNAs from the crRNA array. Additionally, Cas12a-mediated gene disruption was shown to be more effective than Cas9-mediated mutation in flies [193]. It would be interesting to test if CRISPR/Cas12a is more effective in producing a stronger Notch loss-

of-function midgut tumor phenotype compared to CRISPR/Cas9. This system could also be used in the future to target many other tumor suppressor genes in the fly midgut, facilitating the generation of additional tumor models for further studies.

4.2 Nerfin-1 regulates intestinal stem cell proliferation in the fly midgut

The main goal of this section was to identify novel genes required to regulate stem cell proliferation using the Notch loss-of-function midgut tumor model. Tumorigenesis is triggered by the breakdown of the genetic network that controls stem cell proliferation. Misexpression of regulatory genes is a significant event that can be identified through transcriptomics. The recently developed single-cell RNA sequencing (scRNA-seq) technique has successfully been used to capture transcriptomic reads at the single-cell level in the *Drosophila* midgut [142]. By clustering cells with similar transcriptomic profiles along with specific cell type marker genes, we can gain insights into the cellular composition. Direct comparisons between the transcriptomes of different genotypes can be made at the cellular level, making scRNA-seq a powerful tool for decoding genetic interactions. Single-cell RNA sequencing of the Notch loss-of-function midgut tumors revealed a significant increase in ISCs (Esg-positive, Dl-positive), EEPs (Esg-positive, Pros-positive, Su(H)-negative), and EEs (Pros-positive), along with a decrease in EBs (Esg-positive, E(spl)mbeta-HLH-positive) and ECs **(Figure 12A,B, Supplementary Figure S1)**. This finding aligns with previous studies suggesting that suppression of Notch signaling primes ISCs to divide and differentiate into EEs via transient EEPs [5, 33].

A comparison of the transcriptomes of the Esg-positive progenitor population between Notch loss-of-function and control midguts revealed a total of 288 differentially expressed genes. Notably, Enhancer of split complex genes (*E(spl)m3-HLH*, *E(spl)malpha-BFM*, *E(spl)m6-BFM*, and *E(spl)mgamma-HLH*) were significantly downregulated. Bardin *et al.* showed that enhancer-of-split complex genes are key Notch target genes, which are essential for preventing ISC self-renewal in the adult fly midgut. The loss of these genes increased Delta-positive ISCs, mirroring the Notch loss-of-function phenotype [34]. Additionally, I also observed an upregulation of the ISC marker *Delta*, which is typically associated with an increased ISC population [6]. Furthermore, genes required for EE cell fate commitment (*sc*, *ase*, and *pros*) were also upregulated in the progenitor population of the Notch loss-of-function midgut **(Figure 12C)** [5].

Using the Notch loss-of-function midgut tumor as a phenotypic readout, I conducted a reverse genetic screen of the upregulated genes in the progenitor population. For this screen, I chose to suppress Notch using RNAi instead of CRISPR/Cas9 for two major reasons. First, there is a low probability that the guide-RNAs will successfully and simultaneously mutate both *Notch* and the gene of interest in the same cell of the midgut. Variations in editing probabilities can lead to the formation of distinct clones, complicating the interpretation of genetic interactions. Second, the tumor phenotype induced by CRISPR/Cas9 is weaker and takes longer to develop as compared to RNAi-mediated knockdown. Therefore, knocking down *Notch* provides a more effective experimental model for conducting the reverse genetic screen.

By following this reverse genetic screening approach, I identified 28 genes whose knockdown significantly reduced the N^{RNAi}-mediated midgut tumor phenotype. These included genes involved in DNA replication (*PolZ1*), mitosis (*Pen* and *Kmn1*), and regulators of Notch signaling (*sc*, *spdo*, *insb*, and *nerfin-1*) **(Figure 13)**. In this screen, *sc* served as the positive control. Bardin *et al.* showed that the transcription factor Scute (Sc) is expressed in both ISCs and EEs in the adult midgut. They also demonstrated that Sc is essential for specifying EE cell fate from ISCs, as its overexpression led to an expansion of EE cells [34]. Zeng *et al.* further indicated that active Notch signaling in ISCs prevents EE differentiation by restricting *sc* expression [5]. I confirmed that the knockdown of *sc* in N^{RNAi} progenitor cells significantly reduced the number of EE cells as well as stem cell mitosis.

The next candidate gene I chose to study was *nerfin-1*, whose role in intestinal stem cell function has not yet been investigated. Nerfin-1 is a zinc finger transcription factor, which maintains the differentiated state of medullary neurons in the larval central nervous system (CNS). Loss of Nerfin-1 upregulates Notch signaling and promotes de-differentiation of neurons into dividing neuroblasts [144, 145]. Given Nerfin-1's ability to maintain cell fate by negatively regulating Notch signaling in the larval CNS, it is an interesting candidate to study in midgut tumorigenesis. My data indicated that the disruption of Notch signaling in progenitor cells disturbs the cellular differentiation machinery in the midgut. This forces ISCs to either divide or differentiate into EEs to form tumorigenic clusters. Rapidly dividing ISCs in tumor midguts exhibited increased *nerfin-1* expression, and its knockdown reduced both stem cell proliferation and EE differentiation, similar to the effects seen with *sc* knockdown **(Figure 14, Supplementary Figure S2)**. Additionally, suppression of *nerfin-1* mitigated early death in adult

flies caused by midgut tumors **(Figure 15)**. This suggests that active Notch signaling promotes EC differentiation and prevents ISC division by suppressing the expression of *nerfin-1*. In the absence of Notch signaling, *nerfin-1* expression is upregulated in the progenitor population, promoting stem cell proliferation and EE differentiation.

Even under homeostasis, the knockdown of *nerfin-1* resulted in a reduced number of progenitor cells and stem cell proliferation **(Figure 18)**. By tracking the stem cell lineage, I observed that the knockdown of *nerfin-1* in progenitor cells resulted in small clones primarily consisting of large nucleated ECs with very few to no small nucleated progenitors or EEs **(Supplementary Figure S6)**. This suggests that progenitor cells require Nerfin-1 to maintain their identity, the loss of which forces them to differentiate into ECs. This depletes the progenitor cell pool in the midgut. Such a reduction in progenitor cells due to *nerfin-1* knockdown hindered the midgut's ability to regenerate following pathogenic infection **(Figure 17)**. This indicates that Nerfin-1 is an important transcription factor that regulates progenitor proliferation and differentiation in the fly midgut.

While I demonstrated that Nerfin-1 can regulate the proliferation and differentiation of progenitor cells in the fly midgut, the underlying mechanism remains unknown. A previous study in the larval CNS indicated that the loss of Nerfin-1 leads to the upregulation of the Hippo pathway genes [145]. In the adult fly midgut, upregulation of the Hippo pathway prevents stem cell proliferation, which resembles the phenotype I observed upon *nerfin-1* knockdown [194]. Therefore, I speculate that similar to its role in the larval CNS, Nerfin-1 might also regulate the Hippo pathway genes in the midgut, thereby modulating stem cell proliferation.

In another study conducted by Kuzin *et al.*, it was found that Prospero (Pros) regulates axon guidance through Nerfin-1 in the developing fly nervous system [195]. Given that Pros is a well-known EE marker and is essential for EE differentiation in the midgut, it is likely that Nerfin-1 functions downstream of Pros in regulating EE differentiation in the midgut. This could be analysed by checking the expression level of *nerfin-1* in *pros* mutant flies. However, genetically testing this epistatic relationship might be challenging, as overexpression of *pros* does not produce an observable phenotype [5]. Nevertheless, Zeng *et al.* demonstrated that Pros regulates EE cell fate downstream or in parallel to the Achaete-Scute complex (AS-C), whose components, Sc or Ase, significantly increase EE production in progenitors when overexpressed in the midgut [5]. The role of Nerfin-1 in regulating EE cell fate downstream of

the AS-C-Pros axis could be tested by knocking down *nerfin-1* in flies overexpressing Sc or Ase and analyzing EE abundance.

While the loss of *nerfin-1* reduced stem cell proliferation and promoted EC differentiation, overexpression of *nerfin-1* had no significant effect on stem cell proliferation or EE differentiation **(Supplementary Figure S7)**. This may indicate that Nerfin-1 alone is insufficient to elicit changes in progenitor cells and may require additional interacting partners. One potential partner is the Yki transcriptional co-activator Scalloped (Sd), which has been shown to physically interact with Nerfin-1 and maintain the cellular fate of medullary neurons in the fly CNS [145]. I postulate that Nerfin-1 may work in conjunction with Sd to regulate stem cell proliferation and differentiation in the midgut by modulating the Hippo signaling pathway.

Colorectal cancer (CRC) develops due to the accumulation of mutations in various genes, the most common of which are *APC* and *RAS*. Loss-of-function mutation in the tumor suppressor gene *APC* activates Wnt signaling and serves as an initial trigger, leading to the formation of intestinal adenomas [146, 147]. Oncogenic activation of the *KRAS* transform these adenomas into carcinomas [148, 149]. Using the fly intestinal model of CRC, which expresses both Apc^{RNAi} and Ras^{V12} in the progenitor population, I demonstrated that the loss of *nerfin-1* significantly reduced midgut tumor formation **(Figure 16)**. The mouse homologue of Nerfin-1, Insulinoma associated 1 (INSM1) is highly expressed in colorectal tumors of neuroendocrine origin and has been shown to regulate enteroendocrine differentiation fate by acting downstream of Notch signaling in the mouse intestine [196, 197]. Given that in flies *nerfin-1* is regulated by Notch signaling, is required for EE differentiation, and is upregulated in midgut tumors, its function and mechanism are likely conserved across organisms.

4.3 Toll signaling regulates intestinal stem cell proliferation in the fly midgut

Enteric infection triggers a coordinated host response that includes both pathogen elimination and midgut regeneration [79]. In the fly, pathogen killing is primarily regulated by the innate immune pathways, Toll and IMD signaling, which transcribe antimicrobial peptides (AMPs) that are toxic to pathogens [154]. Midgut regeneration is characterized by epithelial damage and the replacement of lost cells by rapidly dividing and differentiating progenitors. Several signaling pathways regulate

midgut regeneration in response to infection, the most important of which is the JNK signaling pathway. I demonstrate that Toll signaling is a multifunctional signaling pathway that not only governs innate immunity, but also regulates midgut regeneration through JNK signaling.

Activation of Toll signaling promotes the transcription of target genes, which include antimicrobial peptides (AMPs) such as *Drs* and *Def*, and the Toll pathway ligand *spz* [112, 154]. I observed that *spz* was upregulated in the progenitor population of Notch loss-of-function mutant midguts **(Supplementary Figure S8)**. Additionally, through RT-qPCR I confirmed that all three Toll pathway target genes *spz*, *Drs*, and *Def* were upregulated in tumorigenic N^{RNAi} midguts, indicating that Notch loss-of-function results in the formation of midgut tumors that activate the Toll signaling pathway **(Figure 19)**.

Canonical Toll signaling relies on the extracellular ligand Spz to activate the transmembrane Toll receptor, which triggers a signaling cascade that promotes Dif- and Dorsal-mediated target gene expression [98]. I found that the Toll pathway genes *Tl*, *Myd88*, *pll*, *Dif*, and *dl* are autonomously required for stem cells to overproliferate and form tumors in Notch mutant midguts **(Figure 20, Supplementary Figure S9)**. One potential mode of regulation of the Toll pathway by Notch signaling could involve the transcriptional regulation of *spz*. Disruption of Notch signaling leads to increased expression of *spz* in progenitor cells. These elevated levels of Spz might bind to the Toll receptor and promote stem cell proliferation. However, the knockdown of *spz* in the progenitors of Notch mutant midguts did not reduce stem cell overproliferation. Given that Spz is not required for Notch loss-of-function-mediated stem cell proliferation, it is likely that the Toll receptor is activated in Notch mutant midguts independently of Spz. Since there are five paralogs of Spz in flies (NT1, Spz3, Spz4, Spz5, Spz6), one of these paralogs might be needed to activate the Toll signaling pathway in progenitor cells. Further studies are required to dissect the mechanism by which Notch signaling activates the Toll signaling pathway in the midgut.

Activation of Toll signaling through a gain-of-function mutation in the Toll receptor (Tl^{10b}) has previously been shown to lead to melanotic tumor formation in the fly larvae [116]. I observed that activating Toll signaling in the progenitor cells of the midgut through the overexpression of Tl^{10b} and *Dif* resulted in a strong stem cell overproliferation phenotype **(Figure 23, Supplementary Figure S12)**. This suggests that active Toll signaling is sufficient to regulate intestinal stem cell proliferation. So far, nine Toll-related receptors have been identified in the fly

genome, with Toll-1 (Tl) being the most studied. Ding *et al.* demonstrated that Toll-7 is required for $Ras^{V12}/lgl^{-/-}$ tumor formation in the fly imaginal disc, and that its overexpression is sufficient to promote tumorigenesis [117]. Given that the overexpression of active Tl^{10b} and *Dif* are sufficient to induce stem cell overproliferation in the midgut, it would be interesting to investigate whether other Toll receptors and Dorsal also exhibit similar pro-proliferative functions in the *Drosophila* midgut.

In *Drosophila*, the outcome of the Toll signaling pathway is primarily regulated by two NF-κB transcription factors, Dif and Dorsal, in a context-dependent manner. For instance, Dorsal is required for dorso-ventral patterning of the embryo, while Dif primarily mediates the anti-fungal immune response in adult flies [198, 199]. Both Dif and Dorsal function redundantly in the fly larvae to regulate the production of the antimicrobial peptide Drosomycin [200]. My data suggest that both Dif and Dorsal can regulate Tl^{10b} mediated stem cell proliferation in the adult midgut **(Figure 24)**. Previous studies have shown that gain-of-function (Tl^{10b}) mutation in the fly larval fat body leads to the nuclear translocation of both Dif and Dorsal, which is necessary for the active transcription of NF-κB target genes [111, 116]. Given that the knockdown of *Dif* and *dl* reduced Tl^{10b}-mediated stem cell proliferation, it is likely that the activation of Toll signaling through overexpression of Tl^{10b} also results in the nuclear accumulation of Dif and Dorsal. This accumulation would lead to the transcription of pro-proliferative genes required for promoting stem cell proliferation.

Damage to the intestinal epithelium caused by enteric infection triggers a regenerative response characterized by accelerated division and differentiation of progenitor cells. The cytoprotective JNK signaling pathway has been identified as a major regulator of epithelial regeneration in response to infection-mediated damage [11]. However, the underlying mechanisms by which pathogens activate JNK signaling are poorly understood. In this study, I propose a model for JNK activation via the Toll pathway, forming a signaling axis that regulates stem cell proliferation in the midgut. I demonstrated that the loss of Toll pathway genes *Tl*, *Dif*, and *dl* reduced infection-induced stem cell overproliferation in the midgut **(Figure 22)**. This phenotype mirrors that observed in JNK mutant midguts [11]. Additionally, I showed that activating Toll signaling through overexpression of Tl^{10b} in progenitor cells resulted in the activation of JNK signaling, which is necessary for mediating stem cell overproliferation **(Figure 25 and 26)**. The relationship between Toll and JNK signaling in regulating cell proliferation was

also established in a previous study by Ding *et al.*, where overexpression of Toll-7 activated JNK signaling and induced cell proliferation in the larval wing disc [117]. This suggests that Toll signaling interacts with JNK signaling to regulate intestinal stem cell proliferation.

Components of the human TLR signaling pathway, which is homologous to the fly Toll signaling pathway, have been shown to regulate CRC in vertebrates. Fukata *et al.* demonstrated that TLR4 is overexpressed in CRC tissues, and its genetic abrogation prevented tumor formation in the mouse colon [201]. In another study, Rakoff *et al.* found that MYD88 deficiency reduced intestinal tumors in $Apc^{Min/+}$ mutant mice [202]. Additionally, several studies have identified the activated form of transcription factor NF-κB in a significant number of CRC patient samples [203, 204]. Target genes of NF-κB including pro-proliferative genes (eg *Cyclin D1*, *c-Myc*) and anti-apoptotic genes (eg *B-cell lymphoma 2* (*Bcl-2*)) may play important roles in promoting tumor growth and preventing apoptosis, respectively [205]. Inhibition of NF-κB through chemical inhibitors has been shown to sensitize CRC cells to apoptosis and reduced cell yield [206]. My data using the fly CRC model driven by Apc^{RNAi};Ras^{V12} indicate that the Toll signaling pathway is activated in tumorigenic midguts. Furthermore, I confirmed that the knockdown of core Toll pathway components *Tl* and *dl* significantly reduced stem cell overproliferation in Apc^{RNAi};Ras^{V12} midguts, and *Dif* knockdown showed a trend in the same direction **(Figure 21)**. This suggests that similar to TLR signaling in higher vertebrate models, the Toll signaling pathway is activated and is essential for tumor growth in the fly midgut.

Apart from intracellular regulation, the Toll signaling pathway has also been shown to regulate biological functions through intercellular communication. For instance, Parisi *et al.* demonstrated that in the presence of *dlg* mutant fly imaginal disc tumors, hemocytes produce Spz, which activates Toll signaling in the fat body. This activation promotes the production of Eiger, which induces tumor cell death [207]. Another study using a wing disc cell competition model suggested that winner cells eliminate loser cells by enhancing SPE production. SPE processes and activates Spz, which triggers Toll-induced cell death in loser cells [119]. In my study, I showed that activating Toll signaling in differentiated ECs through overexpression of Tl^{10b} induced stem cell overproliferation in the midgut **(Figure 27)**. This suggests that active Toll signaling in ECs can non-autonomously regulate intestinal stem cell proliferation.

Intercellular communication between stressed or damaged ECs and proliferating stem cells in the midgut primarily relies on cytokine production and signaling. For instance, during infection, JNK is activated in damaged or stressed ECs, leading to the transcription of cytokines from the Upd family. These secreted Upds activate pro-proliferative JAK/STAT signaling in ISCs, promoting stem cell proliferation [7]. Given that active Toll signaling in ECs non-autonomously enhances stem cell proliferation, it is possible that activating Toll signaling in ECs could lead to JNK-dependent cell death and subsequent cytokine production. This response may then trigger the proliferation of stem cells in the midgut. Since Toll signaling is known to regulate cell death in the *Drosophila* wing disc via JNK signaling, it would be interesting to investigate whether Toll signaling also influences EC cell death via JNK signaling in the midgut [120, 208].

A similar mode of intercellular communication between ECs and tumors has been described in the adult fly midgut. *Notch* mutant tumors in the midgut rely on JNK-dependent niche signals from surrounding dying and delaminating ECs to fuel tumor growth [35]. It would be interesting to investigate whether Toll signaling in ECs can facilitate the process of EC delamination and cell death, thereby non-autonomously promoting tumorigenesis in the *Notch* mutant midgut. To test this, I developed a novel fly line designed to target Toll signaling in the ECs of *Notch* mutant midguts. This fly line employs both binary systems (LexA/LexAOP and Gal4/UAS) to simultaneously target Notch signaling in progenitor cells and Toll signaling in ECs. It consists of an progenitor cell LexA driver: *esg-LexA, LexAOP GFP, tub-Gal80^{ts}* (*esg^{ts}-LexA*), LexAOP-regulated knockdown of Notch receptor: *LexAOP N^{RNAi}*, and the Gal4 driver for EC cells *MexA-Gal4* **(Figure 37)**. By knocking down core Toll signaling components in ECs using the Gal4/UAS system, I can test if this intervention rescues *N^{RNAi}*-dependent tumor formation in the midgut.

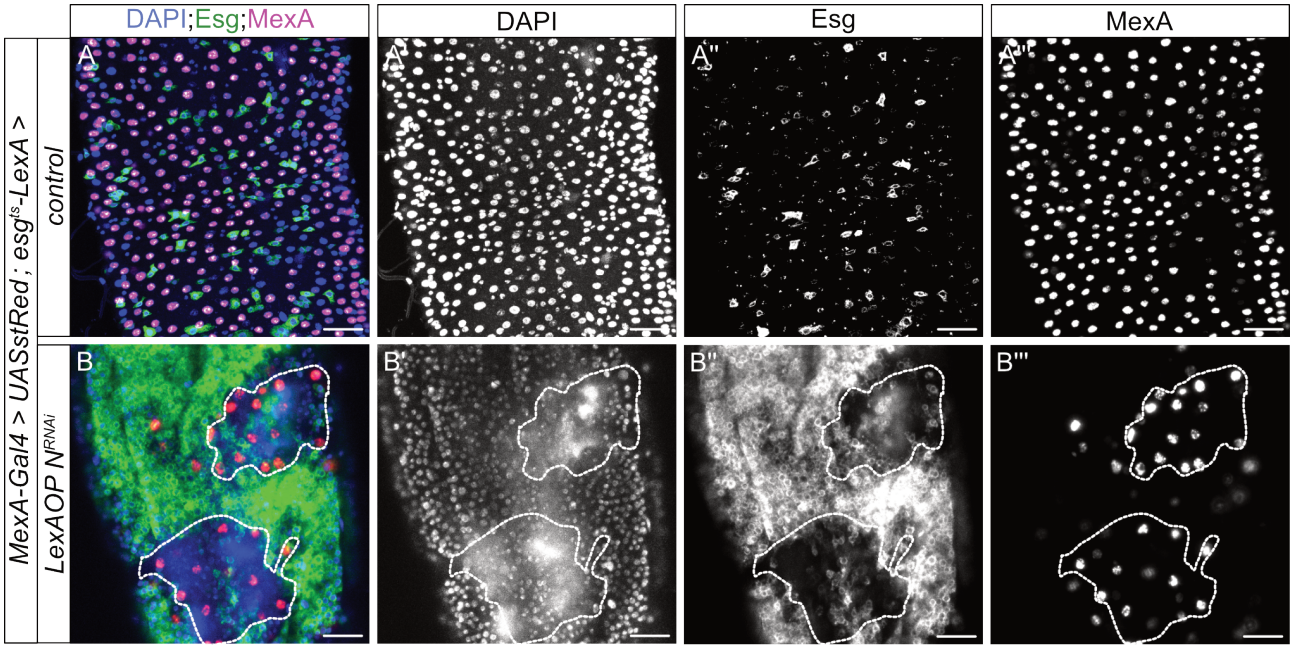

Figure 37 : Generating a fly line to study the non-autonomous regulation of the Notch loss-of-function midgut tumor phenotype. (A-B) Representative images of the posterior midgut showing EC-driven RFP (*MexA-Gal4 > UASstRed);* and progenitor cell-specific *esg^{ts}-LexA* > driven control (*w^{1118}*) **(A)** and *LexAOP N^{RNAi}* **(B).** White dashed lines indicate Esg-negative, MexA-positive ECs in the Notch loss-of-function tumor midgut. Scale bar = 40μm.

4.4 Developing a renal cell carcinoma fly model.

Renal Cell Carcinoma (RCC) is a type of kidney cancer and ranks among the top 10 most common cancers globally. The predominant subtype, clear cell RCC (ccRCC), is characterized by loss-of-function mutations in the E3 ubiquitin ligase VHL, which occur in over 90% of cases. This loss of VHL activity stabilizes hypoxia-inducible factors (HIF-1α and HIF-2α), which transcribe genes necessary for tumorigenesis [163]. I noticed that the knockdown of *Vhl* in Renal Stem Cells (RSCs) of the fly malpighian tubule (MT), which serves as the functional homologue of the human kidney, did not affect RSC proliferation **(Figure 28C)**. Interestingly, several studies in the mouse renal epithelium have also demonstrated that mutating *VHL* alone does not lead to renal cancer, suggesting that the loss of *VHL* by itself is insufficient for tumor formation and may require additional genetic alterations [209].

ccRCC tumors are highly heterogeneous, and exhibit intratumoral heterogeneity. This heterogeneity arises primarily from various combinatorial mutations, leading to the formation of distinct clones. Among these mutations, alterations in *VHL* and the loss of the 3p chromosome

are common occurrences across all analyzed patient samples. A two-hit suppressor gene model has been described for the loss of *VHL*, in which one *VHL* allele has smaller point mutations, while the other *VHL* allele is deleted as a result of the loss of the entire 3p chromosome [210, 211]. The 3p chromosome region harbors three other tumor suppressor genes that are frequently mutated in ccRCC. This includes chromatin and histone modifier genes such as *PBRM1*, *BAP1*, and *SETD2*, all of which are located within a 50-Mb region alongside *VHL* [212]. Studies have shown that deletion of *VHL* together with the loss of either *PBRM1* or *BAP1* in mice leads to the formation of kidney tumors, indicating that carcinogenesis depends on the combined effects of these genetic mutations [213, 214]. I postulate that combined knockdown of *Vhl* along with the fly homologues of *PBRM1* (*polybromo*) or *BAP1* (*caly*) in RSCs of the fly MT might also result in renal stem cell overproliferation.

Genetic mutations serve as initial triggers that drive the activation of oncogenic signaling pathways, which regulate tumorigenesis. The four major signaling pathways commonly active in RCC patients are WNT, PI3K/AKT/mTOR, HGF/MET, and VHL/Hypoxia [165]. Among these, the combined activation of WNT and PI3K/AKT/mTOR signaling in the mouse kidney, achieved through the loss of *APC* and the expression of activated *K-RAS*^{V12}, resulted in RCC formation [150]. I also observed that the combined knockdown of *Apc* and overexpression of *Ras*^{V12} in RSCs led to the formation of rapidly proliferating tumors in the adult fly MT **(Figure 29)**. These MT tumors exhibited the activation of both Wnt and PI3K/Akt/mTor signaling, as indicated by Fz3-RFP **(Figure 30C,D)** and p4EBP staining **(Figure 32)**, respectively.

Activation and requirement of both the WNT and PI3K/AKT/mTOR pathways in the progression of human RCC have been demonstrated in several studies. Canonical WNT signaling components, including WNT ligands such as WNT1 and WNT10A, as well as FZD receptors FZD5 and FZD8, have been shown to be upregulated in RCC samples [167, 168, 169]. Advanced-stage RCC tumors are also characterized by the presence of cytoplasmic β-catenin, indicating the activation of canonical WNT signaling [166]. On the other hand, components of the PI3K/AKT/mTOR pathway, including the growth factor TGFα, the receptor EGFR, and the kinase AKT, have all been found to be upregulated in RCC samples [215, 216, 217]. Additionally, mutations in PI3K/AKT/mTOR pathway components such as PTEN, TSC1/2, PIK3CA, PIK3CG, mTOR, and AKT have been identified in approximately 26-28% of RCC cases [182, 218]. Activated mTOR has also been strongly correlated with poor survival and

tumorigenesis [219, 220].

Several studies have also proposed mechanisms by which the loss of *VHL* and stabilization of HIF2α activate WNT and PI3K/AKT/mTOR signaling in RCC samples. Chitalia *et al.* identified an E3-ubiquitin ligase, Jade-1, which interacts with VHL and ubiquitinates β-catenin promoting its degradation [221]. In another study, Choi *et al.* demonstrated that HIF2α assembles with the β-catenin/TCF complex to enhance Wnt-dependent gene transcription [222]. The activated EGF receptor was also shown to undergo proteasomal degradation mediated by VHL, the absence of which stabilized the activated EGF receptor in RCC cells [223]. Additionally, Doan *et al.* found that stable HIF2α downregulated Deptor, a negative regulator of mTorc1, contributing to tumor proliferation in *VHL* mutant cells [224]. It would be interesting to investigate whether the loss of *Vhl* or overexpression of the fly HIFα protein Sima in RSCs can also activate Wnt and PI3K/Akt/mTor signaling pathways in the fly MT.

Drosophila melanogaster is a powerful *in-vivo* model organism commonly used for large-scale genetic screens to identify novel gene functions and study genetic mechanisms of various diseases. In this study, I utilized the fly MT *Apc*^{RNAi};*Ras*^{V12} tumor model that I established to identify novel genes potentially required for RCC progression. Through a small-scale reverse genetic screen, I identified five genes whose knockdown rescued tumor formation in the fly MT. These genes include *abs*, α-*Man-Ib*, *polo*, *ppan*, and *kibra* **(Figure 36B-G)**.

Human homologues of the above listed genes *DDX41*, *MAN1B1*, *PLK1*, *PPAN*, and *WWC3* are all upregulated in human RCC patients **(Figure 36A)**. Protein expression of DDX41 has been shown to be associated with a worse prognosis in RCC patients. Additionally, DDX41-expressing ccRCC cells along with VHL loss, exhibited increased proliferation through the regulation of the chemokine (C-X-C motif) ligand family [186]. PLK1 has also been associated with high-grade tumorigenesis in RCC tissues. The loss of PLK1 activity through chemical inhibition resulted in a significant decrease in proliferation and invasiveness [187]. While only a few studies have looked at the role of DDX41 and PLK1 in RCC tumorigenesis, very little work has been done to identify the mechanism by which these and other genes regulate tumorigenesis. The fly MT tumor model can serve as a powerful tool to identify more such novel genes and study their mechanism of tumor formation, which can later be translated into higher vertebrate models.

4.5 Conclusion and Outlook

Over the last decade, *Drosophila melanogaster* has been a widely used model organism for studying the genetics of intestinal cancer [158]. Tumorigenesis in the fly midgut is characterized by the disruption of the genetic machinery that regulates stem cell proliferation and differentiation. Among the complex genetic network controlling the stem cell function, only a few signaling pathways have been characterized so far including Notch, JNK, Wnt and EGFR. Many other genes and signaling pathways that are parts of this network remain unknown. In my thesis, I used the Notch loss-of-function midgut tumor model to uncover the role of the transcription factor Nerfin-1 in stem cell proliferation and differentiation. I also identified a novel function of the innate immune signaling Toll pathway in regulating stem cell proliferation in the midgut. Beyond the midgut tumor model, I also established a novel Renal Cell Carcinoma (RCC) fly malpighian tubule (MT) tumor model, which can be used to identify unknown gene functions and mechanisms. In summary, I demonstrated that *Drosophila* tumor models can successfully be used to decode the genetic networks regulating stem cell function in regenerative organs, such as the midgut and MT, providing insights that can be translated to the study of higher model organisms.

4.5.1 Midgut tumor model to identify gene function

The fly midgut comprises intestinal stem cells whose ability to divide and differentiate is regulated by several conserved signaling pathways. One such pathway is the Notch signaling pathway, which determines the differentiation fate of stem cells. High Notch signaling primes stem cells to differentiate into enterocytes (ECs) via transient enteroblasts (EBs), while low Notch signaling promotes enteroendocrine cells (EEs) to differentiate via enteroendocrine progenitors (EEPs). Using CRISPR/Cas9 to perform conditional mutagenesis in the midgut, I showed that the disruption of Notch signaling through mutations in the Notch receptor and E3-ubiquitin ligase Neuralized resulted in the formation of midgut tumors characterized by the accumulation of rapidly dividing stem cells and secretory enteroendocrine cells.

Using single-cell RNA sequencing (scRNA-seq) of the Notch mutant midguts, I together with my colleagues identified all major cell types of the midgut and their associated transcriptomic changes. This represents the first and the most comprehensive scRNA-seq dataset generated for a tumor-bearing fly midgut. More such scRNA-seq datasets can be generated in the future

for different genes whose manipulation induces an intestinal stem cell phenotype. Comparisons between these rich datasets of various genetic manipulations can be used to formulate a genetic network that regulates stem cell function in the fly midgut.

By performing a reverse genetic screen using the Notch loss-of-function midgut tumor phenotype, I identified 28 genes whose knockdown reduced stem tumor formation. Among these genes, *nerfin-1* was particularly interesting, as it has been shown to negatively regulate Notch signaling in the larval CNS [144, 145]. I subsequently demonstrated that Nerfin-1 is required for regulating intestinal stem cell proliferation, the knockdown of which suppresses stem cell proliferation during homeostasis, upon enteric infection, and during tumorigenesis (in the context of Notch loss-of-function and Apc^{RNAi};Ras^{V12}). The mechanism by which Nerfin-1 regulates stem cell proliferation requires further investigation. One possible mechanism of regulation could be through the Hippo signaling pathway since Nerfin-1 has been shown to negatively regulate Hippo signaling in the fly larval CNS [145]. It would be interesting to test whether the loss of Nerfin-1 reduces Notch loss-of-function midgut tumor by activating the Hippo pathway. Additionally, other regulatory genes required for the pro-proliferative effect of Nerfin-1 can be identified through scRNA-seq of *nerfin-1* knockdown midguts. Given that Nerfin-1 is a transcription factor, its target genes can be identified using the DNA adenine methyltransferase identification (DAM-ID) technique. DAM-ID involves identifying sequences bound by the transcription factor through a fused DNA methyltransferase that methylates these sequences [225].

My results also showed that the knockdown of *nerfin-1* suppressed the accumulation of EE cells in the Notch loss-of-function midguts, suggesting that Nerfin-1 may also regulate differentiation decisions. I confirmed through lineage tracing experiments that the loss of *nerfin-1* prevented stem cells from renewing and forced them to differentiate into large nucleated enterocytes. Further experiments can be conducted to confirm if the loss of *nerfin-1* promotes EC differentiation in the midgut. This could be achieved by quantifying EE population in *nerfin-1* knockdown or mutant midguts. A similar experiment was done to demonstrate that Scute and Pros are required for EE differentiation in the midgut [5]. Since the overexpression of components of the Achaete-Scute complex (Asense and Scute), leads to a significant increase in EEs, it would be interesting to test if knocking down *nerfin-1* reduces the number of EEs formed. The role of Nerfin-1 in regulating stem cell proliferation and EE differentiation in the fly

midgut is particularly intriguing, as its human homologue INSM1 has also been shown to be required for the differentiation of enteroendocrine cells in the human intestine, downstream of Notch signaling [197]. Moreover, INSM1 was recently identified as a specific marker for neuroendocrine tumors of intestinal origin [196]. Altogether, this suggests that the role of Nerfin-1 in regulating stem cell proliferation and EE differentiation might be conserved, and its mechanisms can be studied in the fly midgut, with potential translation to higher model organisms.

The Toll signaling pathway in the adult fly is primarily known for its role in mediating innate immunity in response to Gram-positive bacterial and fungal infections. In my previous publication, I identified the multifaceted role of Toll signaling in maintaining gut microbial composition by regulating metabolic genes in the midgut [121]. Interestingly, from the scRNA-seq dataset and RT-qPCR, I found that Notch loss-of-function tumors activated the Toll signaling pathway in the midgut. I also observed similar activation of the Toll signaling pathway in another midgut tumor model induced by Apc^{RNAi};Ras^{V12}. Subsequently, I demonstrated that activated Toll signaling is necessary to promote stem cell overproliferation under tumor conditions. I further confirmed that the abrogation of Toll signaling by knocking down its core components, suppressed stem cell proliferation in response to infection-induced midgut regeneration. Altogether, I uncovered a novel role for Toll signaling in regulating intestinal stem cell proliferation in the midgut.

Interestingly, unlike Nerfin-1, genetic activation of Toll signaling during homeostasis was sufficient to cause stem cell overproliferation. I demonstrated that this stem cell overproliferation phenotype was dependent on the activation of the JNK signaling pathway, acting downstream or in parallel to the Toll pathway. This aligns with several studies that have shown that Toll signaling can regulate JNK signaling [117, 208]. It would be interesting to test whether activated JNK signaling promotes stem cell proliferation via the Toll signaling pathway in the midgut. Lastly, other Toll-dependent stem cell regulatory genes can be identified through RNA sequencing of Tl^{10b} midguts and targeted DAM-ID of the Toll pathway transcription factors Dif and Dorsal. I generated a *UAS Dif-DAM-ID* transgenic fly, which can be used in the future to identify target genes of Dif in the progenitor population of the midgut.

I also discovered that Toll signaling in the ECs can non-autonomously regulate stem cell proliferation in the midgut. Previous studies have shown that activation of JNK signaling in dying ECs promotes stem cell proliferation by transcribing cytokines [7]. It would be interesting to check if Toll signaling regulates EC cell death via JNK signaling and also contributes to the transcription of cytokines that trigger stem cell overproliferation in the midgut. I generated a non-autonomous, screenable Notch loss-of-function fly line that can be used to determine whether the abrogation of Toll signaling in ECs rescues Notch loss-of-function mediated stem cell overproliferation. This first-of-its-kind fly line can be used to identify genes required for intercellular communication between ECs and tumors through a straightforward reverse genetic screening approach.

4.5.2 Malpighian tubule tumor model to identify gene function

The adult fly malpighian tubule (MT) is the functional homologue of the human kidney and is required for the excretion of toxins, ion exchange and fluid transport [159]. The fly MT has been used to model and study several human diseases, such as metabolic disorders and kidney stones; however, very little work has been done to model RCC in the fly [161]. I demonstrated that the knockdown of the most commonly mutated tumor suppressor gene, *Vhl*, in the fly RSCs does not affect their proliferation. Previous studies conducted in mice have shown that the loss of *VHL* requires additional mutations in *PBRM1* or *BAP1* to trigger RCC formation [213, 214]. Therefore, it would be interesting to test if the combined suppression of *Vhl* and *polybromo* or *caly* would result in the formation of MT tumors.

Nevertheless, I showed that the combined activation of the Wnt and PI3K/Akt/mTor pathways in the fly RSCs through the expression of Apc^{RNAi};Ras^{V12} resulted in the formation of MT tumors, characterized by rapidly proliferating renal stem cells. I further showed that these renal stem cells are dependent on the Wnt and PI3K/Akt/mTor pathways for their overproliferation phenotype. These results are consistent with those observed in the mouse renal epithelium, suggesting that the fly MT can be used to model RCC.

Using this established fly MT tumor model, I identified five genes (*abs*, α*-Man-Ib*, *polo*, *ppan*, and *kibra*) whose knockdown rescued Apc^{RNAi};Ras^{V12}-mediated MT tumors. The human homologues of these genes are upregulated in RCC tissues, and very little is known about how they regulate tumorigenesis. It would be interesting to study the mechanism by which these

genes regulate tumorigenesis in the MT. This could be done by sequencing and examining changes in the gene expression pattern in RSCs. Additionally, a larger systematic screening could be conducted using the MT tumor model to identify more regulatory genes, whose effects could later be tested in higher model organisms.

5 Materials and Methods

5.1 Materials

5.1.1 Fly stocks

Fly Name	Genotype	Source
esg^{ts}	esg-GAL4, Tub-$GAL80^{ts}$, UAS-GFP	Jiang *et al.*, 2009
esg^{ts}F/O	UAS-Flp; esg-GAL4, UAS-GFP; Act¿CD2¿GAL4, Tub-$GAL80^{ts}$	Jiang *et al.*, 2009
$MyoIA^{ts}$	MyoIA-GAL4, Tub-$GAL80^{ts}$, UAS-GFP	Jiang *et al.*, 2009
UAS Cas9.P2	UAS Cas9.P2	Port *et al.*, 2016
hep-$gRNA^{2X}$	P{hsFLP}1, y^1 w^{1118}; P{HD_CFD01377}attP40/CyO-GFP	VDRC 342022
Mad-$gRNA^{2X}$	P{hsFLP}1, y^1 w^{1118}; P{HD_CFD00651}attP40/CyO-GFP	VDRC 341570
neur-$gRNA^{2X}$	P{hsFLP}1, y^1 w^{1118}; P{HD_CFD01179}attP40/CyO-GFP	VDRC 341917
N-$gRNA^{2X}$	P{hsFLP}1, y^1 w^{1118}; P{HD_CFD01184}attP40/CyO-GFP	VDRC 341922
sepia-$gRNA^{2X}$	P{hsFLP}1, y^1 w^{1118}; P{HD_CFD00764}attP40/CyO-GFP	VDRC 341664
N^{RNAi}	w^{1118}; P{GD14477}v27228/TM3	VDRC 27228
esg^{ts};N^{RNAi}	esg-GAL4, Tub-GAL80ts, UAS-GFP/Cyo; UAS NRNAi/Tm6b	Generated Stock
$nerfin1^{RNAi}$ #1	y^1 v^1; P{TRiP.JF02956}attP2	BDSC 28324
$nerfin1^{RNAi}$ #2	P{KK105266}VIE-260B	VDRC 101631
UAS nerfin-1	UAS nerfin-1	Vissers *et al.*, 2018
Tl^{RNAi}	P{KK103505}VIE-260B	VDRC 100078
Dif^{RNAi}	P{KK106594}VIE-260B	VDRC 100537
dl^{RNAi}	P{KK107820}VIE-260B	VDRC 105491

pll ^{RNAi}	P{KK102624}VIE-260B	VDRC 103774
Myd88 ^{RNAi}	P{KK102656}VIE-260B	VDRC 106198
Rel^{RNAi}	y[1] sc[*] v[1] sev[21]; P{y[+t7.7] v[+t1.8]=TRiP.HMS00070}attP2	BDSC 33661
UAS Tl^{10b} #1	P{UAS-Tl.10b}11, y^{1} w*	BDSC 58987
UAS Tl^{10b} #2	UAS Tl10b (II)	Shia *et al.*, 2009
UAS Tl^{10b};esg^{ts}	UAS Tl10b; esg-GAL4, Tub-GAL80ts, UAS-GFP/Cyo	Generated Stock (Siamak R)
UAS Dif	M{UAS-Dif.ORF.3xHA.GW}ZH-86Fb	FlyORF F000698
puc-lacz	puc-lacZ^{E69}	Zeitlinger *et al.*, 1999
esg^{ts};puc-lacz	esg-GAL4, Tub-GAL80ts, UAS-GFP/Cyo; puc-lacZE69/Tm6b	Zhou *et al.*, 2020
UAS bsk^{DN}	P{UAS-bsk.DN}3	Rallis *et al.*, 2010
esg^{ts};bsk^{DN}	esg-GAL4, Tub-GAL80ts, UAS-GFP/Cyo; UAS BskDN/Tm6b	Zhou *et al.*, 2020
esg^{ts} lexA	esg-LexA, Tub-GAL80ts, LexAOP-GFP	Chen *et al.*, 2022
lexAOP N^{RNAi}	LexAOP NRNAi	Boukhatmi *et al.*, 2020
MexA Gal4	P{w[+mC]=mex1-GAL4.2.1}9-1, y[1] w[1118]	BDSC 91367
MexA Gal4;esg^{ts} lexA	MexAGal4;esg-LexA, Tub-GAL80ts, LexAOP-GFP	Generated Stock
MexA Gal4;esg^{ts} lexA; lexAOP N^{RNAi}	MexAGal4;esg-LexA, Tub-GAL80ts, LexAOP-GFP;LexAOP NRNAi	Generated Stock
Vhl^{RNAi}	y[1] sc[*] v[1] sev[21]; P{y[+t7.7] v[+t1.8]=TRiP.HMS02963}attP2	BDSC 50727
polybromo^{RNAi}	y^{1} sc* v^{1} sev^{21}; P{TRiP.HMS00531}attP2	BDSC 32840
Set2^{RNAi}	y^{1} w^{1118}; P{UAS-Set2.RNAi}21	BDSC 24108
caly^{RNAi}	y^{1} sc* v^{1} sev^{21}; P{TRiP.HMC04109}attP40	BDSC 56888

Apc^{RNAi}	UAS-Apc1 RNAi	VDRC 51469
Ras^{V12} (II)	w[*]; P{w[+mC]=UAS-Ras85D.V12}2	BDSC 64196
Ras^{V12} (III)	w^{1118}; P{UAS-Ras85D.V12}TL1	BDSC 4847
fz3-RFP	fz3-RFP	Tian *et al.*, 2016
Apc^{RNAi},Ras^{V12}	UAS Apc1RNAi, UAS RasV12/Tm6b	Generated Stock
esg^{ts};Apc^{RNAi}, Ras^{V12}	esg-GAL4, Tub-GAL80ts, UAS-GFP/Cyo; UAS Apc1RNAi, UAS RasV12/Tm6b	Generated Stock
esg^{ts};Apc^{RNAi}, Ras^{V12}, fz3RFP	esg-GAL4, Tub-GAL80ts, UAS-GFP/Cyo; UAS Apc1RNAi, UAS RasV12,fz3-RFP/Tm6b	Generated Stock
wg^{RNAi}	P{KK108857}VIE-260B	VDRC 10459
pan^{DN}	y[1] w[1118]; P{w[+mC]=UAS-pan.dTCFDeltaN}4	BDSC 4784
pan^{DN}	y[1] w[1118]; P{w[+mC]=UAS-pan.dTCFDeltaN}5	BDSC 4785
$Egfr^{RNAi}$	w^{1118}; P{GD1654}v43268/CyO	VDRC 43268
Akt^{RNAi}	P{KK100495}VIE-260B	VDRC 103703
$Dsor^{RNAi}$	y[1] v[1]; P{y[+t7.7] v[+t1.8]=TRiP.HMS00037}attP2	BDSC 33639
abs^{RNAi}	P{KK101165}VIE-260B	VDRC 107031
alpha-Man-Ib^{RNAi}	y[1] sc[*] v[1] sev[21]; P{y[+t7.7] v[+t1.8]=TRiP.HMS05396}attP4	BDSC 66930
$kibra^{RNAi}$	P{KK111409}VIE-260B	VDRC 106507
$ppan^{RNAi}$	y1 sc* v1 sev21; P{TRiP.HMC06628}attP40	BDSC 80392
$polo^{RNAi}$	y1 sc* v1 sev21; P{TRiP.HMS00530}attP2	BDSC 33042
$lili^{RNAi}$	y1 v1; P{TRiP.HMJ03117}attP40	BDSC 51163
dco^{RNAi}	y1 sc* v1 sev21; P{TRiP.GL00001}attP2/TM3, Sb1	BDSC 35134
syd^{RNAi}	y1 v1; P{TRiP.GLC01419}attP2/TM3, Sb1	BDSC 43232
Ack^{RNAi}	y1 sc* v1 sev21; P{TRiP.HMS00839}attP2	BDSC 33899
so^{RNAi}	y1 v1; P{TRiP.JF02201}attP2	BDSC 31912
eIF4A ^{RNAi}	y1 sc* v1 sev21; P{TRiP.HMS00927}attP2	BDSC 33970
Cip4 ^{RNAi}	y1 v1; P{TRiP.JF01437}attP2	BDSC 31646
Fit1 ^{RNAi}	y1 v1; P{TRiP.JF01986}attP2	BDSC 25966
SPARC ^{RNAi}	y1 v1; P{TRiP.HMS02133}attP40	BDSC 40885

Cks30A^{RNAi}	y[1] sc[*] v[1] sev[21]; P{y[+t7.7] v[+t1.8]=TRiP.HMC05072}attP40	BDSC 60078
spz^{RNAi}	y[1] sc[*] v[1] sev[21]; P{y[+t7.7] v[+t1.8]=TRiP.HMS05390}attP40	BDSC 66924
CG17224^{RNAi}	w^{1118}; P{GD5088}v41175	VDRC 41175
CG4250^{RNAi}	P{KK110313}VIE-260B	VDRC 101949
Dgp-1^{RNAi}	P{KK100798}VIE-260B	VDRC 109410
beat-IIIb^{RNAi}	y[1] sc[*] v[1] sev[21]; P{y[+t7.7] v[+t1.8]=TRiP.HMC04424}attP40	BDSC 56984
Delta^{RNAi}	P{KK107312}VIE-260B	VDRC 109491
CG31345^{RNAi}	P{KK108923}VIE-260B	VDRC 104444
Cyp6d2^{RNAi}	P{KK109836}VIE-260B	VDRC 101829
sna^{RNAi}	y[1] sc[*] v[1] sev[21]; P{y[+t7.7] v[+t1.8]=TRiP.HMS01252}attP	BDSC 34906
RhoGAP100F^{RNAi}	P{KK100782}VIE-260B	VDRC 106241
CG6329^{RNAi}	y[1] v[1]; P{y[+t7.7] v[+t1.8]=TRiP.JF02927}attP2	BDSC 28297
dpr6^{RNAi}	P{KK112634}VIE-260B	VDRC 103521
spdo^{RNAi}	y[1] v[1]; P{y[+t7.7] v[+t1.8]=TRiP.JF01806}attP2	BDSC 31227
Mmp2^{RNAi}	y[1] v[1]; P{y[+t7.7] v[+t1.8]=TRiP.HMJ23143}attP40	BDSC 61309
stan^{RNAi}	P{KK100512}VIE-260B	VDRC 107993
CG4702^{RNAi}	P{KK106521}VIE-260B	VDRC 100663
Swim^{RNAi}	P{KK108093}VIE-260B	VDRC 107301
CG9815^{RNAi}	P{KK112426}VIE-260B	VDRC 10278
CG4210^{RNAi}	P{KK107727}VIE-260B	VDRC 104004
Tengl3^{RNAi}	P{KK104451}VIE-260B	VDRC 100187
insb^{RNAi}	P{KK103886}VIE-260B	VDRC 101577
eIF4E7^{RNAi}	P{KK103628}VIE-260B	VDRC 107958
CG14302^{RNAi}	P{KK111946}VIE-260B	VDRC 1067941
GstZ2^{RNAi}	P{KK112682}VIE-260B	VDRC 107660
Sirup^{RNAi}	y[1] v[1]; P{y[+t7.7] v[+t1.8]=TRiP.HMS06021}attP40	BDSC 80441
dpr17^{RNAi}	P{KK106447}VIE-260B	VDRC 100978

kuk^{RNAi}	P{KK109679}VIE-260B	VDRC 106855
$CG9628^{RNAi}$	P{KK104289}VIE-260B	VDRC 107136
$Kmn1^{RNAi}$	P{KK111826}VIE-260B	VDRC 106889
$dimm^{RNAi}$	P{KK100204}VIE-260B	VDRC 103356
sff^{RNAi}	y[1] sc[*] v[1] sev[21]; P{y[+t7.7] v[+t1.8]=TRiP.HMS01280}attP2	BDSC 36656
$CCHa1^{RNAi}$	P{KK112676}VIE-260B	VDRC 104974
$PolZ1^{RNAi}$	P{KK102442}VIE-260B	VDRC 103755
NtR^{RNAi}	P{KK104631}VIE-260B	VDRC 108234
sc^{RNAi}	P{KK100141}VIE-260B	VDRC 105951
$RPA3^{RNAi}$	P{KK109861}VIE-260B	VDRC 101833
Pen^{RNAi}	y[1] v[1]; P{y[+t7.7] v[+t1.8]=TRiP.JF02772}attP2	BDSC 27692

Table 1: Fly lines used in this thesis.

5.1.2 Antibodies

Antibody	**Supplier, Reference**	**Dilution, Host**
anti-Armadillo	DSHB, N2-7A1	1:100, Mouse
anti-Beta Galactosidase	Icllab, RGAL-45A-Z	1:1000, Rabbit
anti-Cas9	Cell signaling, 14697	1:500, Mouse
anti-Discs large 1	DSHB, 4F3	1:100, Mouse
anti-phosphoSer10-Histone 3	Cell signaling, 9701	1:500, Rabbit
anti-phosphoSer10-Histone 3	Cell signaling, 9706	1:500, Mouse
anti-phospho-4EBP	Cell signaling, 2855	1500, Rabbit
anti-Prospero	DSHB, MR1A	1:100, Mouse
anti-Rabbit IgG (H+L) secondary antibody Alexa 594	Thermo Fisher, A11012	1:3000, Goat
anti-Mouse IgG (H+L) secondary antibody Alexa 594	Thermo Fisher, A11005	1:3000, Goat

anti-Rabbit IgG (H+L) secondary antibody Alexa 647	Thermo Fisher, A32733	1:3000, Goat
anti-Mouse IgG (H+L) secondary antibody Alexa 647	Thermo Fisher, A21236	1:3000, Goat

Table 2: Antibodies used in this thesis.

5.1.3 Primers

Primer pair name	**Forward primer sequence (5'-3')** / **Reverse primer sequence (5'-3')**	**Purpose**
spz	GACACCTGGCAGTTAATTGTCA	
	CGAAGTCACAGGGTTGATCCG	
Drosomycin	CTGGGACAACGAGACCTGTC	
	ATCCTTCGCACCAGCACTTC	
Defensin	TGTCCTGGTGCATGAGGATG	
	AGTTCCACTTGGAGAGTAGGTC	
Nerfin1	AGCAGGGAAGCGTAAATTGAG	
	CTTTGACGGGTTTCGCTGGT	
Pros	CTGCCCCAGAGTTTGGACAA	
	CCTGATGCGAGTGACTGGA	
GapDH	CCAATGTCTCCGTTGTGGA	
	TCGGTGTAGCCCAGGATT	RT-qPCR
UAS Ras^{V12}	CCTCCGAGCGGAGTACTGTC	
	TTGCTTTCGGTAAGAGTCCTCGA	
UAS Apc^{RNAi}	CCTCCGAGCGGAGTACTGTC	
	CGCGAATTCAAGCGGATGCAGAAGCGGAAG	Genotyping

Table 3: Primers used in this thesis.

5.1.4 Chemicals, Buffers and Kits

Chemicals and Reagents	Reference	Supplier
16 % Formaldehyde (w/v)	28908	Thermo Fisher
Agarose	2267.4	Carl Roth
BSA Fraction V 99%	1501	Gerbu
DMSO	D8418-50ml	Sigma
Elastase	E0258	Sigma
iTaq™ Universal SYBR® Green Supermix	1725124	Biorad
Kodak Photo-Flo	KPH12	Kodak
LB medium	X968.2	Carl Roth
PBS	P3813-10pak	Sigma
Poly-L-lysine hydrobromide	P1524-1G	Sigma
Proteinase K	EO0491	Thermo Fisher
Q5® Hot Start High-Fidelity 2X Master Mix	M0494S	NEB
Rifampicin	A2220,0001	Applichem
Sucrose	84097-1Kg	Sigma
SYBR Safe DNA Gel Stain	S33102	Thermo Fisher
Triton X-100	T8787	Sigma
VECTASHIELD® Antifade Mounting Medium with DAPI	H-1200-10	Vector Labs

Table 4: Chemicals and Reagents used in this thesis.

Buffers	Composition
LB broth	10g/l Trypton, 5g/l Yeast extract, 10g/l NaCl in ddH_2O, pH 7.0
Normal Fly food	50L H_2O, 360-400g Agar, 1.1Kg Sugar beet syrup, 4Kg Malt, 4kg Corn flour, 500g Soya flour, 900g Beer yeast, 120g Nipagin, 1l 31% Propionic acid, 1l 2.65% Phosphoric acid
PBS (1X)	1 pouch (138mM NaCl, 2.7mM KCl, pH7.4) in 1L ddH_2O
PBST (0.1%)	0.1% Triton X-100 in 1X PBS
PBT (1%)	1% BSA in 0.1% PBST

Poly-L-lysine working solution	30ml 10X Poly-L-lysine, 1.5ml Kodak Photo-Flo, 170ml ddH_2O
Squishing buffer	10mM Tris-Cl pH 8.2, 1mM EDTA, 25mM Nacl. Add 200ug/ml Proteinase K immediately before DNA extraction
TAE buffer	50mM EDTA, 2M Tris, 1M Acetic acid

Table 5: Buffers and their compositions used in this thesis.

Kits	**Reference**	**Supplier**
Chromium Next GEM Single Cell 3 Kit	1000268	10X Genomics
Illumina TruSeq mRNA stranded Kit	20020595	Illumina
QuantiTect Reverse Transcription Kit (50)	205311	Qiagen
RNase-Free DNase Set	79254	Qiagen
RNeasy Mini Kit (250)	74106	Qiagen

Table 6: Kits used in this thesis.

5.1.5 Softwares

Softwares	**Reference**
Affinity designer 2.0	Affinity
Fiji	Schindelin *et al.*, 2012
Inkscape	Inkscape Project. (2020)
Prism	GraphPad

Table 7: Softwares used in this thesis.

5.2 Methods

5.2.1 *Drosophila* husbandry

Drosophila melanogaster were reared at 29°C or 18°C with 12:12 hour light/dark cycle on normal fly food. Fifty litres of normal fly food was prepared using the following ingredients: 360-400g Agar, 1.1kg Sugar beet syrup, 4kg Malt, 4kg Corn flour, 500g Soya flour, 900g Beer yeast, 120g Nipagin, 1 litre 31% Propionic acid, and 1 litre 2.65% Phosphoric acid. Fly crosses for experiments were set up by collecting virgins females and putting them with males on fly food in 18°C. These parent flies were allowed to mate and lay eggs on the fly food in a vial for 3-4 days before being transferred to new food vials. Two to three days post-eclosion, adult progeny of the desired genotypes were collected and maintained at either 29°C or 18°C, depending on the type of experiment. Experimental flies were flipped once every 2-3 days into a new fly food vial. Mated female flies were used for all experiments. Fly stocks were maintained in duplicates at 18°C and flipped once every 40-60 days.

5.2.2 Oral Infection

Enteric infection was performed in adult flies by feeding them the pathogenic bacterium *Erwinia carotovora carotovora 15 (Ecc15)*. *Ecc15* was allowed to grow in 1X LB broth supplemented with 150μg/ml Rifampicin for 2 days at 30°C. The bacterial culture's optical density (OD) was measured and concentrated to an OD600 = 50 using 5% sucrose solution dissolved in PBS. 200μl of this concentrated bacterial solution in sucrose was added to a filter paper, which was then placed in vials on top of the fly food to create infection chambers. For uninfected controls, filter paper soaked with 200μl of only 5% sucrose was placed inside the fly vials.

Flies of the desired genotypes were starved for 4 hours in empty vials, half of which were transferred into vials containing the contaminated filter paper, while the other half were shifted to control vials containing only sucrose. Bacterial feeding and infection were performed at 29°C for 16hrs, after which midguts were dissected and further processed for imaging.

5.2.3 Lifespan

For lifespan experiments, 20-25 esg^{ts} and esg^{ts};N^{RNAi} virgin female flies were crossed with 5-10 control (w^{1118}), *nerfin-1*$^{RNAi\ \#1}$, and *nerfin-1*$^{RNAi\ \#2}$ male flies in large fly food bottles at 18°C. Adult

progeny were collected 3-4 days after eclosion. A total of 5 vials per genotype, each containing 20 females and 2 males, were collected and kept at 29°C to induce the RNAi-mediated knockdown effect. The flies were transferred to fresh food every 2 days, and dead female flies were counted. This was performed until all the flies died naturally. The lifespan data were analyzed and plotted using GraphPad Prism 10 software. A total of 3 biological replicates was performed with only one replicate is shown in the figure.

5.2.4 Poly-L-lysine slide preparation for Immunohistochemistry

The working Poly-L-lysine solution was prepared by mixing the following components: 30ml of 10X Poly-L-lysine stock solution, 170ml of ddH_2O, and 1.5ml of Kodak Photo-Flo. Frosted glass slides were loaded in pairs into the grooves of a glass staining rack. These slides were then completely submerged in the working Poly-L-lysine solution, which was placed on a rocking surface at room temperature for 15min. Afterwards, the glass rack containing the coated slides was removed from the solution and dried at 60°C for 15min. This process of coating and drying was repeated 3 more times to ensure proper coverage of the glass slides with Poly-L-lysine. Following this, the glass slides were removed from the rack and placed, wet side face up, on an aluminium foil in a 4°C cold room for 1 hour. A ring of silicon was then applied on the borders of each slide and allowed to dry overnight. The working solution can be stored at 4°C for several months and can be reused 3-4 times before being discarded.

5.2.5 Immunohistochemistry of *Drosophila* Midgut and Malpighian tubules

Adult female flies of the desired genotype and age were anaesthetized with CO_2, and their midguts and malpighian tubules were carefully dissected in PBS. The tissues were positioned and attached to Poly-L-lysine slides, which allowed the tissues to firmly adhere to the surface. A thick silicone layer on the borders of the slides contains reagents and buffers, preventing spillage. Midguts and malpighian tubules from 3 to 5 different genotypes were placed on the Poly-L-lysine slide, with each genotype grouped together. The tissues were then fixed in 4% FA for 30 to 40min at room temperature, followed by washing once with 1X PBS and twice with 1X PBST (1X PBS + 0.1% Triton X-100). Tissues were then permeabilized in 1X PBST for 30 min and then blocked for another 30 min in 0.1% BSA in 1X PBST (PBT). Subsequently, tissues were incubated with primary antibodies diluted in PBT overnight at 4°C. After incubation, the samples were washed 4 times with 1X PBST (1st wash: 1min, 2nd wash: 10min, 3rd wash:

20min, and 4th wash: 15min) to remove the free-floating primariy antibody. Secondary antibodies, diluted 1:3000 in PBT, were added to the tissues and incubated for 1.5hrs at room temperature, followed by another set of 4 washes with 1X PBST (1st wash: 1min, 2nd wash: 10min, 3rd wash: 20min and 4th wash: 15min) to remove the unbound secondary antibody. After washing the tissues, the silicone layer was carefully removed using a scalpel, and a few drops of VECTASHIELD Antifade Mounting Medium with DAPI were added to the tissues. A coverslip was then placed on the tissues and sealed with transparent nail polish. The final slides were stored at 4°C. Images of the midgut and malpighian tubules were acquired with Nikon A1 and Leica Sp5 microscopes. The images were analysed using Fiji software and compiled into figures using Affinity Designer.

Quantification of pH3-positive mitotic cells The mitotic index for all the genotypes mentioned in the thesis was determined by counting cells undergoing division, identified by antibody staining of Phospho-Histone H3 at Ser10 (pH3 staining). Phosphorylation of histone H3 at Ser10 is associated with chromosomal condensation during mitosis [226]. Dissected midguts and malpighian tubules of the desired genotype were fixed and stained with the pH3 antibody, which was conjugated to the secondary antibody Alexa 594 to enable counting through the eyepiece of the microscope. For the midgut, pH3-positive cells along the entire length of the midgut, from the foregut to the hindgut, were counted. For the malpighian tubules, pH3-positive cells were counted in the stem cell zone, from the midgut-malpighian tubule boundary to the lower tubule.

5.2.6 Genotyping

Two to three whole adult flies, to be genotyped, were collected in an Eppendorf tube and frozen at -20°C. These frozen flies were then crushed using a pipette tip in 50μl squishing buffer supplemented with 1μl Proteinase K. After crushing, the samples were incubated at 37°C for 30min, followed by 98°C for 3min, with a final hold at 4°C. Next, 1μl of the supernatant, which contains the genomic DNA, was carefully pipetted into a PCR tube containing 12.5μl of Q5 Hot Start Mastermix, 1.25μl of forward primer, 1.25μl of reverse primer, and 9μl of water. These samples were then subjected to PCR amplification using the following protocol: 98°C for 30sec, followed by 35 cycles of 98°C for 10sec, 63°C for 30sec, 72°C for 30sec. This was followed by a final extension at 72°C for 2min and a hold at 4°C. The PCR products were run on a 1% agarose gel stained with SYBR Safe at 110V for 45min. The gel was visualized using the

BioRad Gel Doc system.

5.2.7 RT-qPCR

Midguts from 20 female flies of the desired genotypes were dissected in PBS. These midguts were then placed in sterile, empty Eppendorf tubes, flash-frozen in dry ice, and stored in -20°C for several weeks. To isolate RNA, the frozen midguts were crushed using a mortar and pestle. RNA was then extracted using the Qiagen RNeasy Mini kit according to the manufacturer's instructions. An additional DNAse treatment was performed during the RNA isolation procedure, using the RNase-Free DNase kit, as per the manufacturer's instructions, to eliminate contaminating DNA. The concentration of the eluted RNA was measured in ng/μl using a Nanodrop spectrophotometer.

One μg of RNA was used to prepare cDNA by reverse transcription using the Quantitect Reverse transcriptase kit as per the manufacturer's instructions. The cDNA was stored at -20°C until further usage. For RT-qPCR, a cDNA master mix was prepared for each genotype, consisting of 1μl SYBR Green, 0.4μl cDNA, and 3.6ul nuclease-free water per reaction. A primer master mix was also prepared for the genes to be assessed, consisting of 4μl SYBR Green and 1μl of 5μM forward and reverse primers. According to the experimental combinations, 5μl cDNA master mix and 5μl of primer master mix were added in each well of a 384-well plate. The plate was sealed with a LightCycler 480 Sealing Foil (Roche, 04729757001) and briefly centrifuged. The samples were then run in a LightCycler 480 machine (Roche). The experiments were performed in duplicate, with each plate containing 3 independent biological replicates. The 2–$\Delta\Delta$Ct method was used to calculate the relative fold change [227], with GAPDH as the reference gene.

5.2.8 Single cell RNA sequencing of *Drosophila* midguts

For single-cell RNA sequencing experiments, 20-25 *esg^{ts}*;*UAS Cas9.P2* virgin female flies were crossed with 5-10 control (*w^{1118}*) and *N-gRNA^{2X}* male flies in fly food vials at 18°C. Adult female progeny of the correct genotype were collected and incubated at 29°C for 10 days, followed by 30 days at 18°C, and then 29°C for one day. This method was used to temporally regulate Cas9 levels in the midgut and effectively introduce Cas9-induced mutations. These flies were starved for 4 hours, flipped into vials containing filter paper soaked in 5% sucrose (in PBS), and incubated

overnight at 29°C. Midguts from 20 flies were dissected and stored in ice-cold PBS. Whole tissues were then dissociated into single cells using 1 mg/ml Elastase (Sigma, E0258) solution for 45min at room temperature, with gentle vortexing every 15-20min. After dissociation, the samples were centrifuged at 300 RCF for 5min and at 600 RCF for another 5min. The supernatant was carefully discarded without disturbing the cell pellet. One ml of filtered PBS was added and the pellet was gently resuspended. The cell suspension was passed through a 40μm [SKU 43-10040-50, , PluriSelect Life Science] and 20μm [43-10020-50, PluriSelect Life Science] cell strainers coated with PBST. The filtrate was then centrifuged for 2.5min at 300 RCF and for another 2.5min at 600 RCF. After centrifugation, 900μl of the PBS was carefully removed, and the cell pellet was resuspended in the remaining 100μl of PBS. The total number of cells was counted using the Luna cell counter.

Library from approximately 20,000 cells was prepared for single-cell RNA sequencing using the 10X Genomics 3' kit according to the manufacturer's instructions. Before sequencing, library fragment size was measured using an Agilent Bioanalyzer high-sensitivity chip and quantified using Qubit. Libraries were multiplexed and sequenced using a Nextseq 550 at the Deep Sequencing Facility, BioQuant, Heidelberg University. The library preparation and sequencing were performed by Svejna Leible from the Boutros lab (DKFZ, Heidelberg).

A CellRanger index (version 7.0.1) was created using the genome sequence of *Drosophila melanogaster* along with the associated GTF file (Ensembl release 102). Single-cell count matrices were produced by aligning reads to the reference with the cellranger count tool, utilizing the include-introns option. Quality control and analysis of single-cell RNA-seq data were carried out using the R package Seurat (version 4.3.0). The raw gene expression count matrices were pre-processed and filtered with scran53 (version 1.24.0), adhering to the protocols outlined by Amezquita *et al.* [228]. In summary, droplets with RNA content below each library's inflection point were discarded, as well as cells that met any of the following criteria: (a) less than 250 detected genes, (b) in the top 1 percentile of cells by UMI count, or (c) a high percentage of mitochondrial reads. All subsequent analyses were conducted using Seurat (version 4.1.1) unless noted otherwise. These analyses included log normalization of counts, data scaling, cell cycle inference, and the identification of the 3000 most variable genes for each replicate. The replicates were then integrated, and batch effects were corrected using Seurat's IntegrateData method. Dimensionality reduction was performed with RunPCA, followed by constructing

UMAPs from the first 20 principal components. Data clustering was executed using the Louvain algorithm. Cell-type labels were manually assigned to clusters based on the expression of specific marker genes. For analyzing differential cell type abundance, the number of cells per type and replicate was quantified and the resulting data was modelled as a negative binomial distribution with DESeq2 (version 1.36.0). The size factors were set equal to the total number of cells per replicate.

In order to identify differentially expressed genes, pseudobulk expression profiles were created by aggregating counts from all cells sharing the same cell type label across each replicate. Genes with fewer than 75 counts in total across all replicates were excluded. The differential expression analysis was conducted with default parameters using DESeq2 (version 1.36.0) [229]. Differentially expressed genes were classified as those with an absolute log2 fold change greater than 1 and adjusted P value below 0.05. All the data analysis was performed by Nick Hirschmueller from the Huber lab (EMBL, Heidelberg).

5.2.9 Bulk RNA sequencing

A total of 20 adult female flies were dissected in PBS to isolate midguts, and 40 adult female flies were dissected to isolate malpighian tubules. These tissues were placed in empty sterile Eppendorf tubes and flash-frozen in dry ice. Frozen tissues were crushed using a mortar and pestle, and total RNA was isolated using the Qiagen RNeasy Mini kit. RNA was isolated from three independent biological replicates for each genotype.

Sequencing libraries were prepared using the Illumina TruSeq mRNA stranded Kit following the manufacturer's instructions. Briefly, mRNA was purified from 500ng (or 400ng in the case of sample DAM3) of total RNA using oligo(dT) beads. Then poly(A)+ RNA was fragmented to 150 bp and converted to cDNA. The cDNA fragments were then end-repaired, adenylated on the 3' end, adapter-ligated and amplified with 15 cycles of PCR. The final libraries were validated using Qubit (Invitrogen) and Tapetstation (Agilent Technologies). 2x 50 bp paired-end sequencing was performed on the Illumina NovaSeq 6000 SP according to the manufacturer's protocol. The libraries were prepared by the DKFZ NGS core facility (DKFZ, Heidelberg).

Adapter sequences were trimmed from raw reads using cutadapt (version 1.18) [230]. *Drosophila melanogaster* genome sequences were downloaded from Ensembl (release 108)

and a salmon index was built with a k-mer size of 23. Reads were aligned to the reference genome using salmon (version 1.9.0) with default parameters [231]. Differential gene expression analysis was performed using DESeq2 (version 1.36.0) [229] along with logFC shrinkage using the apeglm algorithm (version 1.18.0) [232]. Genes with an absolute logFC greater than 1 and an adjusted p-value below 0.05 were considered significant. The data was analysed by Nick Hirschmueller from the Huber lab (EMBL, Heidelberg).

5.2.10 Identification of genes from the clear cell Renal Cell Carcinoma dataset

mRNA expression z-scores relative to normal samples for the Kidney Renal Clear Cell Carcinoma (TCGA, PanCancer Atlas, 2018) were downloaded from cbioportal. Genes having mean or median (or both) z-score above 2 were selected. Fly homologs of these human genes were then identified, a few of which were screened in the fly MT tumor model. This data was extracted by Erica Valentini from the Boutros lab (DKFZ, Heidelberg).

5.2.11 Statistical analysis

Statistical analysis was performed using the GraphPad Prism 10 software. An Ordinary-one way ANOVA test was used to compare three or more conditions, while the Mann-Whitney T-test was used to compare two independent conditions. The Log-rank (Mantel-Cox) test was employed to analyze the lifespan data. Specific statistical tests used for each experiment are mentioned in the figure legends.

6 References

[1] Irene Miguel-Aliaga, Heinrich Jasper, and Bruno Lemaitre. “Anatomy and physiology of the digestive tract of Drosophila melanogaster”. In: *Genetics* 210.2 (2018), pp. 357–396.

[2] Elena M Lucchetta and Benjamin Ohlstein. “The Drosophila midgut: a model for stem cell driven tissue regeneration”. In: *Wiley Interdisciplinary Reviews: Developmental Biology* 1.5 (2012), pp. 781–788.

[3] Benjamin Ohlstein and Allan Spradling. “The adult Drosophila posterior midgut is maintained by pluripotent stem cells”. In: *Nature* 439.7075 (2006), pp. 470–474.

[4] Craig A Micchelli and Norbert Perrimon. “Evidence that stem cells reside in the adult Drosophila midgut epithelium”. In: *Nature* 439.7075 (2006), pp. 475–479.

[5] Xiankun Zeng and Steven X Hou. “Enteroendocrine cells are generated from stem cells through a distinct progenitor in the adult Drosophila posterior midgut”. In: *Development* 142.4 (2015), pp. 644–653.

[6] Benjamin Ohlstein and Allan Spradling. “Multipotent Drosophila intestinal stem cells specify daughter cell fates by differential notch signaling”. In: *Science* 315.5814 (2007), pp. 988–992.

[7] Huaqi Jiang et al. “Cytokine/Jak/Stat signaling mediates regeneration and homeostasis in the Drosophila midgut”. In: *Cell* 137.7 (2009), pp. 1343–1355.

[8] Guonan Lin, Na Xu, and Rongwen Xi. “Paracrine Wingless signalling controls self-renewal of Drosophila intestinal stem cells”. In: *Nature* 455.7216 (2008), pp. 1119–1123.

[9] Wen-Chih Lee et al. “Adenomatous polyposis coli regulates Drosophila intestinal stem cell proliferation”. In: (2009).

[10] Huaqi Jiang et al. “EGFR/Ras/MAPK signaling mediates adult midgut epithelial homeostasis and regeneration in Drosophila”. In: *Cell stem cell* 8.1 (2011), pp. 84–95.

[11] Nicolas Buchon et al. “Invasive and indigenous microbiota impact intestinal stem cell activity through multiple pathways in Drosophila”. In: *Genes & development* 23.19 (2009), pp. 2333–2344.

[12] Julian AT Dow, Sue Ann Krause, and Pawel Herzyk. “Updates on ion and water transport by the Malpighian tubule”. In: *Current Opinion in Insect Science* 47 (2021), pp. 31–37.

[13] Shree Ram Singh, Wei Liu, and Steven X Hou. “The adult Drosophila malpighian tubules are maintained by multipotent stem cells”. In: *Cell stem cell* 1.2 (2007), pp. 191–203.

[14] Shigeo Takashima et al. “Migration of Drosophila intestinal stem cells across organ boundaries”. In: *Development* 140.9 (2013), pp. 1903–1911.

[15] Chenhui Wang and Allan C Spradling. “An abundant quiescent stem cell population in Drosophila Malpighian tubules protects principal cells from kidney stones”. In: *Elife* 9 (2020), e54096.

[16] Mark E Fortini. “Notch signaling: the core pathway and its posttranslational regulation”. In: *Developmental cell* 16.5 (2009), pp. 633–647.

[17] Christine M Blaumueller et al. “Intracellular cleavage of Notch leads to a heterodimeric receptor on the plasma membrane”. In: *Cell* 90.2 (1997), pp. 281–291.

[18] Robert J Lake et al. “In vivo analysis of the Notch receptor S1 cleavage”. In: *PloS one* 4.8 (2009), e6728.

[19] Christel Brou et al. “A novel proteolytic cleavage involved in Notch signaling: the role of the disintegrin-metalloprotease TACE”. In: *Molecular cell* 5.2 (2000), pp. 207–216.

[20] Eric C Lai et al. “Drosophila neuralized is a ubiquitin ligase that promotes the internalization and degradation of delta”. In: *Developmental cell* 1.6 (2001), pp. 783–794.

[21] Elias Pavlopoulos et al. “neuralized Encodes a peripheral membrane protein involved in delta signaling and endocytosis”. In: *Developmental cell* 1.6 (2001), pp. 807–816.

[22] Eric C Lai et al. “The ubiquitin ligase Drosophila Mind bomb promotes Notch signaling by regulating the localization and activity of Serrate and Delta”. In: (2005).

[23] Jeffrey S Mumm et al. “A ligand-induced extracellular cleavage regulates γ-secretase-like proteolytic activation of Notch1”. In: *Molecular cell* 5.2 (2000), pp. 197–206.

[24] Gary Struhl and Iva Greenwald. “Presenilin is required for activity and nuclear access of Notch in Drosophila”. In: *Nature* 398.6727 (1999), pp. 522–525.

[25] Bart De Strooper et al. “A presenilin-1-dependent γ-secretase-like protease mediates release of Notch intracellular domain”. In: *Nature* 398.6727 (1999), pp. 518–522.

[26] Gary Struhl and Atsuko Adachi. “Nuclear access and action of notch in vivo”. In: *Cell* 93.4 (1998), pp. 649–660.

[27] Mark E Fortini and Spyros Artavanis-Tsakonas. “The suppressor of hairless protein participates in notch receptor signaling”. In: *Cell* 79.2 (1994), pp. 273–282.

[28] Lizi Wu et al. “MAML1, a human homologue of Drosophila mastermind, is a transcriptional co-activator for NOTCH receptors”. In: *Nature genetics* 26.4 (2000), pp. 484–489.

[29] Magalie Lecourtois and Francois Schweisguth. “The neurogenic suppressor of hairless DNA-binding protein mediates the transcriptional activation of the enhancer of split complex genes triggered by Notch signaling.” In: *Genes & development* 9.21 (1995), pp. 2598–2608.

[30] Adina M Bailey and James W Posakony. “Suppressor of hairless directly activates transcription of enhancer of split complex genes in response to Notch receptor activity.” In: *Genes & development* 9.21 (1995), pp. 2609–2622.

[31] Takahisa Furukawa et al. “Suppressor of Hairless, the Drosophila homologue of RBP-Jκ, transactivates the neurogenic gene E (spl) m8”. In: *The Japanese Journal of Genetics* 70.4 (1995), pp. 505–524.

[32] Jerome Korzelius et al. “The WT1-like transcription factor Klumpfuss maintains lineage commitment of enterocyte progenitors in the Drosophila intestine”. In: *Nature Communications* 10.1 (2019), p. 4123.

[33] Jun Chen et al. “Transient Scute activation via a self-stimulatory loop directs enteroendocrine cell pair specification from self-renewing intestinal stem cells”. In: *Nature cell biology* 20.2 (2018), pp. 152–161.

[34] Allison J Bardin et al. “Transcriptional control of stem cell maintenance in the Drosophila intestine”. In: *Development* 137.5 (2010), pp. 705–714.

[35] Parthive H Patel, Devanjali Dutta, and Bruce A Edgar. “Niche appropriation by Drosophila intestinal stem cell tumours”. In: *Nature cell biology* 17.9 (2015), pp. 1182–1192.

[36] Satoshi Ikeda et al. “Axin, a negative regulator of the Wnt signaling pathway, forms a complex with GSK-3β and β-catenin and promotes GSK-3β-dependent phosphorylation of β-catenin”. In: *The EMBO journal* (1998).

[37] Bonnee Rubinfeld et al. “Binding of GSK3β to the APC-β-catenin complex and regulation of complex assembly”. In: *Science* 272.5264 (1996), pp. 1023–1026.

[38] Jennifer L Stamos and William I Weis. “The β-catenin destruction complex”. In: *Cold Spring Harbor perspectives in biology* 5.1 (2013), a007898.

[39] Hermann Aberle et al. “β-catenin is a target for the ubiquitin–proteasome pathway”. In: *The EMBO journal* 16.13 (1997), pp. 3797–3804.

[40] M Hart et al. “The F-box protein β-TrCP associates with phosphorylated β-catenin and regulates its activity in the cell”. In: *Current biology* 9.4 (1999), pp. 207–211.

[41] Robert A Cavallo et al. “Drosophila Tcf and Groucho interact to repress Wingless signalling activity”. In: *Nature* 395.6702 (1998), pp. 604–608.

[42] Purnima Bhanot et al. “A new member of the frizzled family from Drosophila functions as a Wingless receptor”. In: *Nature* 382.6588 (1996), pp. 225–230.

[43] Keiko Tamai et al. “LDL-receptor-related proteins in Wnt signal transduction”. In: *Nature* 407.6803 (2000), pp. 530–535.

[44] Daniele VF Tauriello et al. “Wnt/β-catenin signaling requires interaction of the Dishevelled DEP domain and C terminus with a discontinuous motif in Frizzled”. In: *Proceedings of the National Academy of Sciences* 109.14 (2012), E812–E820.

[45] Gary Davidson et al. “Casein kinase 1 γ couples Wnt receptor activation to cytoplasmic signal transduction”. In: *Nature* 438.7069 (2005), pp. 867–872.

[46] Jürgen Behrens et al. “Functional interaction of β-catenin with the transcription factor LEF-1”. In: *Nature* 382.6592 (1996), pp. 638–642.

[47] Nicholas S Tolwinski and Eric Wieschaus. “A nuclear function for armadillo/β-catenin”. In: *PLoS biology* 2.4 (2004), e95.

[48] Nicolas Buchon et al. “Morphological and molecular characterization of adult midgut compartmentalization in Drosophila”. In: *Cell reports* 3.5 (2013), pp. 1725–1738.

[49] Jessica Perochon, Lynsey R Carroll, and Julia B Cordero. “Wnt signalling in intestinal stem cells: lessons from mice and flies”. In: *Genes* 9.3 (2018), p. 138.

[50] Julia Cordero, Marcos Vidal, and Owen Sansom. “APC as a master regulator of intestinal homeostasis and transformation: from flies to vertebrates”. In: *Cell Cycle* 8.18 (2009), pp. 2927–2932.

[51] Ai Tian et al. “Regulation of stem cell proliferation and cell fate specification by Wingless/Wnt signaling gradients enriched at adult intestinal compartment boundaries”. In: *PLoS genetics* 12.2 (2016), e1005822.

[52] Julia B Cordero et al. “Non-autonomous crosstalk between the Jak/Stat and Egfr pathways mediates Apc1-driven intestinal stem cell hyperplasia in the Drosophila adult midgut”. In: *Development* 139.24 (2012), pp. 4524–4535.

[53] AJ Rowan et al. “APC mutations in sporadic colorectal tumors: A mutational “hotspot” and interdependence of the “two hits””. In: *Proceedings of the National Academy of Sciences* 97.7 (2000), pp. 3352–3357.

[54] Chenhui Wang et al. “APC loss-induced intestinal tumorigenesis in Drosophila: Roles of Ras in Wnt signaling activation and tumor progression”. In: *Developmental biology* 378.2 (2013), pp. 122–140.

[55] Saskia JE Suijkerbuijk et al. “Cell competition drives the growth of intestinal adenomas in Drosophila”. In: *Current Biology* 26.4 (2016), pp. 428–438.

[56] Julia B Cordero et al. “Inducible progenitor-derived Wingless regulates adult midgut regeneration in Drosophila”. In: *The EMBO journal* 31.19 (2012), pp. 3901–3917.

[57] Robert Clifford and T Schüpbach. “Molecular analysis of the Drosophila EGF receptor homolog reveals that several genetically defined classes of alleles cluster in subdomains of the receptor protein.” In: *Genetics* 137.2 (1994), pp. 531–550.

[58] Barbara J Rutledge et al. “The Drosophila spitz gene encodes a putative EGF-like growth factor involved in dorsal-ventral axis formation and neurogenesis.” In: *Genes & development* 6.8 (1992), pp. 1503–1517.

[59] Aderet Reich and Ben-Zion Shilo. “Keren, a new ligand of the Drosophila epidermal growth factor receptor, undergoes two modes of cleavage”. In: *The EMBO journal* (2002).

[60] Bruce Schnepp et al. “Vein is a novel component in the Drosophila epidermal growth factor receptor pathway with similarity to the neuregulins.” In: *Genes & development* 10.18 (1996), pp. 2302–2313.

[61] F Shira Neuman-Silberberg and Trudi Schüpbach. “The Drosophila dorsoventral patterning gene gurken produces a dorsally localized RNA and encodes a TGFα-like protein”. In: *Cell* 75.1 (1993), pp. 165–174.

[62] Joseph Schlessinger. “Ligand-induced, receptor-mediated dimerization and activation of EGF receptor”. In: *Cell* 110.6 (2002), pp. 669–672.

[63] Jean Paul Olivier et al. “A Drosophila SH2-SH3 adaptor protein implicated in coupling the sevenless tyrosine kinase to an activator of Ras guanine nucleotide exchange, Sos”. In: *Cell* 73.1 (1993), pp. 179–191.

[64] Michael A Simon et al. “Ras1 and a putative guanine nucleotide exchange factor perform crucial steps in signaling by the sevenless protein tyrosine kinase”. In: *Cell* 67.4 (1991), pp. 701–716.

[65] Laura Bonfini et al. “The Son of sevenless gene product: a putative activator of Ras”. In: *Science* 255.5044 (1992), pp. 603–606.

[66] David Stokoe et al. “Activation of Raf as a result of recruitment to the plasma membrane”. In: *Science* 264.5164 (1994), pp. 1463–1467.

[67] R Marais et al. “Ras recruits Raf-1 to the plasma membrane for activation by tyrosine phosphorylation.” In: *The EMBO journal* 14.13 (1995), pp. 3136–3145.

[68] Leo Tsuda et al. “A protein kinase similar to MAP kinase activator acts downstream of the raf kinase in Drosophila”. In: *Cell* 72.3 (1993), pp. 407–414.

[69] WH Biggs 3rd et al. “The Drosophila rolled locus encodes a MAP kinase required in the sevenless signal transduction pathway.” In: *The EMBO Journal* 13.7 (1994), pp. 1628–1635.

[70] Sergio Astigarraga et al. “A MAPK docking site is critical for downregulation of Capicua by Torso and EGFR RTK signaling”. In: *The EMBO journal* 26.3 (2007), pp. 668–677.

[71] Chenge Zhang et al. “EGFR signaling activates intestinal stem cells by promoting mitochondrial biogenesis and β-oxidation”. In: *Current Biology* 32.17 (2022), pp. 3704–3719.

[72] Tsutomu Kodaki et al. “The activation of phosphatidylinositol 3-kinase by Ras”. In: *Current biology* 4.9 (1994), pp. 798–806.

[73] Pablo Rodriguez-Viciana et al. “Phosphatidylinositol-3-OH kinase direct target of Ras”. In: *Nature* 370.6490 (1994), pp. 527–532.

[74] Thomas F Franke et al. “The protein kinase encoded by the Akt proto-oncogene is a target of the PDGF-activated phosphatidylinositol 3-kinase”. In: *Cell* 81.5 (1995), pp. 727–736.

[75] Ken Inoki et al. “TSC2 is phosphorylated and inhibited by Akt and suppresses mTOR signalling”. In: *Nature cell biology* 4.9 (2002), pp. 648–657.

[76] Na Xu et al. “EGFR, Wingless and JAK/STAT signaling cooperatively maintain Drosophila intestinal stem cells”. In: *Developmental biology* 354.1 (2011), pp. 31–43.

[77] Jinyi Xiang et al. “EGFR-dependent TOR-independent endocycles support Drosophila gut epithelial regeneration”. In: *Nature communications* 8.1 (2017), p. 15125.

[78] Benoıt Biteau and Heinrich Jasper. “EGF signaling regulates the proliferation of intestinal stem cells in Drosophila”. In: *Development* 138.6 (2011), pp. 1045–1055.

[79] Nicolas Buchon et al. “Drosophila EGFR pathway coordinates stem cell proliferation and gut remodeling following infection”. In: *BMC biology* 8 (2010), pp. 1–19.

[80] Jiae Lee et al. “Dissemination of Ras V12-transformed cells requires the mechanosensitive channel Piezo”. In: *Nature communications* 11.1 (2020), p. 3568.

[81] Erdem Bangi et al. “Functional exploration of colorectal cancer genomes using Drosophila”. In: *Nature communications* 7.1 (2016), pp. 1–16.

[82] Xiankun Zeng et al. “Tumor suppressors Sav/scrib and oncogene ras regulate stem-cell transformation in adult Drosophila malpighian tubules”. In: *Journal of cellular physiology* 224.3 (2010), pp. 766–774.

[83] Amandine Rambur et al. “Sequential Ras/MAPK and PI3K/AKT/mTOR pathways recruitment drives basal extrusion in the prostate-like gland of Drosophila”. In: *Nature Communications* 11.1 (2020), p. 2300.

[84] Tatsushi Igaki et al. “Eiger, a TNF superfamily ligand that triggers the Drosophila JNK pathway”. In: *The EMBO journal* (2002).

[85] Hiroshi Kanda et al. “Wengen, a member of the Drosophila tumor necrosis factor receptor superfamily, is required for Eiger signaling”. In: *Journal of Biological Chemistry* 277.32 (2002), pp. 28372–28375.

[86] Ditte S Andersen et al. “The Drosophila TNF receptor Grindelwald couples loss of cell polarity and neoplastic growth”. In: *Nature* 522.7557 (2015), pp. 482–486.

[87] Yi-Chi Su, Jessica E Treisman, and Edward Y Skolnik. “The Drosophila Ste20-related kinase misshapen is required for embryonic dorsal closure and acts through a JNK MAPK module on an evolutionarily conserved signaling pathway”. In: *Genes & development* 12.15 (1998), pp. 2371–2380.

[88] Yoshihiro Takatsu et al. “TAK1 participates in c-Jun N-terminal kinase signaling during Drosophila development”. In: *Molecular and cellular biology* (2000).

[89] Bruno Glise, Henri Bourbon, and Stephane Noselli. “hemipterous encodes a novel Drosophila MAP kinase kinase, required for epithelial cell sheet movement”. In: *Cell* 83.3 (1995), pp. 451–461.

[90] Juan R Riesgo-Escovar et al. “The Drosophila Jun-N-terminal kinase is required for cell morphogenesis but not for DJun-dependent cell fate specification in the eye.” In: *Genes & development* 10.21 (1996), pp. 2759–2768.

[91] Karen K Perkins, Gina M Dailey, and Robert Tjian. “Novel Jun-and Fos-related proteins in Drosophila are functionally homologous to enhancer factor AP-1.” In: *The EMBO journal* 7.13 (1988), pp. 4265–4273.

[92] Jun Zhou and Michael Boutros. “JNK-dependent intestinal barrier failure disrupts host–microbe homeostasis during tumorigenesis”. In: *Proceedings of the National Academy of Sciences* 117.17 (2020), pp. 9401–9412.

[93] Benoıt Biteau, Christine E Hochmuth, and Heinrich Jasper. “JNK activity in somatic stem cells causes loss of tissue homeostasis in the aging Drosophila gut”. In: *Cell stem cell* 3.4 (2008), pp. 442–455.

[94] Zongzhao Zhai et al. “Accumulation of differentiating intestinal stem cell progenies drives tumorigenesis”. In: *Nature communications* 6.1 (2015), p. 10219.

[95] Fanju W Meng and Benoıt Biteau. “A Sox transcription factor is a critical regulator of adult stem cell proliferation in the Drosophila intestine”. In: *Cell reports* 13.5 (2015), pp. 906–914.

[96] Juliane Mundorf et al. “Ets21c governs tissue renewal, stress tolerance, and aging in the Drosophila intestine”. In: *Cell reports* 27.10 (2019), pp. 3019–3033.

[97] Daniel Jun-Kit Hu and Heinrich Jasper. “Control of intestinal cell fate by dynamic mitotic spindle repositioning influences epithelial homeostasis and longevity”. In: *Cell reports* 28.11 (2019), pp. 2807–2823.

[98] Susanna Valanne, Jing-Huan Wang, and Mika Rämet. “The Drosophila toll signaling pathway”. In: *The Journal of Immunology* 186.2 (2011), pp. 649–656.

[99] Tatiana Michel et al. “Drosophila Toll is activated by Gram-positive bacteria through a circulating peptidoglycan recognition protein”. In: *Nature* 414.6865 (2001), pp. 756–759.

[100] Vanessa Gobert et al. “Dual activation of the Drosophila toll pathway by two pattern recognition receptors”. In: *Science* 302.5653 (2003), pp. 2126–2130.

[101] Marie Gottar et al. “Dual detection of fungal infections in Drosophila via recognition of glucans and sensing of virulence factors”. In: *Cell* 127.7 (2006), pp. 1425–1437.

[102] Nicolas Buchon et al. “A single modular serine protease integrates signals from pattern-recognition receptors upstream of the Drosophila Toll pathway”. In: *Proceedings of the National Academy of Sciences* 106.30 (2009), pp. 12442–12447.

[103] In-Hwan Jang et al. “A Spätzle-processing enzyme required for toll signaling activation in Drosophila innate immunity”. In: *Developmental cell* 10.1 (2006), pp. 45–55.

[104] Miranda Lewis et al. “Cytokine Spätzle binds to the Drosophila immunoreceptor Toll with a neurotrophin-like specificity and couples receptor activation”. In: *Proceedings of the National Academy of Sciences* 110.51 (2013), pp. 20461–20466.

[105] Christoph Parthier et al. “Structure of the Toll-Spätzle complex, a molecular hub in Drosophila development and innate immunity”. In: *Proceedings of the National Academy of Sciences* 111.17 (2014), pp. 6281–6286.

[106] Alexander NR Weber et al. “Ligand-Receptor and Receptor-Receptor Interactions Act in Concert to Activate Signaling in the Drosophila Toll Pathway*”. In: *Journal of Biological Chemistry* 280.24 (2005), pp. 22793–22799.

[107] Tiffany Horng and Ruslan Medzhitov. “Drosophila MyD88 is an adapter in the Toll signaling pathway”. In: *Proceedings of the National Academy of Sciences* 98.22 (2001), pp. 12654–12658.

[108] Huaiyu Sun et al. “A heterotrimeric death domain complex in Toll signaling”. In: *Proceedings of the National Academy of Sciences* 99.20 (2002), pp. 12871–12876.

[109] Louisa P Wu and Kathryn V Anderson. “Regulated nuclear import of Rel proteins in the Drosophila immune response”. In: *Nature* 392.6671 (1998), pp. 93–97.

[110] JEAN-MARC Reichhart et al. “Expression and nuclear translocation of the rel/NF-kappa B-related morphogen dorsal during the immune response of Drosophila”. In: *Comptes rendus de l’Académie des sciences. Série III, Sciences de la vie* 316.10 (1993), pp. 1218–24.

[111] Y Tony Ip et al. “Dif, a dorsal-related gene that mediates an immune response in Drosophila”. In: *Cell* 75.4 (1993), pp. 753–763.

[112] Jean-Luc Imler and Jules A Hoffmann. “Signaling mechanisms in the antimicrobial host defense of Drosophila”. In: *Current opinion in microbiology* 3.1 (2000), pp. 16–22.

[113] Zongzhao Zhai, Jean-Philippe Boquete, and Bruno Lemaitre. “Cell-specific Imd-NF-κB responses enable simultaneous antibacterial immunity and intestinal epithelial cell shedding upon bacterial infection”. In: *Immunity* 48.5 (2018), pp. 897–910.

[114] Jun Zhou, Erica Valentini, and Michael Boutros. “Microenvironmental innate immune signaling and cell mechanical responses promote tumor growth”. In: *Developmental cell* 56.13 (2021), pp. 1884–1899.

[115] Kristina Petkau et al. “Constitutive immune activity promotes tumorigenesis in Drosophila intestinal progenitor cells”. In: *Cell reports* 20.8 (2017), pp. 1784–1793.

[116] Bruno Lemaitre et al. “Functional analysis and regulation of nuclear import of dorsal during the immune response in Drosophila.” In: *The EMBO journal* 14.3 (1995), pp. 536–545.

[117] Xiang Ding et al. “Toll-7 promotes tumour growth and invasion in Drosophila”. In: *Cell Proliferation* 55.2 (2022), e13188.

[118] SN Meyer et al. “An ancient defense system eliminates unfit cells from developing tissues during cell competition”. In: *Science* 346.6214 (2014), p. 1258236.

[119] Lale Alpar, Cora Bergantiños, and Laura A Johnston. “Spatially restricted regulation of Spätzle/Toll signaling during cell competition”. In: *Developmental cell* 46.6 (2018), pp. 706–719.

[120] Zhuojie Li et al. “Toll signaling promotes JNK-dependent apoptosis in Drosophila”. In: *Cell Division* 15 (2020), pp. 1–11.

[121] Shivohum Bahuguna et al. “Bacterial recognition by PGRP-SA and downstream signalling by Toll/DIF sustain commensal gut bacteria in Drosophila”. In: *PLoS genetics* 18.1 (2022), e1009992.

[122] Edward Giniger, Susan M Varnum, and Mark Ptashne. “Specific DNA binding of GAL4, a positive regulatory protein of yeast”. In: *Cell* 40.4 (1985), pp. 767–774.

[123] Andrea H Brand and Norbert Perrimon. “Targeted gene expression as a means of altering cell fates and generating dominant phenotypes”. In: *development* 118.2 (1993), pp. 401–415.

[124] Maximiliano L Suster et al. “Refining GAL4-driven transgene expression in Drosophila with a GAL80 enhancer-trap”. In: *genesis* 39.4 (2004), pp. 240–245.

[125] Sen-Lin Lai and Tzumin Lee. “Genetic mosaic with dual binary transcriptional systems in Drosophila”. In: *Nature neuroscience* 9.5 (2006), pp. 703–709.

[126] Andrew Fire et al. “Potent and specific genetic interference by double-stranded RNA in Caenorhabditis elegans”. In: *nature* 391.6669 (1998), pp. 806–811.

[127] Emily Bernstein et al. “Role for a bidentate ribonuclease in the initiation step of RNA interference”. In: *Nature* 409.6818 (2001), pp. 363–366.

[128] Scott M Hammond et al. “An RNA-directed nuclease mediates post-transcriptional gene silencing in Drosophila cells”. In: *Nature* 404.6775 (2000), pp. 293–296.

[129] Scott M Hammond et al. “Argonaute2, a link between genetic and biochemical analyses of RNAi”. In: *Science* 293.5532 (2001), pp. 1146–1150.

[130] Martin Jinek et al. “A programmable dual-RNA–guided DNA endonuclease in adaptive bacterial immunity”. In: *science* 337.6096 (2012), pp. 816–821.

[131] Fillip Port et al. “Optimized CRISPR/Cas tools for efficient germline and somatic genome engineering in Drosophila”. In: *Proceedings of the National Academy of Sciences* 111.29 (2014), E2967–E2976.

[132] Fillip Port and Simon L Bullock. “Augmenting CRISPR applications in Drosophila with tRNA-flanked sgRNAs”. In: *Nature methods* 13.10 (2016), pp. 852–854.

[133] Zhasmine Mirzoyan et al. “Drosophila melanogaster: A model organism to study cancer”. In: *Frontiers in genetics* 10 (2019), p. 51.

[134] Wei Liu, Shree Ram Singh, and Steven X Hou. “JAK–STAT is restrained by Notch to control cell proliferation of the Drosophila intestinal stem cells”. In: *Journal of cellular biochemistry* 109.5 (2010), pp. 992–999.

[135] Jennifer A Doudna and Emmanuelle Charpentier. “The new frontier of genome engineering with CRISPR-Cas9”. In: *Science* 346.6213 (2014), p. 1258096.

[136] Tianzuo Zhan et al. “CRISPR/Cas9 for cancer research and therapy”. In: *Seminars in cancer biology*. Vol. 55. Elsevier. 2019, pp. 106–119.

[137] Fillip Port et al. “A large-scale resource for tissue-specific CRISPR mutagenesis in Drosophila”. In: *Elife* 9 (2020), e53865.

[138] Jun Zhou et al. “Dpp/Gbb signaling is required for normal intestinal regeneration during infection”. In: *Developmental biology* 399.2 (2015), pp. 189–203.

[139] Shivohum Bahuguna et al. “Conditional CRISPR-cas genome editing in Drosophila to generate intestinal tumors”. In: *Cells* 10.11 (2021), p. 3156.

[140] Hongjie Li. “Single-cell RNA sequencing in Drosophila: Technologies and applications”. In: *Wiley Interdisciplinary Reviews: Developmental Biology* 10.5 (2021), e396.

[141] Devanjali Dutta et al. “Regional cell-specific transcriptome mapping reveals regulatory complexity in the adult Drosophila midgut”. In: *Cell reports* 12.2 (2015), pp. 346–358.

[142] Ruei-Jiun Hung et al. “A cell atlas of the adult Drosophila midgut”. In: *Proceedings of the National Academy of Sciences* 117.3 (2020), pp. 1514–1523.

[143] Yumei Li et al. “Transcription factor antagonism controls enteroendocrine cell specification from intestinal stem cells”. In: *Scientific reports* 7.1 (2017), p. 988.

[144] Jiajun Xu et al. “Prevention of medulla neuron dedifferentiation by Nerfin-1 requires inhibition of Notch activity”. In: *Development* 144.8 (2017), pp. 1510–1517.

[145] Joseph HA Vissers et al. “The Scalloped and Nerfin-1 transcription factors cooperate to maintain neuronal cell fate”. In: *Cell reports* 25.6 (2018), pp. 1561–1576.

[146] Kenneth W Kinzler and Bert Vogelstein. “Lessons from hereditary colorectal cancer”. In: *Cell* 87.2 (1996), pp. 159–170.

[147] Owen J Sansom et al. “Loss of Apc in vivo immediately perturbs Wnt signaling, differentiation, and migration”. In: *Genes & development* 18.12 (2004), pp. 1385–1390.

[148] Johannes L Bos et al. “Prevalence of ras gene mutations in human colorectal cancers”. In: *Nature* 327.6120 (1987), pp. 293–297.

[149] Klaus–Peter Janssen et al. “APC and oncogenic KRAS are synergistic in enhancing Wnt signaling in intestinal tumor formation and progression”. In: *Gastroenterology* 131.4 (2006), pp. 1096–1109.

[150] Owen J Sansom et al. “Loss of Apc allows phenotypic manifestation of the transforming properties of an endogenous K-ras oncogene in vivo”. In: *Proceedings of the National Academy of Sciences* 103.38 (2006), pp. 14122–14127.

[151] Nicolas Buchon et al. “Drosophila intestinal response to bacterial infection: activation of host defense and stem cell proliferation”. In: *Cell host & microbe* 5.2 (2009), pp. 200–211.

[152] Dani Osman et al. “Autocrine and paracrine unpaired signaling regulate intestinal stem cell maintenance and division”. In: *Journal of cell science* 125.24 (2012), pp. 5944–5949.

[153] Shichao Yu et al. “Drosophila innate immunity involves multiple signaling pathways and coordinated communication between different tissues”. In: *Frontiers in Immunology* 13 (2022), p. 905370.

[154] Ennio De Gregorio et al. “The Toll and Imd pathways are the major regulators of the immune response in Drosophila”. In: *The EMBO journal* 21.11 (2002), pp. 2568–2579.

[155] David S Schneider et al. “Dominant and recessive mutations define functional domains of Toll, a transmembrane protein required for dorsal-ventral polarity in the Drosophila embryo.” In: *Genes & development* 5.5 (1991), pp. 797–807.

[156] Bruno Lemaitre et al. “The dorsoventral regulatory gene cassette spätzle/Toll/cactus controls the potent antifungal response in Drosophila adults”. In: *Cell* 86.6 (1996), pp. 973–983.

[157] Takahiro Tanji, Eun-Young Yun, and Y Tony Ip. “Heterodimers of NF-κB transcription factors DIF and Relish regulate antimicrobial peptide genes in Drosophila”. In: *Proceedings of the National Academy of Sciences* 107.33 (2010), pp. 14715–14720.

[158] Jun Zhou and Michael Boutros. “Intestinal stem cells and their niches in homeostasis and disease”. In: *Cells & Development* 175 (2023), p. 203862.

[159] Aylin R Rodan. “The Drosophila Malpighian tubule as a model for mammalian tubule function”. In: *Current opinion in nephrology and hypertension* 28.5 (2019), pp. 455–464.

[160] Jun Xu et al. “Transcriptional and functional motifs defining renal function revealed by single-nucleus RNA sequencing”. In: *Proceedings of the National Academy of Sciences* 119.25 (2022), e2203179119.

[161] Erez Cohen et al. “Physiology, development, and disease modeling in the Drosophila excretory system”. In: *Genetics* 214.2 (2020), pp. 235–264.

[162] Keiji Tanimoto et al. “Mechanism of regulation of the hypoxia-inducible factor-1α by the von Hippel-Lindau tumor suppressor protein”. In: *The EMBO journal* (2000).

[163] James J Hsieh et al. “Renal cell carcinoma”. In: *Nature reviews Disease primers* 3.1 (2017), pp. 1–19.

[164] Valerie H Le and James J Hsieh. “Genomics and genetics of clear cell renal cell carcinoma: a mini-review”. In: *Journal of Translational Genetics and Genomics* 2 (2018), N–A.

[165] Gowrishankar Banumathy and Paul Cairns. “Signaling pathways in renal cell carcinoma”. In: *Cancer biology & therapy* 10.7 (2010), pp. 658–664.

[166] Gyula Kovacs et al. “Cytoplasmic expression of β-catenin is an independent predictor of progression of conventional renal cell carcinoma: a simple immunostaining score”. In: *Histopathology* 70.2 (2017), pp. 273–280.

[167] Ren-Jun Hsu et al. “WNT10A plays an oncogenic role in renal cell carcinoma by activating WNT/β-catenin pathway”. In: (2012).

[168] Stephan Kruck et al. “Impact of an altered Wnt1/β-catenin expression on clinicopathology and prognosis in clear cell renal cell carcinoma”. In: *International journal of molecular sciences* 14.6 (2013), pp. 10944–10957.

[169] Nico Janssens et al. “Alteration of frizzled expression in renal cell carcinoma”. In: *Tumor Biology* 25.4 (2004), pp. 161–171.

[170] Kazumori Kawakami et al. “Functional significance of Wnt inhibitory factor-1 gene in kidney cancer”. In: *Cancer Research* 69.22 (2009), pp. 8603–8610.

[171] Ken Kawamoto et al. “DNA methylation and histone modifications cause silencing of Wnt antagonist gene in human renal cell carcinoma cell lines”. In: *International journal of cancer* 123.3 (2008), pp. 535–542.

[172] Nives Pećina-Šlaus, Krešimir Pavelić, and Jasminka Pavelić. “Loss of heterozygosity and protein expression of APC gene in renal cell carcinomas”. In: *Journal of molecular medicine* 77 (1999), pp. 446–453.

[173] Nives Pećina-Šlaus et al. “Genetic changes of the E-cadherin and APC tumour suppressor genes in clear cell renal cell carcinoma”. In: *Pathology* 36.2 (2004), pp. 145–151.

[174] Yen-Chein Lai and Wen-Chung Wang. “Genetic Analysis Reveals the Important Role of the APC Gene in Clear Cell Renal Cell Carcinoma”. In: *Anticancer Research* 41.9 (2021), pp. 4295–4304.

[175] Owen J Sansom et al. “Apc deficiency predisposes to renal carcinoma in the mouse”. In: *Oncogene* 24.55 (2005), pp. 8205–8210.

[176] Ai Tian et al. “Intestinal stem cell overproliferation resulting from inactivation of the APC tumor suppressor requires the transcription cofactors Earthbound and Erect wing”. In: *PLoS genetics* 13.7 (2017), e1006870.

[177] Joel Johansson et al. “RAL GTPases drive intestinal stem cell function and regeneration through internalization of WNT signalosomes”. In: *Cell Stem Cell* 24.4 (2019), pp. 592–607.

[178] Michelle C Mendoza, E Emrah Er, and John Blenis. “The Ras-ERK and PI3K-mTOR pathways: cross-talk and compensation”. In: *Trends in biochemical sciences* 36.6 (2011), pp. 320–328.

[179] Ryan C Gimple and Xiuxing Wang. “RAS: Striking at the Core of the Oncogenic Circuitry”. In: *Frontiers in oncology* 9 (2019), p. 965.

[180] Allan J Pantuck et al. “Prognostic relevance of the mTOR pathway in renal cell carcinoma: implications for molecular patient selection for targeted therapy”. In: *Cancer* 109.11 (2007), pp. 2257–2267.

[181] Daniela Miricescu et al. “PI3K/AKT/mTOR signalling pathway involvement in renal cell carcinoma pathogenesis”. In: *Experimental and Therapeutic Medicine* 21.5 (2021), pp. 1–7.

[182] Yusuke Sato et al. “Integrated molecular analysis of clear-cell renal cell carcinoma”. In: *Nature genetics* 45.8 (2013), pp. 860–867.

[183] Yinhua Jin et al. “EGFR/Ras signaling controls Drosophila intestinal stem cell proliferation via Capicua-regulated genes”. In: *PLoS genetics* 11.12 (2015), e1005634.

[184] Christopher J Ricketts et al. “The cancer genome atlas comprehensive molecular characterization of renal cell carcinoma”. In: *Cell reports* 23.1 (2018), pp. 313–326.

[185] Ethan Cerami et al. “The cBio cancer genomics portal: an open platform for exploring multidimensional cancer genomics data”. In: *Cancer discovery* 2.5 (2012), pp. 401–404.

[186] Kohei Kobatake et al. “DDX41 expression is associated with tumor necrosis in clear cell renal cell carcinoma and in cooperation with VHL loss leads to worse prognosis”. In: *Urologic Oncology: Seminars and Original Investigations*. Vol. 40. 10. Elsevier. 2022, 456–e9.

[187] Guojun Zhang, Zhe Zhang, and Zhuogang Liu. “Polo-like kinase 1 is overexpressed in renal cancer and participates in the proliferation and invasion of renal cancer cells”. In: *Tumor Biology* 34 (2013), pp. 1887–1894.

[188] Wenzhi Jiang et al. “Successful transient expression of Cas9 and single guide RNA genes in Chlamydomonas reinhardtii”. In: *Eukaryotic cell* 13.11 (2014), pp. 1465–1469.

[189] Su Yang, Shihua Li, and Xiao-Jiang Li. “Shortening the half-life of Cas9 maintains its gene editing ability and reduces neuronal toxicity”. In: *Cell reports* 25.10 (2018), pp. 2653–2659.

[190] Jaime Miquel et al. “Effects of temperature on the life span, vitality and fine structure of Drosophila melanogaster”. In: *Mechanisms of ageing and development* 5 (1976), pp. 347–370.

[191] Imilce A Rodriguez-Fernandez, Helen M Tauc, and Heinrich Jasper. “Hallmarks of aging Drosophila intestinal stem cells”. In: *Mechanisms of ageing and development* 190 (2020), p. 111285.

[192] Marilyn Kozak. “Constraints on reinitiation of translation in mammals”. In: *Nucleic acids research* 29.24 (2001), pp. 5226–5232.

[193] Fillip Port, Maja Starostecka, and Michael Boutros. “Multiplexed conditional genome editing with Cas12a in Drosophila”. In: *Proceedings of the National Academy of Sciences* 117.37 (2020), pp. 22890–22899.

[194] Rachael L Shaw et al. “The Hippo pathway regulates intestinal stem cell proliferation during Drosophila adult midgut regeneration”. In: *Development* 137.24 (2010), pp. 4147–4158.

[195] Alexander Kuzin et al. “Nerfin-1 is required for early axon guidance decisions in the developing Drosophila CNS”. In: *Developmental biology* 277.2 (2005), pp. 347–365.

[196] Anne-Sophie Litmeyer et al. “High expression of insulinoma-associated protein 1 (INSM1) distinguishes colorectal mixed and pure neuroendocrine carcinomas from conventional adenocarcinomas with diffuse expression of synaptophysin”. In: *The Journal of Pathology: Clinical Research* 9.6 (2023), pp. 498–509.

[197] Mathias S Gierl et al. “The zinc-finger factor Insm1 (IA-1) is essential for the development of pancreatic β cells and intestinal endocrine cells”. In: *Genes & development* 20.17 (2006), pp. 2465–2478.

[198] David Stein et al. “The Dorsal-related immunity factor (Dif) can define the dorsal-ventral axis of polarity in the Drosophila embryo”. In: *Development* 125.11 (1998), pp. 2159–2169.

[199] Sophie Rutschmann et al. “The Rel protein DIF mediates the antifungal but not the antibacterial host defense in Drosophila”. In: *Immunity* 12.5 (2000), pp. 569–580.

[200] Pascal Manfruelli et al. “A mosaic analysis in Drosophila fat body cells of the control of antimicrobial peptide genes by the Rel proteins Dorsal and DIF”. In: *The EMBO journal* (1999).

[201] Masayuki Fukata et al. “Toll-like receptor-4 promotes the development of colitis-associated colorectal tumors”. In: *Gastroenterology* 133.6 (2007), pp. 1869–1869.

[202] Seth Rakoff-Nahoum and Ruslan Medzhitov. “Regulation of spontaneous intestinal tumorigenesis through the adaptor protein MyD88”. In: *Science* 317.5834 (2007), pp. 124–127.

[203] Gen Lin et al. “KRAS mutation and NF-κB activation indicates tolerance of chemotherapy and poor prognosis in colorectal cancer”. In: *Digestive diseases and sciences* 57 (2012), pp. 2325–2333.

[204] Nikhil Moorchung, Shova Kunwar, and Kashif W Ahmed. “An evaluation of nuclear factor kappa B expression in colorectal carcinoma: an analysis of 50 cases”. In: *Journal of Cancer Research and Therapeutics* 10.3 (2014), pp. 631–635.

[205] Michael Karin et al. “NF-κB in cancer: from innocent bystander to major culprit”. In: *Nature reviews cancer* 2.4 (2002), pp. 301–310.

[206] Nadine K Clemo et al. “BAG-1 is up-regulated in colorectal tumour progression and promotes colorectal tumour cell survival through increased NF-κB activity”. In: *Carcinogenesis* 29.4 (2008), pp. 849–857.

[207] Federica Parisi et al. “Transformed epithelia trigger non-tissue-autonomous tumor suppressor response by adipocytes via activation of Toll and Eiger/TNF signaling”. In: *Cell reports* 6.5 (2014), pp. 855–867.

[208] Dawei Liu et al. “Chromosomal instability triggers cell death via local signalling through the innate immune receptor Toll”. In: *Oncotarget* 6.36 (2015), p. 38552.

[209] Weibin Hou and Zhigang Ji. “Generation of autochthonous mouse models of clear cell renal cell carcinoma: mouse models of renal cell carcinoma”. In: *Experimental & molecular medicine* 50.4 (2018), pp. 1–10.

[210] Marco Gerlinger et al. “Intratumor heterogeneity and branched evolution revealed by multiregion sequencing”. In: *New England journal of medicine* 366.10 (2012), pp. 883–892.

[211] Marco Gerlinger et al. “Genomic architecture and evolution of clear cell renal cell carcinomas defined by multiregion sequencing”. In: *Nature genetics* 46.3 (2014), pp. 225–233.

[212] Samuel Pena-Llopis et al. “Cooperation and antagonism among cancer genes: the renal cancer paradigm”. In: *Cancer research* 73.14 (2013), pp. 4173–4179.

[213] Judit Espana-Agusti et al. “Loss of PBRM1 rescues VHL dependent replication stress to promote renal carcinogenesis”. In: *Nature communications* 8.1 (2017), p. 2026.

[214] Shan-Shan Wang et al. “Bap1 is essential for kidney function and cooperates with Vhl in renal tumorigenesis”. In: *Proceedings of the National Academy of Sciences* 111.46 (2014), pp. 16538–16543.

[215] Natalie De Paulsen et al. “Role of transforming growth factor-α in von Hippel–Lindau (VHL)-/- clear cell renal carcinoma cell proliferation: A possible mechanism coupling VHL tumor suppressor inactivation and tumorigenesis”. In: *Proceedings of the National Academy of Sciences* 98.4 (2001), pp. 1387–1392.

[216] Aleksandra Franovic et al. “Translational up-regulation of the EGFR by tumor hypoxia provides a nonmutational explanation for its overexpression in human cancer”. In: *Proceedings of the National Academy of Sciences* 104.32 (2007), pp. 13092–13097.

[217] Martina Hager et al. “Increased activated Akt expression in renal cell carcinomas and prognosis”. In: *Journal of cellular and molecular medicine* 13.8b (2009), pp. 2181–2188.

[218] Huifang Guo et al. “The PI3K/AKT pathway and renal cell carcinoma”. In: *Journal of genetics and genomics* 42.7 (2015), pp. 343–353.

[219] Victoria A Robb et al. “Activation of the mTOR signaling pathway in renal clear cell carcinoma”. In: *The Journal of urology* 177.1 (2007), pp. 346–352.

[220] Athina Ganner et al. “VHL suppresses RAPTOR and inhibits mTORC1 signaling in clear cell renal cell carcinoma”. In: *Scientific reports* 11.1 (2021), p. 14827.

[221] Vipul C Chitalia et al. “Jade-1 inhibits Wnt signalling by ubiquitylating β-catenin and mediates Wnt pathway inhibition by pVHL”. In: *Nature cell biology* 10.10 (2008), pp. 1208–1216.

[222] Hyunsung Choi et al. “HIF-2α enhances β-catenin/TCF-driven transcription by interacting with β-catenin”. In: *Cancer research* 70.24 (2010), pp. 10101–10111.

[223] Liang Zhou and Haifeng Yang. “The von Hippel-Lindau tumor suppressor protein promotes c-Cbl-independent poly-ubiquitylation and degradation of the activated EGFR”. In: *PloS one* 6.9 (2011), e23936.

[224] Hong Doan et al. “HIF-mediated suppression of DEPTOR confers resistance to mTOR kinase inhibition in renal cancer”. In: *Iscience* 21 (2019), pp. 509–520.

[225] Tony D Southall et al. “Cell-type-specific profiling of gene expression and chromatin binding without cell isolation: assaying RNA Pol II occupancy in neural stem cells”. In: *Developmental cell* 26.1 (2013), pp. 101–112.

[226] Michael J Hendzel et al. “Mitosis-specific phosphorylation of histone H3 initiates primarily within pericentromeric heterochromatin during G2 and spreads in an ordered fashion coincident with mitotic chromosome condensation”. In: *Chromosoma* 106 (1997), pp. 348–360.

[227] Kenneth J Livak and Thomas D Schmittgen. “Analysis of relative gene expression data using real-time quantitative PCR and the 2- $\triangle\triangle$CT method”. In: *methods* 25.4 (2001), pp. 402–408.

[228] Robert A Amezquita et al. “Orchestrating single-cell analysis with Bioconductor”. In: *Nature methods* 17.2 (2020), pp. 137–145.

[229] Michael I Love, Wolfgang Huber, and Simon Anders. “Moderated estimation of fold change and dispersion for RNA-seq data with DESeq2”. In: *Genome biology* 15 (2014), pp. 1–21.

[230] Marcel Martin. “Cutadapt removes adapter sequences from high-throughput sequencing reads”. In: *EMBnet. journal* 17.1 (2011), pp. 10–12.

[231] Rob Patro et al. “Salmon provides fast and bias-aware quantification of transcript expression”. In: *Nature methods* 14.4 (2017), pp. 417–419.

[232] Anqi Zhu, Joseph G Ibrahim, and Michael I Love. “Heavy-tailed prior distributions for sequence count data: removing the noise and preserving large differences”. In: *Bioinformatics* 35.12 (2019), pp. 2084–2092.

7 Appendix

7.1 Supplementary Figures

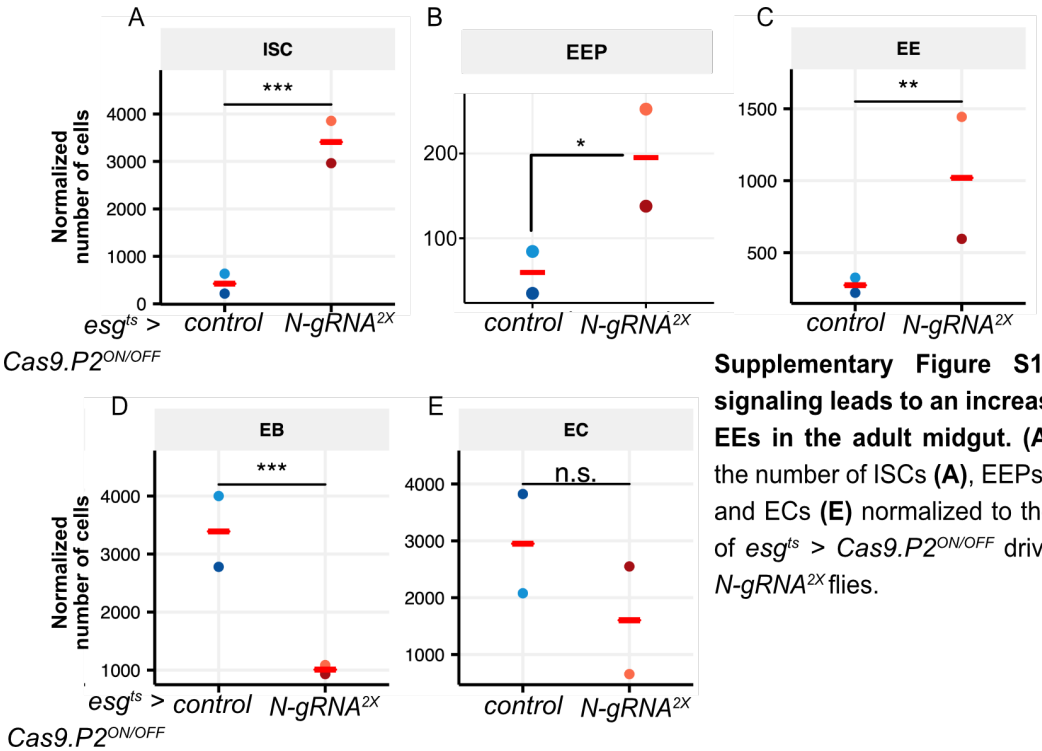

Supplementary Figure S1 : Loss of Notch signaling leads to an increase in ISCs, EEPs, and EEs in the adult midgut. (A-B) Graphs indicating the number of ISCs **(A)**, EEPs **(B)**, EEs **(C)**, EBs **(D)**, and ECs **(E)** normalized to the total number of cells of *esg*^{ts} > *Cas9.P2*$^{ON/OFF}$ driven control (*w*^{1118}), and *N-gRNA*^{2X} flies.

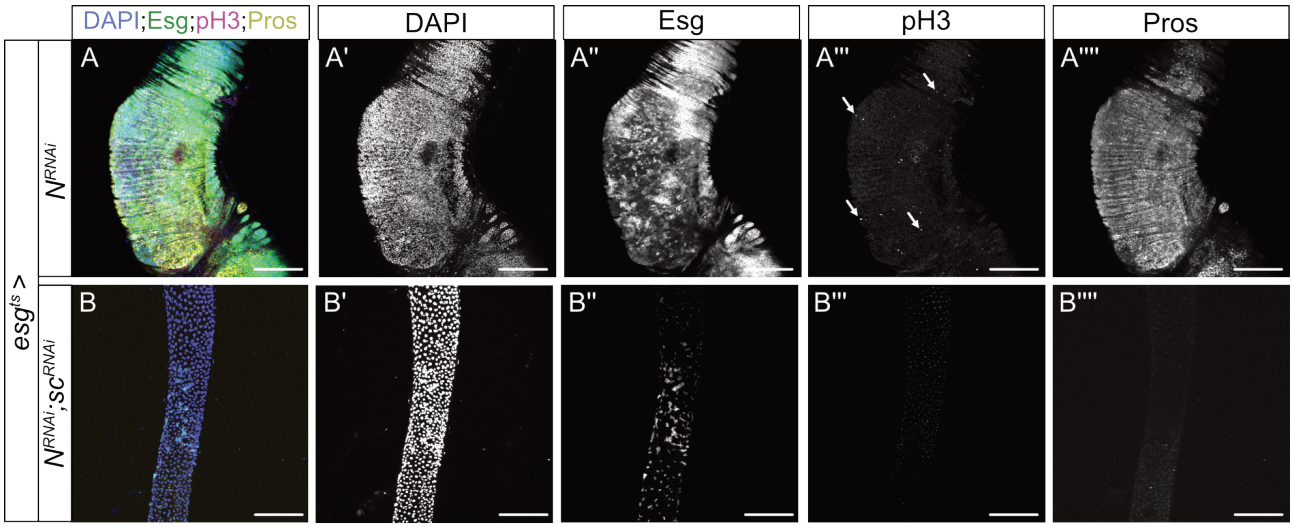

Supplementary Figure S2 : Scute is required for the Notch loss-of-function midgut tumor phenotype. (A-B) Representative images of the posterior midgut of *esg*^{ts} > driven *N*^{RNAi} **(A)**, and *N*^{RNAi};*sc*^{RNAi} **(B)** flies stained with anti-pH3 and anti-Pros antibodies. White arrows indicate pH3 positive mitotic cells in the midgut. Scale bar = 80μm.

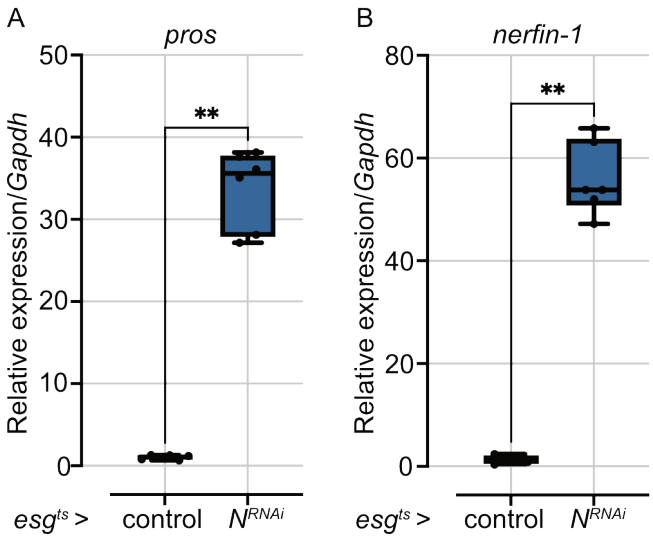

Supplementary Figure S3 : Nerfin-1 is upregulated in Notch loss-of-function midgut tumors. RT-qPCR graph showing upregulation of EE marker *pros* **(A)**, and *nerfin-1* **(B)** expression with respect to house-keeping gene *Gapdh* in esg^{ts} > driven N^{RNAi} vs control (w^{1118}) flies. All experiments were performed in technical duplicates, with 3 independent biological replicates; Mann-Whitney t-test; Significance values are marked by asterisks: $**P < 0.01$.

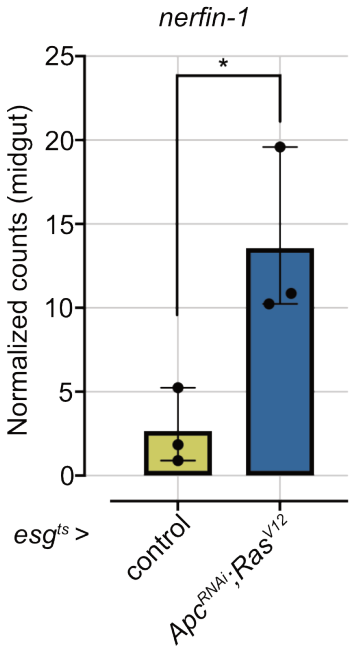

Supplementary Figure S4 : Nerfin-1 is upregulated in $Apc^{RNAi};Ras^{V12}$ midgut tumors. Normalized *nerfin-1* counts from bulk RNA sequencing of midgut of esg^{ts} > driven control and $Apc^{RNAi};Ras^{V12}$ flies; Wald test and benjamini hochberg correction to obtain adj p-value; Significance values are marked by asterisks: $*P \leq 0.05$.

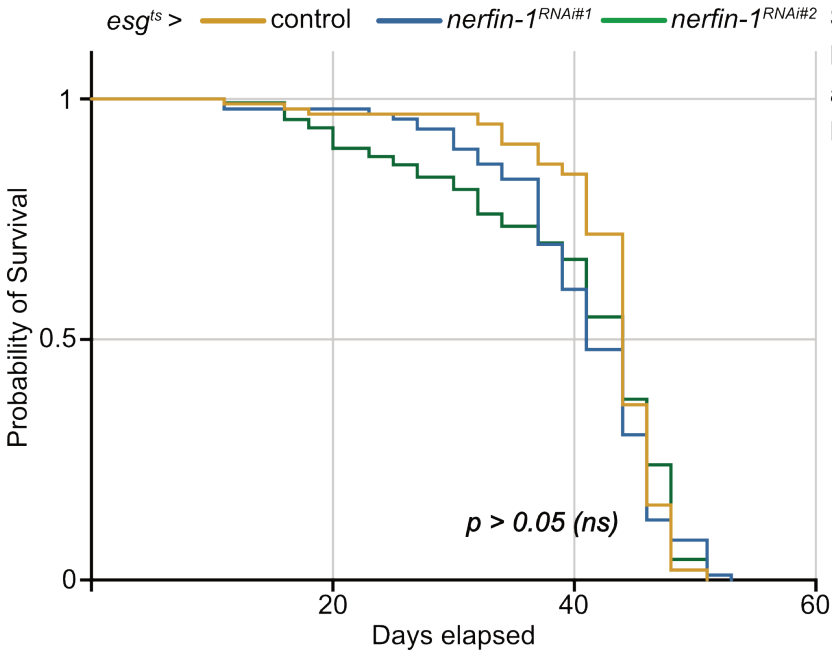

Supplementary Figure S5 : Nerfin-1 has no impact on the lifespan of the adult fly during homeostasis. Lifespan curves of female flies of *esg*^{ts} > driven *control* (*w*^{1118}) (N = 96), *nerfin-1*$^{RNAi\#1}$ (N = 96), and *nerfin-1*$^{RNAi\#2}$ (N = 117) at 29°C. Log-rank *p value* > *0.05*.

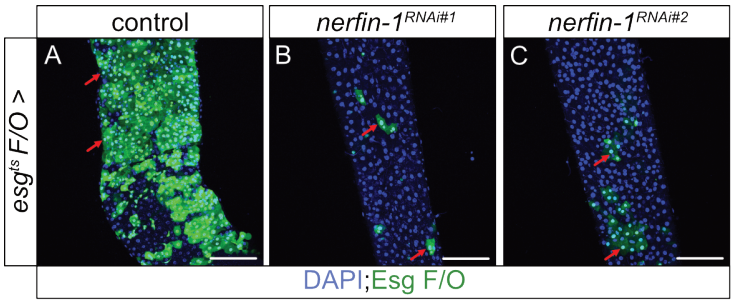

Supplementary Figure S6 : Knockdown of *nerfin-1* forces differentiation of progenitor cells into enterocytes. (A-C) Representative images of the posterior midgut of *esg*^{ts} > *F/O* driven control **(A)**, *nerfin1*$^{RNAi\#1}$ **(B),** and *nerfin1*$^{RNAi\#2}$ **(C)** flies. Red arrows indicate large nucleated EC cells. Note that while a complete turnover of the midgut takes place in the control, suppression of *nerfin1* forces ISC/EBs to differentiate into ECs thereby depleting the progenitor pool. Scale bar = 80μm.

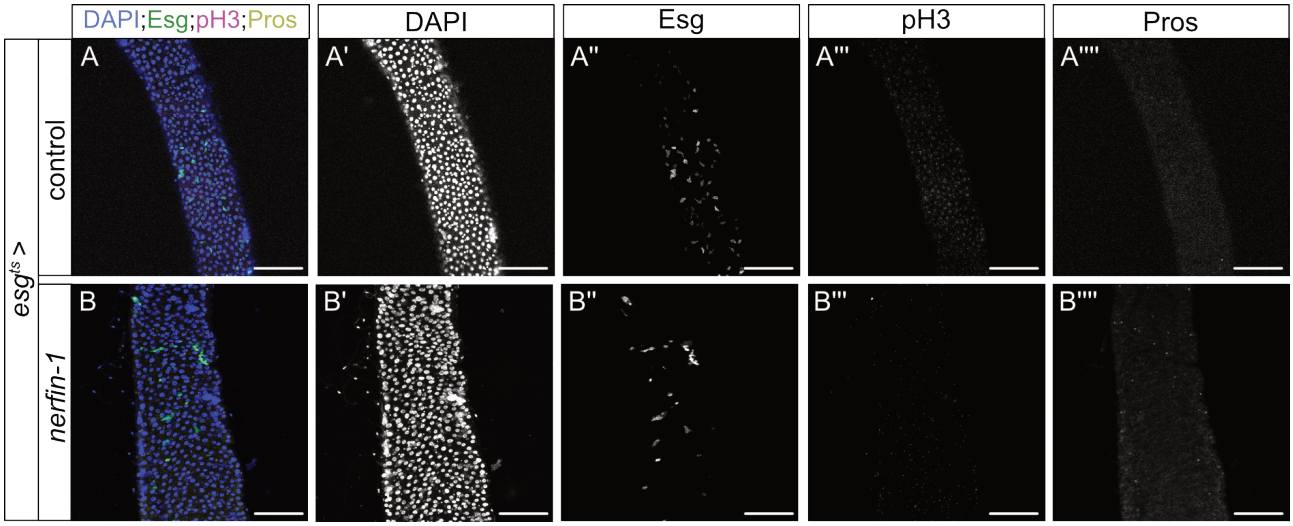

Supplementary Figure S7 : Ectopic expression of *nerfin-1* has no effect on the progenitor cells. (A-C) Representative images of the posterior midgut of *esg*^{ts} > driven *control* (*w*^{1118}) **(A)**, and *nerfin-1* **(B),** stained with anti-pH3 and anti-Pros antibodies. Note that overexpression of *nerfin-1* does not alter progenitor or EE cell numbers. Scale bar = 80μm.

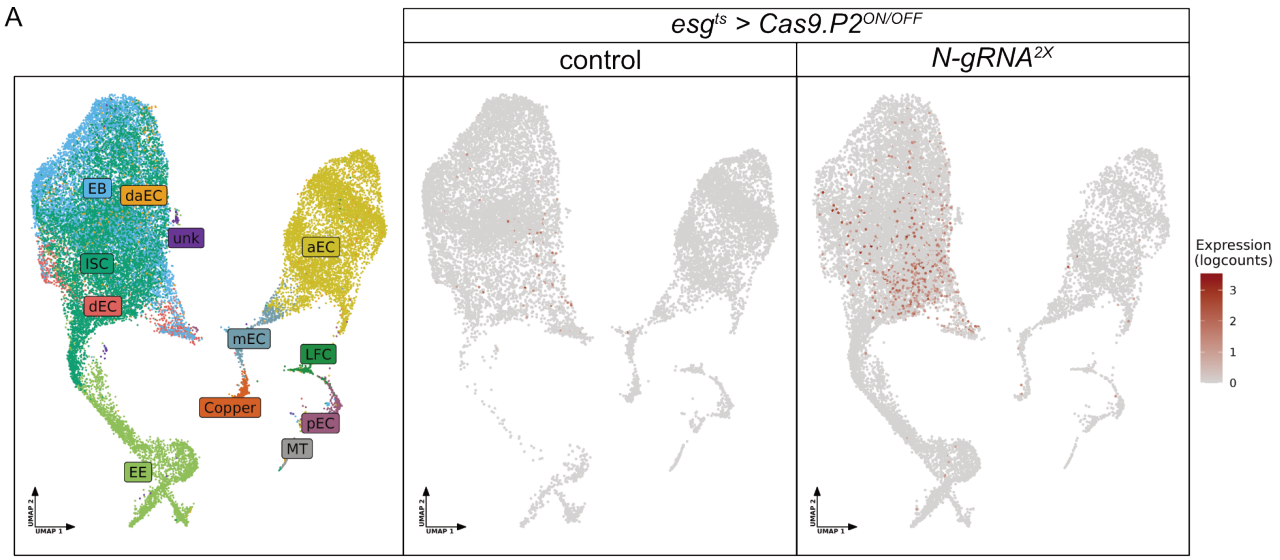

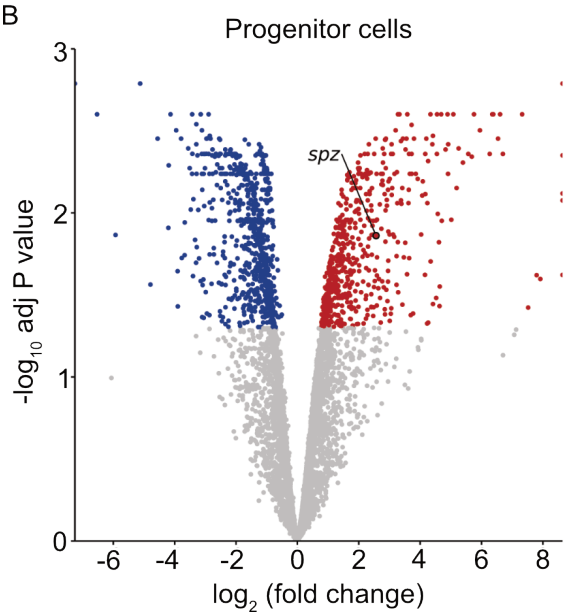

Supplementary Figure S8 : Spz is upregulated in Notch knockout midgut tumors. UMAP representing an increase in *spz* expressing cells in *esg*^{ts} > *Cas9.P2*$^{ON/OFF}$ driven *N-gRNA*^{2X} vs control (*w*^{1118}) **(A).** Volcano plot indicating *spz* is upregulated progenitor cells of *N-gRNA*^{2X} as compared to control (*w*^{1118}) flies **(B)**.

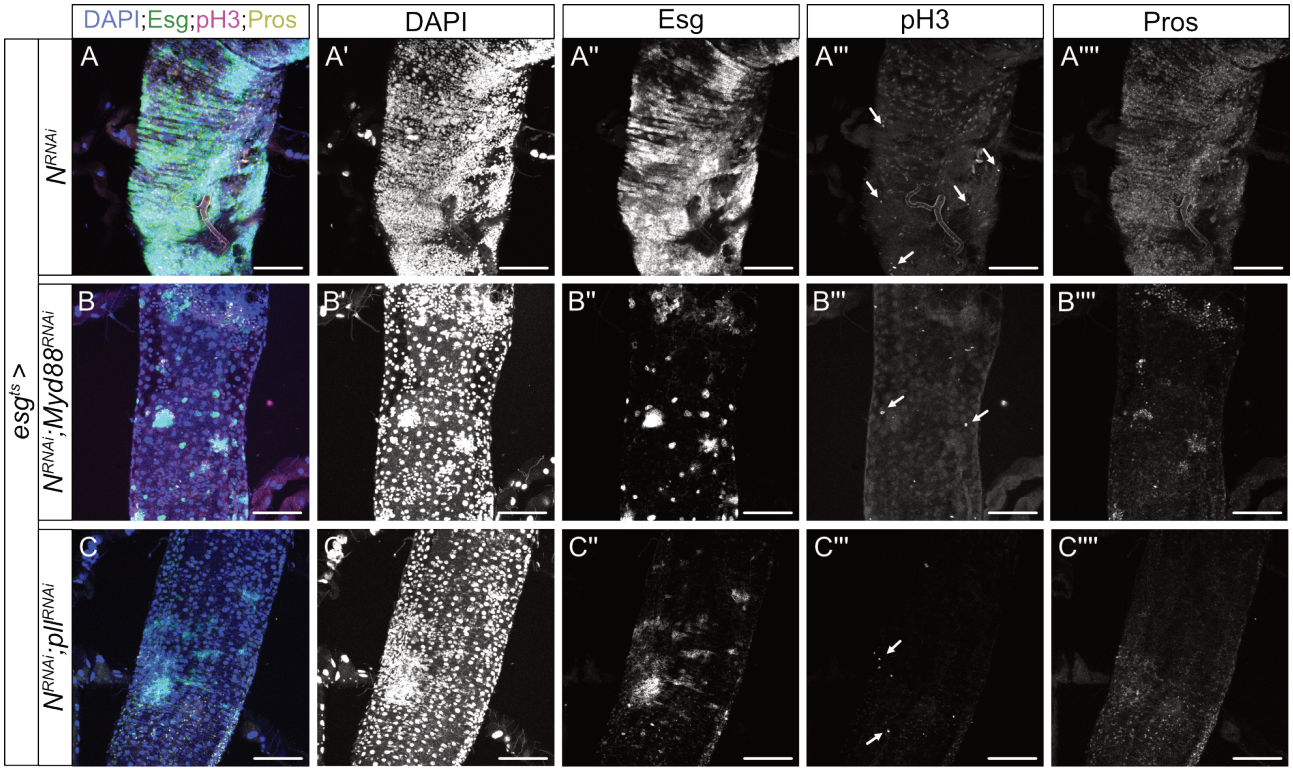

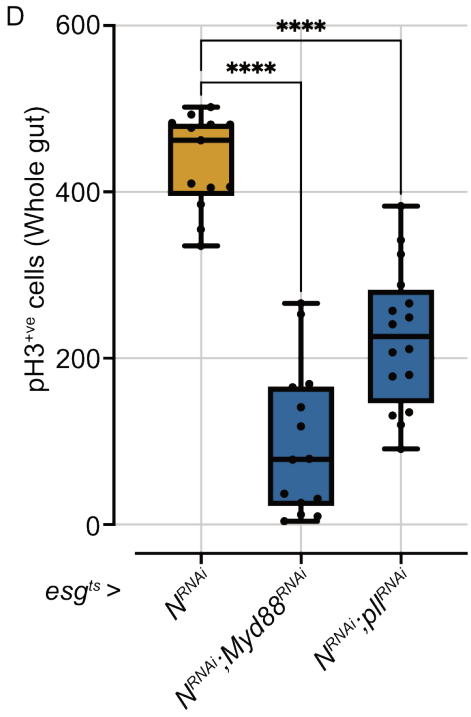

Supplementary Figure S9 : Toll signaling core pathway components Myd88 and Pll are required for the Notch loss-of-function midgut tumor phenotype. (A-D) Representative images of the posterior midgut of *esg*^{ts} > driven *N*^{RNAi} **(A)**, *N*^{RNAi};*Myd88*^{RNAi} **(B)**, and *N*^{RNAi};*pll*^{RNAi} **(C)** flies stained with anti-pH3 and anti-Pros antibodies. White arrows indicate pH3 positive mitotic cells in the midgut. **(D)** Quantification of pH3-positive cells per midgut of the mentioned genotypes. Note that loss of *Myd88* and *pll* can suppress *N*^{RNAi} tumor phenotype. N = 13-16 flies; Significance values are marked by asterisks: ****$P < 0.0001$; Ordinary one-way ANOVA; Scale bar = 80μm.

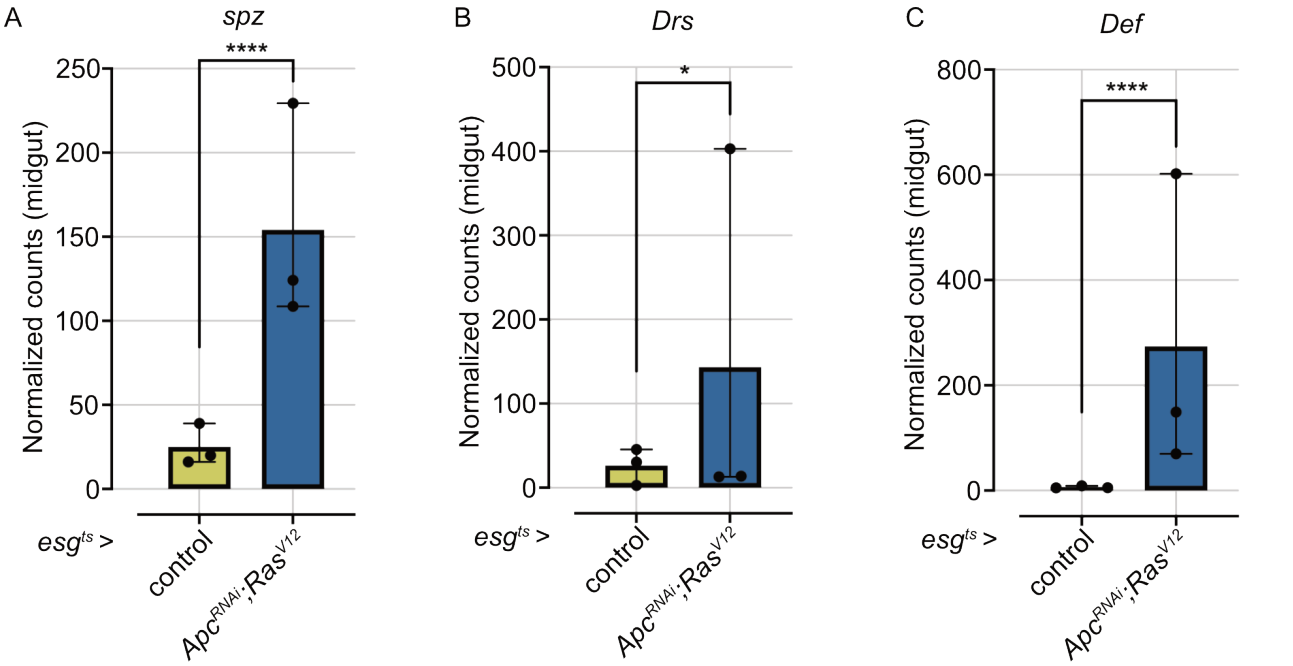

Supplementary Figure S10 : Toll pathway target genes are upregulated in *Apc^{RNAi};Ras^{V12}* midgut tumors. Normalized counts of *spz* **(A),** *Drs* **(B),** *Def* **(C)** from bulk RNA sequencing of the midgut of *esg^{ts}* > driven control and *Apc^{RNAi};Ras^{V12}* flies; Wald test and benjamini hochberg correction to obtain adj p-value; Significance values are marked by asterisks: **P ≤ 0.05, ****P < 0.0001*.

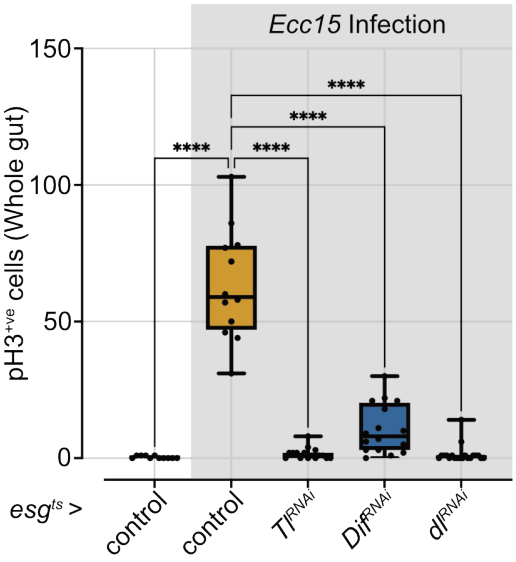

Supplementary Figure S11 : Infection-induced mitotic response is regulated by the Toll signaling pathway in the midgut. Quantification of pH3-positive cells per midgut of *esg^{ts}* > driven uninfected, and *Ecc15* infected control (*w^{1118}*), *Tl^{RNAi}*, *Dif^{RNAi}*, and *dl^{RNAi}* flies. N = 11-20 flies; Significance values are marked by asterisks: *****P < 0.0001*; Ordinary one-way ANOVA.

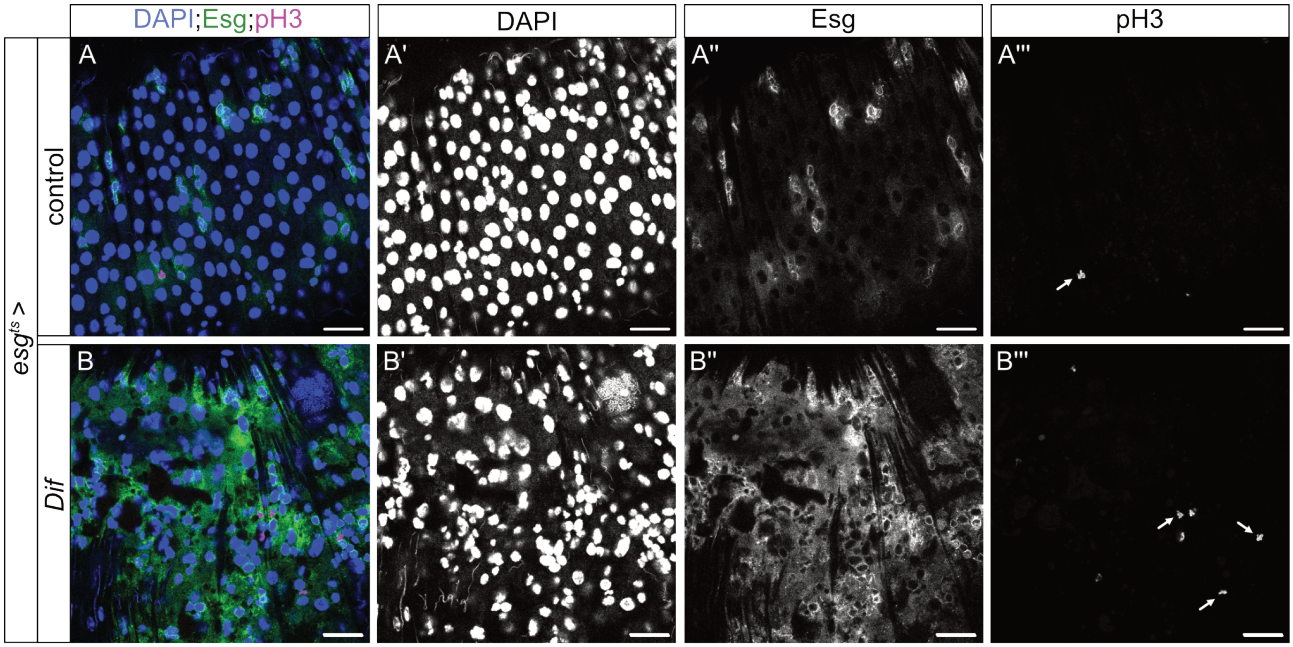

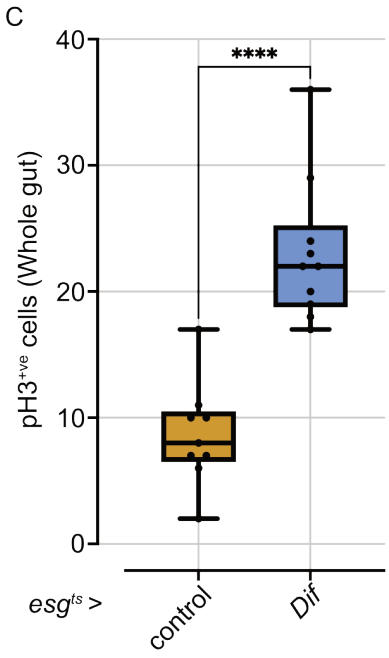

Supplementary Figure S12 : Ectopic expression of *Dif* in progenitor cells induces stem cell overproliferation in the midgut. (A-B) Representative images of the posterior midgut of esg^{ts} > driven control (w^{1118}) **(A)**, and *Dif* **(B)**, flies stained with anti-pH3 antibody. White arrows indicate pH3-positive mitotic cells in the midgut. **(C)** Quantification of pH3-positive cells per midgut of the mentioned genotypes. N = 9-10 flies; Significance values are marked by asterisks: ****$P < 0.0001$; Unpaired t-test; Scale bar = 25μm.

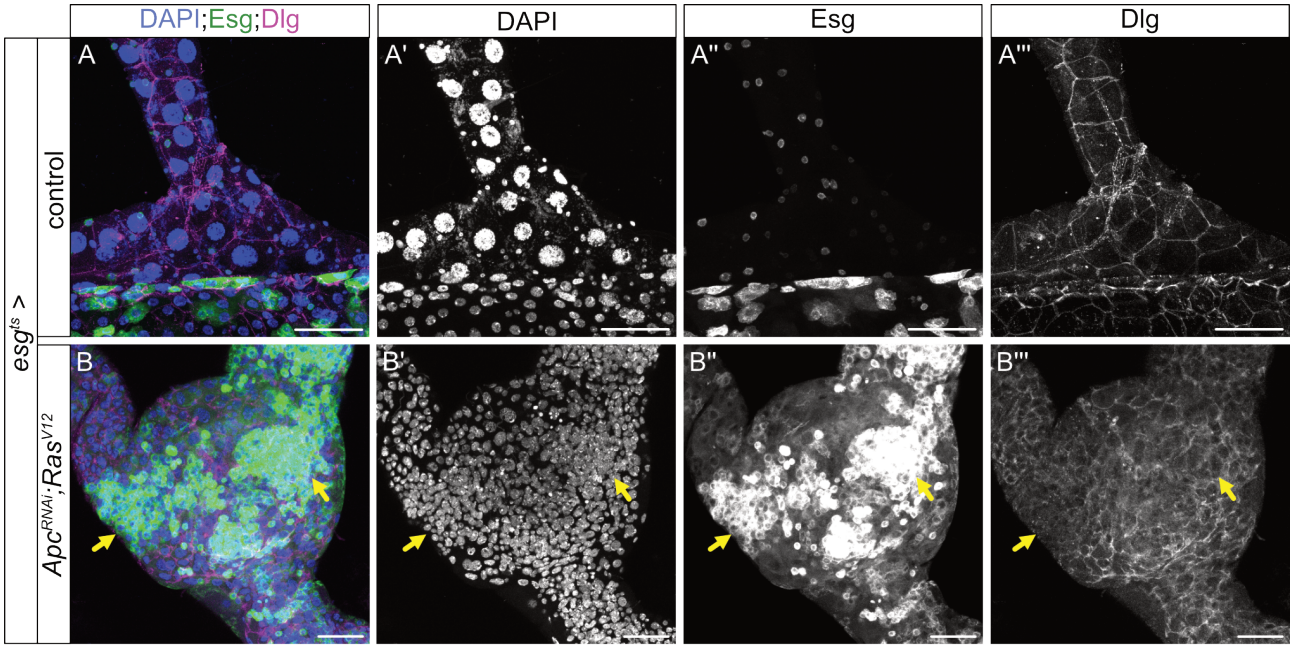

Supplementary Figure S13 : *Apc^{RNAi};Ras^{V12}*-expressing RSCs have disrupted adult malpighian tubule barrier integrity. (A-B) Representative images of the ureter of *esg^{ts}* > driven control (*w^{1118}*) **(A)** and *Apc^{RNAi}; Ras^{V12}* **(B)** flies stained with anti-Dlg antibody. Yellow arrows indicate disrupted Dlg staining in the region with increased RSC proliferation. Scale bar = 45μm.

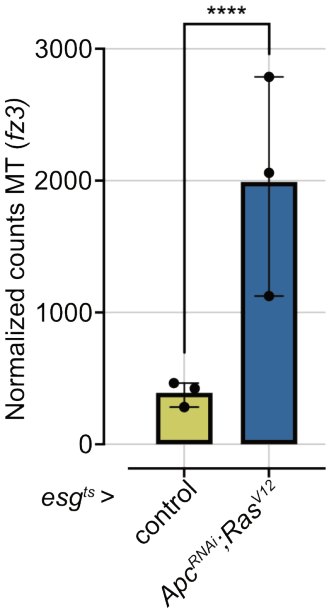

Supplementary Figure S14 : *Apc^{RNAi};Ras^{V12}* display increased expression of Wnt signaling target gene *fz3* in the adult malpighian tubules. Normalized *fz3* counts from bulk RNA seq of malpighian tubules of the mentioned genotypes; Wald test and benjamini hochberg correction to obtain adj p-value; Significance values are marked by asterisks: *****P < 0.0001*.

7.2 Scientific Publications

Bahuguna, S., Atilano, M., Glittenberg, M., Lee, D., Arora, S., Wang, L., Zhou, J., Redhai, S., **Boutros, M**. and Ligoxygakis, P., 2022. Bacterial recognition by PGRP-SA and downstream signalling by Toll/DIF sustain commensal gut bacteria in Drosophila. PLoS genetics, 18(1), p.e1009992.

Bahuguna, S., Redhai, S., Zhou, J., Wang, T., Port, F. and **Boutros, M**., 2021. Conditional CRISPR-cas genome editing in Drosophila to generate intestinal tumors. Cells, 10(11), p.3156.

Udayakumar, A., Stavropoulos, F., Peng, G., **Bahuguna, S**., MacClay, C., Lee, J., Xiao, Q., Xia, Y., **Boutros, M**., Zhou, J., Apidianakis, Y., Pitsouli, C. and Ligoxygakis, P., Toll signalling controls intestinal regeneration in Drosophila. Submitted, Under Review

Redhai, S., Hirschmüller, N., Wang, T., **Bahuguna, S**., Leible, S., Peidli, S., Valentini, E., Kharuk, S., Holzem, M., Bräckow, L., Port, F., Ibberson, D., Huber,W. and **Boutros,M** 2024. Proliferation and differentiation of intestinal stem cells depends on the zinc finger transcription factor BCL11/Chronophage. bioRxiv, pp.2024-09.

Redhai, S., Wang, T., Boonekamp, K.E., Rueter, S., Klemens, T.C., Leible,S., **Bahuguna, S**., Port, F., Pavlovic, B., Holzem, M., Doll, R., Rindtorff, N., Valentini,E., Schmitt,B., Richter,K., Engel,U., Huber,W. and **Boutros,M** 2024. Restraining Wnt activation and intestinal tumorigenesis by a Rab35 dependent GTPase relay. bioRxiv, pp.2024-02.

7.3 Acknowledgements

Doctoral studies is a unique adventure, filled with difficulties and challenges, but these challenges provide wonderful opportunities for learning and growth. During my PhD, I have learnt more than just science and have truly understood the meaning of ”It is the journey not just the destination”. I am grateful to all the people who have been part of this incredible journey, and I cannot imagine reaching the end of my PhD without their support. I am thankful to everyone that I have mentioned here, as well as to those who are not listed.

Michael Boutros, my primary supervisor, gave me the opportunity to pursue a PhD in his laboratory. He supported me in working on my ideas and provided me with both resources and guidance throughout my research. I am also grateful to my TAC members, Aurelio Teleman and Jan Lohmann, for their valuable feedback and recommendations on my project. I would like to thank the members of the DECODE team with whom I worked, including Filip Port, Siamak Redhai, Vaishali, Tianyu Wang, and Svejna Leible. Nick Hirschmüller was a bright bioinformatician, who was very talented and extremely helpful. I truly believe that he has a very bright future ahead.

Petros Ligoxygakis, my M.Sc. supervisor from Oxford, not only helped me publish my first paper after my master’s degree, but we also continued collaborating on another exciting new project exploring how Toll signaling regulates stem cell function. Aiswarya Udayakumar was a talented master’s student from the Ligoxygakis lab, who in one year made remarkable contributions to the project which is going to be published soon. Jun Zhou has held a very special position for me as a guide and advisor. He taught me how to do good science and steer a project. He was always available for scientific advice whenever I needed it. It was especially rewarding for me to have the opportunity to collaborate with him and Petros Ligoxygakis in developing the papers about Toll signaling and stem cell papers.

The members of my lab, especially Ulrike Hardeland, Felicitas Olschowsky and Caroline Diefenbach, Claudia Blass, Mona Stricker, Claudia Strein, Alma Spahic, Florian Heigwer, Filip Port, Erica Valentini, Jan Gerwin, Oksana Voloshanenko, Michaela Holzem, Kim Boonekamp, Antonia Schubert, Martina Zowada, Jan Gleixner, Siu Wang Ng, Nadine Winkler, and Saskia Reuter.

Cornelia Redel and Bojana Pavlovic, who patiently and carefully reviewed my thesis, suggested corrections, supported me when I felt lost, and taught me so much about scientific writing. Cornelia was my first choice for reviewing my thesis because of her ability to grasp concepts from a different field of research, her remarkable scientific rigor, and her skill to critically analyze scientific data. Bojana Pavlovic was not just a reviewer of my thesis, but also a fly colleague, and more importantly, a dear friend in the lab. She helped me navigate through the tough times during my PhD, gave me some wonderful advice, and had great discussions with me during lunch and flipping.

Two people from my lab deserve special gratitude: Pradhipa Karuna Manivannan and Philipp Albrecht. They were not just colleagues, but also amazing friends and people who I could blindly trust. They are one of the major reasons why I completed my thesis with a smile.

The organizing team members of the Career Day R and D team, 2021 (Sabine Kuznia, Jonas Bohn, Julia Peterson, Martha Carreno Gonzalez, Ekaterina Nikitina, Anne Jenseit, and Samantha Zottnick), who allowed me to connect with several company sponsors and host them for the event. This helped me develop the interpersonal skills that I had always been lacking.

PhD Council 2022 members Aga Seretny, Simay Çelikyürekli, Nooraldeen Tarade, Francisco Yanqui-Rivera, and Nina Decker were some of the best teammates I have had. Working with them made everything feel easier. Within the council, leading the PhD Retreat Team 2022 together with Simay Çelikyürekli and the graduate office (Lindsay Murrells and Anne Rölz) was a challenging yet rewarding experience. It taught me the spirit of teamwork and leadership, skills and memories that I will cherish throughout my life.

Sustainability is an important value for me and I am lucky to have worked for nearly 2 years with Hollyn Hartlep, the Sustainability Coordinator of DKFZ. She is a very hardworking, collaborative, and supportive leader who allowed me to communicate sustainability through the sustainability seminar series and participate in plantation/cleanup drives.

Members of our very own DKFZ Life Science Consulting club, including Bryce Lim, Dimitri Kasakovski, Damian Carvajal Ibanez, Jussara Rios de los Rios Resendiz, Aurelia Saftien, Chun Ho Chan, Umberto Pozza, and Arushi Gupta, have been an incredible team. With the goal of promoting researchers to become the next generation of decision-makers, I had the privilege of

watching this team being born and grow into a successful club. Throughout this journey, our career offices, Barbara J and Marion G provided invaluable guidance and support for my ideas, both during the Career Day and in the process of setting up the club. We are very fortunate to have them as our career advisors at DKFZ.

I have been lucky to have wonderful friends outside of work who have been with me throughout the PhD at different times. Kavan Gor, Rashi Agarwal and Pratika Agarwal were particularly important friends in Heidelberg, with whom I always spent my ”brain-free” time to keep my inner fun child alive. I am fortunate to still have my friends from Oxford, especially Aditya Agarwal, Shree Sowndarya, and Natasha Jeppu, with whom I spent the COVID lockdown playing games, chatting for long hours, and even attending a wedding in India. I am proud of their achievements and I have no doubts that they will be very successful in life (I’m counting on it). Anshika Chawla has also been an amazing travel companion, and I cherish the beautiful places we visited together, especially the Dolomites and Croatia—two of the most memorable trips I’ve ever had. Siddhi Rathi-Maniyar and Siddharth were some of the nicest friends, couples, chefs and people who I looked up to.

I have also shared some great coffee breaks and Villager and Warewolf nights with Pradhipa, Anand, Swathi, Vishnu, Suma, Nachiket, Praveen, Amrita, Reshmika, Mohan and Asha. I discovered the excitement of playing badminton much later in my PhD and I am grateful to the friends who played with during my writing phase: Shubhanshu, Dhruv, Avi, Debanjan, Daniel, Valentine, Jana, Denise, and Palkin. Without them, my writing phase would have been extremely difficult.

My constant support before, during, and potentially after my PhD have been my parents, Deepak Bahuguna and Priya Bahuguna, and my partner, Harshita Mishra. Since the beginning of my PhD, Harshita welcomed me into her house during the COVID lockdown when I had no place to stay. She took care of me during long lab hours, when I was sick, and also many other times when I needed it the most. She was there during my toughest times, pushing me to fight another day, and also during my happiest times, always ready to celebrate with me. I am proud of her for succeeding in her own PhD position and for her wonderful research. I’m so glad that, out of all the friends we know, we are the only couple in which both partners hold a PhD degree.

Last but definitely not least, my parents, Deepak Bahuguna and Priya Bahuguna, who stood by me through thick and thin, comforted me with their love and affection, motivated me when I needed it, and selflessly cared for me from the bottom of their hearts. Deciding to pursue a PhD was a tough decision for me but also daunting for them as well since they are not scientists. Nevertheless, they supported me in following my dreams and I will continue to work very hard and make them proud.